Structures of Physical and Visual Light Fields
Measurement, Comparison and Visualization

Kartashova, Tatiana

DOI
10.4233/uuid:fd7e7b74-5719-49f5-856a-a5ee3784c2ea

Publication date
2018

Document Version
Final published version

Citation (APA)
Kartashova, T. (2018). *Structures of Physical and Visual Light Fields: Measurement, Comparison and Visualization*. [Dissertation (TU Delft), Delft University of Technology].
https://doi.org/10.4233/uuid:fd7e7b74-5719-49f5-856a-a5ee3784c2ea

Important note
To cite this publication, please use the final published version (if applicable).
Please check the document version above.

STRUCTURES OF PHYSICAL AND VISUAL LIGHT FIELDS

MEASUREMENT, COMPARISON AND VISUALIZATION

STRUCTURES OF PHYSICAL AND VISUAL LIGHT FIELDS

MEASUREMENT, COMPARISON AND VISUALIZATION

Proefschrift

ter verkrijging van de graad van doctor
aan de Technische Universiteit Delft,
op gezag van de Rector Magnificus Prof.dr.ir. T.H.J.J. van der Hagen,
voorzitter van het College voor Promoties,
in het openbaar te verdedigen op
donderdag 8 November 2018 om 12:30 uur

door

Tatiana KARTASHOVA

Ingenieur in Computertechniek en Informatica,
Sint-Petersburg Elektrotechnisch Universiteit, Sint-Petersburg, Rusland,
geboren te Ermak, USSR.

Dit proefschrift is goedgekeurd door de

promotor: Prof. dr. S. C. Pont
promotor: Prof. dr. H. de Ridder
promotor: Prof. dr. S. F. te Pas

Samenstelling promotiecommissie:

Rector Magnificus,	voorzitter
Prof. dr. S. C. Pont,	Technische Universiteit Delft
Prof. dr. H. de Ridder,	Technische Universiteit Delft
Prof. dr. S. F. te Pas,	Utrecht Universiteit

Onafhankelijke leden:

Dr. I. M. L. C. Vogels,	Technische Universiteit Eindhoven
Prof. dr. R. W. Fleming,	Justus-Liebig University Giessen
Prof. ir. M. A. Voûte,	Technische Universiteit Delft
Prof. dr. E. Eisemann,	Technische Universiteit Delft

Printed by: Ipskamp Printing

This research was funded by the European Commission through the EU FP7 Marie Curie ITN project PRISM, Perceptual Representation of Illumination, Shape and Material (PITN-GA-2012-316746).

An electronic version of this dissertation is available at
http://repository.tudelft.nl/.

To Stefano
and my parents, biologic and academic.

CONTENTS

1

INTRODUCTION

1

Many things are so common and natural that they are taken for granted. Technologies, services, our own bodies — if they work, usually nobody thinks about these "things", except the concerned professionals. However, most of such entities contain multiple layers of complexity, like onions (and ogres).

The human visual system is not an exception. Seeing is an intricate process that includes receiving light through the eyes' optic system onto the retinal cells, delivering information to the brain and the processing of two flat images (one per eye). The result is a rich 3D impression of objects, materials and illumination of the surrounding world. Each part and subpart of this process constitutes a fruitful field of research. In this thesis, I focused on one of those fields, the perception of light in spaces. There might be infinite combinations of shape, material and illumination forming a certain resulting image. For example, Figure 1.1 is physically a flat image on a page, but we can perceive the images of an object having a volume, material and illumination through visual cues that the image of it provides. Most likely, it is an image of a specular sphere under a spotlight, but it also might be a matte sphere with an elliptical drop of white paint under a spot light or a flat disk printed with a black-green gradient with a paint drop under a fully diffuse illumination. The second seems less likely, because the highlight perfectly fits the shading on the sphere. The third seems very unlikely because such gradients are much more likely to be caused by illumination and shape than material (Hoffman & Marshall; 1998). The visual system solves this probability task in an instance using knowledge about our environment.

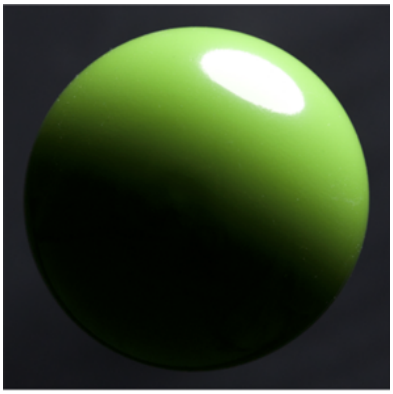

Figure 1.1: Example of an ambiguous image. From van Assen, J.J.R., Wijntjes, M. W. A., Pont, S.C. (2016) Highlight shapes and perception of gloss for real and photographed objects. Journal of Vision;16(6):6. doi: 10.1167/16.6.6. Reprinted with permission.

From a single glance one can estimate the illumination in an observed scene and define if there is a mismatch of illumination or fit a light on an object according to the rest of the scene (Koenderink et al., 2007; Xia et al., 2014, 2017). It is rather fascinating, because one cannot see the light itself in an empty space, since there is nothing there reflecting rays into eyes. Thus, the inferences are made using surrounding objects. But to what extent are humans able to make estimations of spatial variations of light in empty space? In order to approach this question, several concepts should be introduced.

First, what are veridical spatial variations of light and how to capture them? In section 1.2, I list studies on the physical light field that provided the ground truth for my studies. Next, the perceptual aspect should be described in more detail. Light perception research is tightly related to multiple visual perception fields. Relevant studies on mutual influences between perceived light, materials and shapes are discussed in section 1.3. Then, I introduce the challenges from a light visualization perspective in section 1.4. Finally, in section 1.5 of this introduction, I systematize the content of this thesis and explain the relations between the chapters.

1.1. THE PHYSICAL LIGHT FIELD

Illumination in natural scenes depends on many factors, including the properties and position of light sources, scene geometry and materials. Relations between these factors create a complex resulting illumination that is reflected in the variation of light properties over a scene. For example, consider an elongated room such as in Figure 1.2, with a single highly directed light source on one side of it. Obviously, the intensity of light will be different at a point under the lamp (point 1) and a point in another part of the room (point 2). Next, most of the light which reaches point 2 is due to reflections, so the average light direction at this point is almost the opposite of that at point 1, where the lamp is shining straight down. The resulting distribution is clear when presented for a simple schematic example. But in a real scene, it is difficult to capture and analyze light variations, because light travels through every point of 3D space in all directions and has complicated optical interactions with the environment.

Gershun (1939) was the first to create a systematic physical theory describing light in space. He proposed a 5-dimensional function that defined the radiance arriving at a point (x, y, z) from all directions (θ, ϕ). Gershun also introduced the notion of the light vector that represents the average light direction weighted over all directions. The light field can be imagined as a set of numerous panoramic images, one for each point in space. Such a representation of the light field would contain a tremendous amount of information that is extremely difficult to analyze.

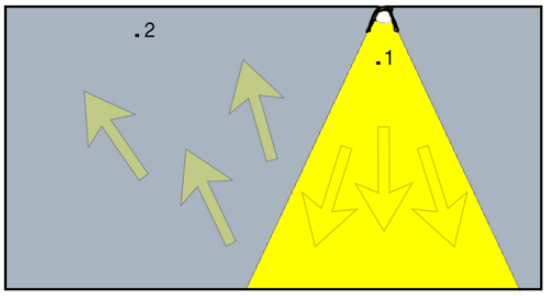

Figure 1.2: Light distribution in a room with a single spotlight.

It is possible to simplify the local light field (illumination in a single point) represen-

tation by extracting only a few important properties from radiance measurements. One way is through components of spherical harmonics decomposition: constant, vector, squash tensor and higher order components (Mury et al., 2007). They have equivalents in lighting design (Pont, 2013). The zeroth order component, a constant, corresponds to ambient light. The first order component, a dipole, corresponds to a light vector or to a directed light. The second order component, a squash tensor, relates to a light clamp (two light sources shining from the opposite sides) or a light ring. The higher order components correspond to brilliance, "light texture" (Kelly, 1952; Pont, 2018). Additionally, the relationship between zeroth and first order components can be used as a measure of diffuseness (Xia et al., 2016ab). These components together describe light completely and provide the scientific basis for Kelly's (1952) design approach in which light plans are built up as a combination of ambient (fully diffuse) light, focal (very directed) light and the "play of brilliants", i.e. mathematical higher order light components. Another approach for extracting light properties from measurements was introduced in the light design research field. Cuttle (2003, 2013) proposed calculations for obtaining the illumination vector direction and magnitude, scalar illuminance, and diffuseness from cubic light measurements.

Findings of Mury et al. (2007, 2009) also made the natural light field more approachable. They coupled the spherical harmonics (SH) development to Gershun's theory and the physical meaning. Moreover, they demonstrated that the low-order components of natural light fields vary smoothly over scenes. Therefore, it is possible to reconstruct a physical light field through interpolation between a relatively small number of measurement points.

In this thesis, I adopted the framework describing light through its components (Pont, 2013). In particular, I use the direction of the light vector, mean illuminance and diffuseness, representing the zeroth and first order components of the spherical harmonics decomposition. These properties were extracted from physical and virtual measurements using Cuttle's (2003, 2013) formulas. The structures of natural light fields were modelled using Mury et al's (2009) approach.

1.2. VISUAL PERCEPTION

Illumination perception has been studied from multiple perspectives in the vision research field. This is not surprising, because illumination is always involved in visual perception. There are, for example, extensive studies on the relation between illumination and perceived lightness (Bloj et al., 2004; Gilchrist, 1977; Gilchrist et al., 1999; Ripamonti et al., 2004; Rutherford & Brainard, 2002; Toscani & Gegenfurtner, 2017), shape (Berbaum et al., 1983; Koenderink & van Doorn, 2003; O'Shea et al., 2010), materials (Anderson, 2011; Fleming et al., 2003; Ho et al., 2006; Kingdom, 2008; Maloney & Brainard, 2010; Marlow et al., 2012; Pont & te Pas, 2006; Pont, 2009; Zhang et al., 2015).

Fewer studies have focused on the perception of light properties. The majority of them have tested only light direction and cues for its estimation (Boyaci et al., 2006; Gerhard & Maloney, 2010; Koenderink et al., 2003; Lopez-Moreno, 2010; O'Shea et al., 2008; Pont et al., 2011). Some have taken into account several light properties at the same time

(Pont & Koenderink, 2007; Xia et al., 2014, 2017), but investigated only the local light field. So far, no studies have conducted systematic measurements of the global visual light field. Yet, it is an interesting topic, because it could reveal a higher level of human awareness of the luminous environment (Pont, 2013).

The most relevant paper to my research is The Visual Light Field conducted by Koenderink et al. (2007). They have proposed a probing method for inferring the perception of light conditions in empty space. The probe was a white sphere superimposed on binocularly viewed images of a scene such that the position of the sphere in the scene was rendered through disparity. An observer could control the sphere's illumination direction, intensity and directedness. The task was to match the illumination of the sphere so that it fits the scene. The inferences were made over several positions under three distinctly different light conditions. The participants' settings were close to the veridical for all tested light conditions, demonstrating sensitivity to the intensity, direction and directedness of light, which was named the visual light field. This study is a conceptual basis for my research. Additionally, I used this approach for probing the light field.

1.3. LIGHT VISUALIZATION

In applied fields, such as architecture and computer graphics, lighting is a very important matter. It is a powerful tool that can influence the appearance of objects and spaces, help to tell story by highlighting elements of scenes, create an atmosphere. Nowadays, light design results are often evaluated via creating virtual models, rendering them and visually evaluating if the results satisfy practical and esthetical requirements. However, such renderings might not provide a clear understanding of the illumination environment. They might be ambiguous due to a lack of clear light cues, especially if the rendered spaces are empty. Moreover, renderings typically have a limited dynamic range. The solution to this issue might be a different approach to light visualization.

An important question in designing a light visualization is choosing its positioning. Or, in other words, in which parts of scenes illumination is important and should be visualized. Light design researchers argue that the design profession should move from thinking in terms of planes to creating light in volumes (Boyce, 2013; Cuttle, 2010) and taking into account more than elimination of discomfort (Boyce, 2003; Lam, 1992). Yet, existing light visualization methods are either limited to surfaces (e.g., the very common false color plot depicting (il)luminance values over planes / a planar section), or focusing on specific light effects (e.g., visualization of caustics in computer graphics).

In this thesis, we developed and tested a perception-based approach to light visualization in volumes and made the concept and the tool available for the light design community.

1.4. THIS THESIS

Previous studies showed that it is possible to reconstruct the physical light field and that human observers are sensitive to its local properties. The next interesting question ex-

tends to observers inferring global structures of light fields. The first aim of this thesis is to further investigate perception of illumination over (images of) volumetric scenes. It is approached through combining volumetric physical light measurements and psychophysical methods for subjective, perceptual measurements. The second aim is to use our knowledge on measurement and perception of light fields to create a visualization of light properties in volumes.

The core of this thesis consists of five chapters. Each chapter is based on a publication (see Publications List), is self-contained, and can be read independently. Below I list the main research questions and short summaries of the chapters' motivations.

- Chapter 2. **Can we reconstruct the visual light field and compare it to the physical light field?**

  In previous research it was shown that human observers are sensitive to local properties of the physical light field (Koenderink et al., 2007; Xia et al., 2014). In this study, we investigated if the human data is robust and consistent enough to reconstruct the structure of the visual light field. Using grids of light probes to capture multiple local inferences we obtained the visual light fields and compared them to the measured physical light fields.

- Chapter 3. **Are inferences of light on objects (based on a single object appearance) and in empty space (based on appearance of surrounding objects) congruent with each other?**

  Artists were probably the first explorers of light qualities in their strive to picture the surrounding world. Through the evolution of techniques they achieved almost photorealistic results. We were interested in lighting representation in paintings. We performed experiments using the light probe approach in order to test if illumination was perceived consistently between the whole scene and on objects.

- Chapter 4. **How does the presence and mutual orientation of light zones (i.e. neighboring light fields with contrasting differences in one or more light properties) influence the perception of light properties in them?**

  The results of the previous study suggested that the presence of light zones might lead to idiosyncratic differences in observers' settings. We investigated the perception of illumination differences over depicted spaces in a systematic manner, performing experiments in scenes containing light zones of two different orientations with respect to an observer: in the image plane (differing between the left and right sides of a scene) and in depth (differing between the front and back parts of a scene).

- Chapter 5. **Do visualizations of light properties in a volume show light fields structures better than renderings?**

  The most common existing approach to light visualization is a false color plot showing the (il)luminance on surfaces of a scene itself or on planar cross sections of a scene. It might be extended from a single to multiple light properties, and from surfaces to volumes. We developed and tested volumetric visualizations of

light that show perceptually relevant light properties, accessible to a user after a brief instruction.

- Chapter 6 **How can volumetric light visualizations be used in lighting design?**

  Light design researchers (Boyce, 2003, 2013; Cutttle, 2010) suggest that the lighting profession (and, therefore, lighting standards and tools) should be extended beyond illumination on horizontal and vertical planes to thinking in terms of 3D spaces. We propose and demonstrate a light visualization tool that supports this idea and shows the light flow structure in the whole volume of a scene.

Chapter 7 summarizes the main results and contributions of this thesis and suggests possibilities for future work.

BIBLIOGRAPHY

Anderson, B. L. (2011). Visual perception of materials and surfaces. Current Biology, 21(24), R978—R983.

Berbaum, K., Bever, T., & Chung, C. S. (1983). Light source position in the perception of object shape. Perception, 12(4), 411—416.

Bloj, M., Ripamonti, C., Mitha, K., Hauck, R., Greenwald, S., & Brainard, D. H. (2004). An equivalent illuminant model for the effect of surface slant on perceived lightness. Journal of Vision, 4, 735—746.

Boyaci, H., Doerschner, K., & Maloney, L. T. (2006). Cues to an equivalent lighting model. Journal of Vision, 6(2), 106—118. https://doi.org/10.1167/6.2.2.

Boyce, P. R. (2003) Human factors in lighting. 2nd ed. Boca Raton, FL: CRC Press.

Boyce, P. R. (2013). Lighting Quality for All. CISBE & SLL International Lighting Conference - Dublin 2013. Session 3, 1—5.

Cuttle, C. (2003). Lighting by Design. Oxford: Architectural Press.

Cuttle, C. (2013). Research Note: A practical approach to cubic illuminance measurement. Lighting Research and Technology, 46(1), 31—34.

Gerhard, H. E., & Maloney, L. T. (2010). Estimating changes in lighting direction in binocularly viewed three-dimensional scenes. Journal of Vision, 10, 14.

Gershun, A. (1939). The light field (P. Moon & G. Timoshenko, Trans.). Journal of Mathematics and Physics, 18, 51—151.

Gilchrist, A. (1977). Perceived lightness depends on perceived spatial arrangement. Science (New York, N.Y.), 195(4274), 185—187.

Fleming, R. W., Dror, R. O., & Adelson, E. H. (2003). Real-world illumination and the perception of surface reflectance properties. Journal of Vision, 3, 347—368.

Gilchrist, A., Kossyfidis, C., Bonato, F., Agostini, T., Cataliotti, J., Li, X., ? Economou, E. (1999). Anchoring Theory of Lightness Perception. Psychological Review, 106(4), 795—834.

Ho, Y.-X., Landy, M. S., & Maloney, L. T. (2006). How direction of illumination affects visually perceived surface roughness. Journal of Vision, 6, 634—648.

Hoffman, D. D., & Marshall, J. C. (1998). Visual intelligence: How we create what we see. Nature, 396, 36—36.

Kelly, R. (1952). Lighting as an Integral Part of Architecture. College Art Journal, 12(1), 24—30.

Kingdom, F. a a. (2008). Perceiving light versus material. Vision Research, 48(20), 2090—105.

Koenderink, van Doorn, A. J., Kappers, A. M. L., te Pas, S. F., & Pont, S. C. (2003). Illumination direction from texture shading. Journal of the Optical Society of America. A, Optics, Image Science, and Vision, 20(6), 987—995.

Koenderink, J. J., & van Doorn, A. J. (2003). Shape and Shading. In The visual neurosciences (pp. 1090—1105). Springer US.

Koenderink, Pont, S. C., van Doorn, A. J., Kappers, A. M. L., & Todd, J. T. (2007). The visual light field. Perception, 36(11), 1595—1610.

Lopez-Moreno, J., Sundstedt, V., Sangorrin, F., & Gutierrez, D. (2010). Measuring the perception of light inconsistencies. Proceedings of the 7th Symposium on Applied Perception in Graphics and Visualization - APGV '10, 1(212), 25.

Maloney, L. T., & Brainard, D. H. (2010). Color and material perception: achievements and challenges. Journal of Vision, 10.

Marlow, P. J., Kim, J., & Anderson, B. L. (2012). The perception and misperception of specular surface reflectance. Current Biology, 22(20), 1909—1913.

Mury, A. a, Pont, S. C., & Koenderink, J. J. (2007). Light field constancy within natural scenes. Applied Optics, 46(29), 7308—7316.

Mury, A. A., Pont, S. C., & Koenderink, J. J. (2009). Structure of light fields in natural scenes. Appl Opt, 48(28), 5386—5395.

Lam, W. M. (1992). Perception and Lighting as formgivers for architecture. New York: Van Nostrand Reinhold.

Lopez-Moreno, J., Sundstedt, V., Sangorrin, F., & Gutierrez, D. (2010). Measuring the perception of light inconsistencies. Proceedings of the 7th Symposium on Applied Perception in Graphics and Visualization - APGV '10, 1(212), 25.

O'Shea, J., Agrawala, M., & Banks, M. S. (2010). The influence of shape cues on the perception of lighting direction. Journal of Vision, 10(12), 21.

Pont, S. C., & te Pas, S. F. (2006). Material - Illumination ambiguities and the perception of solid objects. Perception, 35(10), 1331—1350.

Pont, S. C., & Koenderink, J. J. (2007). Matching illumination of solid objects. Perception & Psychophysics, 69(3), 459—468.

Pont, S. C. (2009). Ecological optics of natural materials and light fields. Human Vision and Electronic Imaging XIV, Edited by Bernice E. Rogowitz, 7240, 724009-724009—

12.

Pont, S. C., Wijntjes, M. W. a, Oomes, A. H. J., van Doorn, A. J., van Nierop, O., de Ridder, H., & Koenderink, J. J. (2011). Cast shadows in wide perspective. Perception, 40(8), 938—948.

Pont, S. C. (2013). Spatial and Form-Giving Qualities of Light. In L. Albertazzi (Ed.), Handbook of Experimental Phenomenology. John Wiley and Sons, Ltd.

Pont, S.C. (2018) Optical and Perceptual Phenomena of Light - and the brilliance of fire flies. Schering Stiftung: Berlin, Germany, Chapter In: Ivana Franke: Retreat into Darkness. Towards a Phenomenology of the Unknown.

Ripamonti, C., Bloj, M., Hauck, R., Mitha, K., Greenwald, S., Maloney, S. I., & Brainard, D. H. (2004). Measurements of the effect of surface slant on perceived lightness. Journal of Vision, 4(9), 747—763.

Rutherford, M. d, & Brainard, D. H. (2002). Lightness Constancy: A Direct Test of the Illumination-Estimation Hypothesis. Psychological Science.

Toscani, M., Zdravkovic, S., & Gegenfurtner, K. R. (2017). Lightness perception for surfaces moving through different illumination levels. Journal of Vision, 16(2016), 1—18.

Xia, L., Pont, S. C., & Heynderickx, I. (2014). The visual light field in real scenes. I-Perception, 5(7), 613—629. Retrieved from unknown

Xia, L., Pont, S. C., & Heynderickx, I. (2016). Light diffuseness metric Part 1?: Theory. Lighting Res. Technol., 49(4), 411—427.

Xia, L., Pont, S. C., & Heynderickx, I. (2016). Light diffuseness metric , Part 2?: Describing , measuring and visualising the light flow and diffuseness in three-dimensional spaces. Lighting Res. Technol., 49(4), 428—445.

Xia, L., Pont, S. C., & Heynderickx, I. (2017). Effects of scene content and layout on the perceived light direction in 3D spaces. Journal of Vision, 16(10), 1—13.

Zhang, F., de Ridder, H., & Pont, S. C. (2015). The influence of lighting on visual perception of material qualities, 9394(0), 93940Q.

LIST OF PUBLICATIONS

INTERNATIONAL PEER-REVIEWED PAPERS

1. **Kartashova, T.**, de Ridder, H., te Pas, S. F., Schoemaker, M., & Pont, S. C. (2015) *The visual light field in paintings of Museum Prinsenhof: comparing settings in empty space and on objects*, Proceedings of SPIE 9394, Human Vision and Electronic Imaging XX **9394**, 93941M. https://doi.org/10.1117/12.2085030

2. **Kartashova, T.**, Sekulovksi, D., de Ridder, H., Pas, S. F., & Pont, S. C. (2016) *The global structure of the visual light field and its relation to the physical light field*, Journal of Vision **16**, 9. https://doi.org/10.1167/16.10.9.doi

3. **Kartashova, T.**, de Ridder, H., te Pas, S. F., & Pont, S. C. (2018) *The visual light Zones*, i-Perception **9**, 3 (1-20). doi:10.1177/2041669518781381.

4. **Kartashova, T.**, de Ridder, H., te Pas, S. F., & Pont, S. C. (2018) *Light Shapes: Perception-Based Visualizations of the Global Light Transport*, Transactions on applied Perception **(in press)**, x (xx).

5. **Kartashova, T.**, de Ridder, H., te Pas, S. F., & Pont, S. C. (201x) *A toolbox for volumetric visualization of light properties*, Lighting Research and Technology **(under review)**, x (xx).

OTHER PUBLICATIONS

1. **Kartashova, T.**,Heynderickx, I, Sekulovski, D., & Pont S. C. (2014) Relating physical and visual global ight field structures. Experiencing Light 20014, 118.

2. **Kartashova, T.**, Sekulovksi, D., de Ridder, H., Pas, S. F., & Pont, S. C. (2015) *A Comparison of Physical and Visual Light Fields*, Proceedings of VSS, Journal of Vision **15**, 12, 634-634.

3. **Kartashova, T.**, de Ridder, H, te Pas, S. F., & Pont S. C.(2016) Inferring light characteristics in spaces with multiple light zones. European Conference on Visual Perception (ECVP) Annual Meeting 2016.

4. Wijntjes, M., te Pas, S., Schoemaker, M. P., Pont, S., Zhang, F., **Kartashova, T.**, & van Middelkoop, C. (2016). The influence of illumination on perception of works by Jan Schoonhoven. Poster session presented at Visual Science of Art Conference, Barcelona, Spain.

5. **Kartashova, T.**, te Pas, S. F., de Ridder, H, & Pont S. C. (2016) Visualizations of Perceptually Relevant Light Parameters. SIGGRAPH Asia 2016.

6. **Kartashova, T.**, de Ridder, H, te Pas, S. F., & Pont S. C.(2017) Light zones in Depth. European Conference on Visual Perception (ECVP) Annual Meeting 2017.

7. Pont, S., Xia, L., & **Kartashova, T.** (2017). The optics, perception and design of light diffuseness in real scenes. Journal of Vision, 17(10), 1-1.

2

THE GLOBAL STRUCTURE OF THE VISUAL LIGHT FIELD

Abstract

Human observers have been demonstrated to be sensitive to the local (physical) light field, or more precisely, to the primary direction, intensity, and diffuseness of the light at a point in a space. In the present study we focused on the question of whether it is possible to reconstruct the global visual light field, based on observers' inferences of the local light properties. Observers adjusted the illumination on a probe in order to visually fit it in three diversely lit scenes. For each scene they made 36 settings on a regular grid. The global structure of the first order properties of the light field could then indeed be reconstructed by interpolation of light vectors coefficients representing the local settings. We demonstrate that the resulting visual light fields (individual and averaged) can be visualized and we show how they can be compared to physical measurements in the same scenes. Our findings suggest that human observers have a robust impression of the light field that is simplified with respect to the physical light field. In particular, the subtle spatial variations of the physical light fields are largely neglected and the visual light fields were more similar to simple diverging fields than to the actual physical light fields.

Published as: Kartashova, T., Sekulovksi, D., de Ridder, H., Pas, S. F., & Pont, S. C. (2016) The global structure of the visual light field and its relation to the physical light field. Journal of Vision, 16(9).

2.1. INTRODUCTION

It is fascinating how light manipulations can change the appearance of an object or a scene (Cuttle, 1973; Ganslandt & Hofmann, 1992; Hunter, Biver, & Fuqua, 2007). Many professionals — artists, photographers, light designers, and architects — use practical knowledge about light in their work. They put things in a spotlight to put attention on them, they use diffuse lighting to make surfaces look smoother, or play more sophisticated tricks with our visual system to create illusions. So far, the theory behind such lighting techniques is not particularly extensive (Cuttle, 2003; Gilchrist & Radonjic, 2009). Moreover, we are not aware of any lighting design books that address how complicated optical interactions between lighting, spatial geometry, materials, and objects result in the light distribution or light field in a space. Most literature in this field focuses on providing enough light (intensity) on working surfaces, people, and objects (Boyce, 1981). Only a few lighting designers address the issue that human-centered lighting design should be based on the observer's experience of light arriving at the eye, which is determined not only by the light sources, but also by a scene geometry, furnishing objects, and materials as well as the position and motion of the observer and the people in the scene (Cuttle, 2003; Ganslandt & Hofmann, 1992). These lighting designers provide some ideas on how to progress toward working with the light field, but none were able to describe the global structure of light distributions in three-dimensional spaces. Thus, a deeper understanding of visual qualities of light might help to improve multiple fields of knowledge.

How an image is perceived depends on the light in the image's scene but at the same time, the light can be judged through the objects in that scene (Koenderink, Pont, van Doorn, Kappers, & Todd, 2007). There are many studies on perceptual interrelations between light and object shape (Berbaum, Bever, & Chung, 1983; Koenderink & van Doorn, 2006; O'Shea, Agrawala, & Banks, 2010), light and surfaces properties (Doerschner, Boyaci, & Maloney, 2007; Fleming, Dror, & Adelson, 2003; Ho, Landy, & Maloney, 2006; Marlow, Kim, & Anderson, 2012), and light and spatial geometry (Madsen, 2007; Yamauchi, Ikeda, & Shinoda, 2003). However, there are only few studies with the light field as the main focus in physics (Dror, Willsky, & Adelson, 2004; Gershun, 1939; Moon & Spencer, 1981; Mury, Pont, & Koenderink, 2007, 2009) and in visual perception (Adelson & Bergen, 1991; Gerhard & Maloney, 2010; Koenderink et al., 2007; Maloney, Gerhard, Boyaci, & Doerschner, 2010; Morgenstern, Geisler, & Murray, 2014; Pentland, 1982; Pont, 2013; Pont & Koenderink, 2007; Pont, van Doorn, de Ridder, & Koenderink, 2010; Xia, Pont, & Heynderickx, 2014). Of those studies, we list the most relevant findings, on which we based our study of the reconstruction of the spatial structure of a perceived light field and its relation to its physical counterpart.

Gershun (1939) was one of the pioneers working on the definition of light in a space. He introduced the term light field, which is a function that describes the amount of light traveling in every direction through every point. It describes light as a function of position in space and direction resulting in a five-dimensional spherical function, describing the radiance arriving to a point x, y, z from direction θ, ϕ. One may interpret this description as a huge collection of panoramic images for all positions in a space. Gershun (1939)

introduced radiant flux density — the net flux that passes through any given surface element from either side; and the light vector — the magnitude and direction of the net flux. He also introduced light tubes as a manner to describe the net light transport through a space. Adelson and Bergen (1991) described an equivalent of the physical light field, the plenoptic function (from plenus, meaning "all," plus optic), which specifies the structure of light as a function of position, direction, wavelength, and time. In our work, we ignore the variables wavelength and time and focus on the luminance distribution — as in Gershun's (1939) definition. This concerns a five- dimensional function, which is quite complex for most real scenes.

The development of mathematical and computer modeling tools provided the means for further elaboration of the topic. Mury et al. (2007, 2009) studied the spatial structure of physical light fields. They developed methods to describe the physical light field by extending Gershun's (1939) definition of light's components, as well as methods to measure and visualize its (global) structure. They found experimentally that the low-order components of the light field vary smoothly over scenes, implying that it is possible to make a reconstruction of the physical light field of a scene based on a relatively small number of measurement points. Mury et al. (2007, 2009) also demonstrated a strong relationship between the low-order components and the geometrical layouts of the scenes, concluding that, in some way, the physical light field can be thought of as a property of the geometry.

The visual light field was measured by Koenderink et al. (2007). In order to test human sensitivity to various parameters of the physical light field, they introduced a white sphere as a gauge object. Their setup consisted of stereoscopic photographs of a scene under three light conditions and a probe (a white matte sphere). The task was to set the lighting (light direction, intensity, diffuseness) on the probe so that it appeared to belong to the scene. The resulting probe images were compared to the photographs of a real sphere in the same positions. Koenderink et al. (2007) concluded that human observers have expectations of how a given object would appear if it was introduced in a scene at some arbitrary position and named this awareness the visual light field.

Xia et al. (2014) tested the findings of Koenderink et al. (2007) for real scenes. They created a real setup in which the lighting on a scene and on a probe could be manipulated separately, and the scene and probe could be fused using a semitransparent mirror. Twenty participants were asked to judge whether the probe fitted the scene with regard to illumination intensity, direction, and diffuseness. The observers were found to be sensitive to variations in light intensity, direction, and diffuseness.

In reviewing studies on illumination, lightness and brightness perception, Schirillo (2013) argued the necessity "to develop a broader perceptual theory, including the crucial variable of how light is inferred in open space" (p. 905). Throughout the paper, he provided several examples of experiments in which the same test patch was perceived significantly lighter or darker depending on its apparent position in space — under dim or bright illumination, respectively. Schirillo (2013) discussed the possibility that we infer light itself, raising questions such as "why does the object appear colored, but not the space in front of it, in that this space contains light of the same wavelengths as that at the surface of the object" (p. 908). In the end, he draws the conclusion that there ex-

ists a mental representation of the light in three-dimensional space. He notes that such awareness must be derived from reflecting surfaces in a scene, but that the quality is not brightness. He concluded that the awareness of light extending into the space between the surfaces and the eye is phenomenologically real and measurable.

Schirillo (2013) also noted that our awareness of the light in empty space does not necessarily mirror physical illumination. For example, neutral light in a room furnished in red may be perceived as reddish. Ostrovsky, Cavanagh, and Sinha (2005) found that the structure of the physical light field can also be misperceived. They demonstrated that humans often neglect inconsistencies in illumination, which would not be the case if the light field is perceived in a physically veridical way. This "deficiency" was explained by the visual system not trying to verify the global consistency of the local estimates because, they speculated, human evolution in a single light source environment yields a fast local analysis sufficient for obtaining the illumination information needed. Likewise, in Koenderink et al.'s (2007) experiment there was a condition in which the judgments of all but one observer were inconsistent with the physical truth. It was the condition in which a probe was in the volume of a cast shadow of an object, implying that observers were not aware of certain details of the light field's structure. Van Doorn, Koenderink, Todd, and Wagemans (2012) recently studied the perception of several global structures in natural light fields. They showed that human observers can perceive uniform, diverging, and converging light fields (which can be represented by sunlight, candlelight, and a ring or sphere of light surrounding a scene or object of interest, respectively) but are insensitive to rotational and deformation light flow patterns (Cuttle, 1973), which are less common and may be formed by complicated lighting/geometry. In conclusion, there is growing evidence that although the visual and physical light fields show similarities, they are not identical to each other. However, we are not aware of any studies in which the global structure of the visual light field was actually measured and compared to the physical light field. One reason for this gap certainly concerns the lack of a proper method to measure the visual light field.

The aim of the present study is to fill this gap in measuring and comparing the global structures of corresponding physical and visual light fields. In doing so, an important question is whether measuring many instances of a local visual light field in a scene allows the reconstruction of its global structure by interpolating its lower order features in a similar way as Mury et al. (2009) did for the physical light field. We found that our data was sufficiently smooth to accomplish this.

The measurements were done on a real scene, a living room, in which the type of illumination was varied to create three different light fields. We took measurements over nearly regular grids, sufficiently capturing the variations in the light field over the three illumination types. In this study, we focused mostly on the directional component of the light field, the light vector, but we also measured the ambient component in order to make diffuseness comparisons. The paper is organized as follows: First, we present the methods we used to measure and reconstruct the visual light fields, demonstrate approaches for their visualization, and discuss the measurements results. Second, we explain the physical measurements and their processing. Finally, we compare the visual and physical light fields and discuss the overall results of the study.

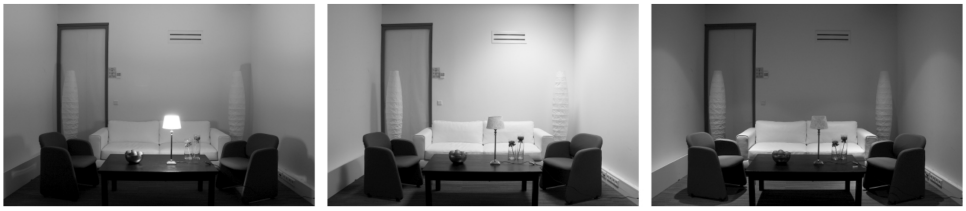

Figure 2.1: Light conditions: visible light source (LAMP), diffused light sources in the ceiling on the right side of the scene (DIFFUSE), two collimated light sources in the ceiling, one on the left and the other on the right side of the scene (SPOTLIGHTS).

2.2. THE VISUAL LIGHT FIELD

2.2.1. METHODS

SCENE

The scene was part of a laboratory room, furnished as a common living room (see Figure 2.1). The scene width was 340 cm, the depth (from the back wall to the front-most line of measurements) was 255 cm, and the height was 300 cm. Most of the objects in the scene had matte surfaces varying in roughness. Some surfaces were shiny, including a smooth specular tabletop, a metal fruit plate and lamp stand, and a transparent glass flower vase. We used the following light conditions: a lamp on the table (LAMP); two sets of fluorescent lamps, one behind another, on the right side of the ceiling creating a diffusely lit scene (DIFFUSE); and two spotlights, one on the left and the other on the right side of the room with their center of symmetry slightly to the left of the room center, to create a more focused lighted scene (SPOTLIGHTS).

We photographed the scene under each of the three light conditions. The camera was standing 5 m away from the back wall of the scene with the following camera settings: f-number equal to 7.1 and exposure times equal to 1/2, 1/15, and 1/8 s for LAMP, DIFFUSE, and SPOTLIGHTS, respectively, because of the differences between illumination levels. We then converted the photographs to grayscale, with each picture ranging in pixel brightness from 0 to 255, and cropped them to hide a part of the ceiling. Thus, the images were made so that the light source was visible for the first scene and invisible for the other two scenes. The resulting pictures can be seen in Figure 2.1.

PROBE

To measure the visual light field for each light condition, we used a grid of 36 positions in the photographs in three depth layers (see Figure 2.2, left). At each position, a computer-generated rendering of a probe was superposed on the photographed image to assess the perceived light in that position. The probe, similar to the one introduced by Koenderink et al. (2007), is a white matte sphere on a black monopod (the "pole") superimposed on predetermined locations in the image. Observers could control both the direction and

the intensity of a collimated light beam on the sphere and the intensity of the ambient light. The direction was controlled by mouse movements and the intensities by keyboard buttons. In this experiment, the diffuseness was defined as the ratio of collimated and ambient luminances (Xia, Pont, & Heynderickx, 2016b), ranging from fully collimated light (e.g., spotlight) to fully diffuse or Ganzfeld illumination (e.g., as in mist or a snowy field on a cloudy day). The diffuseness could be controlled by adjusting the ratio between the collimated and ambient intensities instead of by an explicit extra parameter, as in Koeanderink et al. (2007). This adjustment simplified the interface and is based on studies into diffuseness characterization (Cuttle, 2003; Xia et al., 2016a, 2016b, 2016c, 2016d).

The poles indicated the probe position in the scene. This method can be safely used to replace the stereoscopic representation of the probe location, because in Koenderink et al. (2007) the stereoscopic representation served solely for defining the probe location. Moreover, on Pont's (2011) poster, the methods of Wijntjes and Pont (2010) were used to test whether the representation of the probe's position using a pole resulted in robust spatial percepts. The relative depth structure was found to be robust up to condition- and observer-dependent depth range scaling. The poles always had to be entirely visible to the observer, which restricted the available space for probe placement (e.g., one probe on the sofa was moved up in order to not occlude the lamp; see Figure 2.2, left). We estimated the probe coordinates in the space of the scene (a) in depth and width by placing the pole end on objects with known positions; (b) in height, by relating to a reference object (photographs of the cubic light meter; see Methods of the section on the physical light field measurements). The sphere size was scaled according to the perspective in the photographs depending on its position (see Figure 2.2, right).

SETUP

The experiment was performed on a high-resolution 15-in. computer screen (2880 x 1800 pixels, Retina Display, luminance range from 0.4 cd/m2 to 330.8 cd/ m2), with software developed using the Psychtoolbox library (Brainard, 1997). The light in the room was switched off. The images and the screen were calibrated linearly; in other words, the

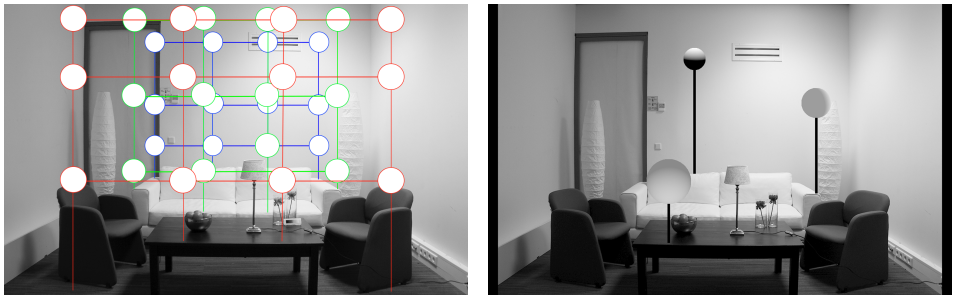

Figure 2.2: Left, all probe positions in the scene. Lines of the same color connect the positions at the same depth and the vertical lines denote the ends of the poles. Right, examples of the probes for each depth. The shading on the probes demonstrates a few possible variations of settings. These are not observers' results.

monitor luminances in the image were linearly related to the original luminances in the scene. The viewing distance of the observer was fixed with a chin rest at 27 cm from the monitor in order to keep the same viewing angle as the camera (62 degrees). Participants

PARTICIPANTS

Ten observers (five men, five women) participated in this experiment. The participants were naive with respect to the setup and purpose of this experiment. All participants had normal or corrected-to-normal vision. They all gave written, informed consent. All experiments were done in agreement with the Declaration of Helsinki, Dutch Law, local ethical guidelines, and approved by the TUDelft Human Research Ethics Committee.

PROCEDURE

Before the start of the experiment, we explained the experiment procedure, the probe, and its controls to the observers. In both training and trial sessions, the task was to set the parameters of the probe's lighting (direction, intensities of directed and ambient light) to make it appear like it fit in the scene. In order to prevent misunderstanding of the position of the probe in the scene, it was explicitly stated that the end of the pole was always standing on a visible object. We then showed photographs of a real white sphere under each light condition and ensured that the participant understood how to control the probe by doing three training trials. The following main part of the experiment consisted of 108 trials, including 36 probe positions for each light condition. We ceded the trial repetitions to be able to test a larger number of probe locations, taking into account that in the Koenderink et al. (2007) experiment, the reproducibility over sessions was stated as "fair" (medians of the quartile deviations over all observers of 5.78 were found for the slant, 4.98 for the tilt, 0.023 for the intensity, which was defined on a range from 0 to 1, and 0.093 for the directedness, which was defined on a range from -1 to 1). The order of the 108 trials was randomized per observer. After the first 54 trials, the observers were given a break. Altogether, the experiment took between 1 and 2 hr, with an average of 1 hr and 20 min. After the experiment, we asked the participants to draw where they thought the light source(s) were positioned on pictures of the three scenes, and to describe the position of the source(s) in words.

2.2.2. RESULTS

SOURCE ESTIMATION

The results of the survey on the inferred light sources positions are presented in Figure 2.3. For the LAMP condition with the visible light source, all observers pointed at the lamp. For the DIFFUSE condition, there was more variation but most of the light sources were "placed" in the upper right part of the ceiling. The observer who pointed a light source on the left part of the picture still stated that it is directed to the right. Another observer positioned the light source above the standing lamp next to the ventilation hole and commented that it is an invisible light source floating next to the wall. Finally, only 4 of 10 observers noticed that there were two light sources in the SPOTLIGHTS condition.

Figure 2.3: Visual light field visualization methods: spheres, arrows, and tubes. For one of the observers, each column illustrates the settings in one of the light conditions: from left to right, LAMP, DIFFUSE, and SPOTLIGHTS. The spheres show the appearance of the adjusted probes per depth plane. The arrows show the adjusted direction of the light pointing in the direction from which the light arrives with the arrows' lengths corresponding to the relative strengths of the directed light. The thickness of the tubes is inversely proportional to the relative strength of the directed light and their direction is locally tangential to the adjusted light direction.

Of the others, three stated that the light source was in the middle of the ceiling, one claimed that there was only one elongated source in the middle, one placed the light source on the right, and one placed it in front of the scene.

LOCAL SETTINGS

For each light parameter and each condition, we evaluated the intersubjective spread in the parameter settings by calculating the medians of the quartile deviations over all observers per point using the same statistics that were used in Koenderink et al.'s (2007) experiment. Overall, the intersubjective spreads in the settings (called spread in the rest of this section) seem to stay within reasonable percentages of the full ranges. The directional settings were decomposed into two angles, polar angle and azimuth. Polar angle indicates an angle perpendicular to the picture plane, varying from 0 degree (frontal illumination from the point of view of the observer) to 180 degrees (backward illumination). Azimuth indicates an angle in the picture plane, varying from 0 degree (right side of the probe illuminated) to 360 degrees, counter-clockwise. For these angles, we used circular statistics. There does not seem to be a strong dependency of polar angle spread on light condition (medians of 11.3 degrees, 14.5 degrees, and 15.0 degrees for LAMP, DIFFUSE, and SPOTLIGHTS, respectively). However, there was a strong dependency of azimuth spread on light condition, increasing from a median of 7.1 degrees in the LAMP light condition to 14.6 degrees in the DIFFUSE condition, and 18.3 degrees in the SPOTLIGHTS condition. Please note that these intersubjective spreads of the probe settings correlate with the apparent spread of the subjective light sources' positions in Figure 2.3.

The photographs were taken with varying exposure times, so there is no meaning in direct comparisons between light intensities of the settings. However, the ratio of the directed and ambient intensity, or the diffuseness, is relative and will be addressed extensively in the comparison of the visual with the physical qualities. The spread of the diffuseness (on a range 0-1) was 0.19 for the LAMP condition, 0.14 for the DIFFUSE condition, and 0.18 for the SPOTLIGHTS condition. Compared to spreads for diffuseness found by others (reviewed in Xia et al., 2016a), these values are typical and also stay

within reasonable percentages of the full range.

Thus, the local settings show rather robust behaviour, allowing comparison of the average structure of the light field over observers with the physical light field (see Comparison of visual and physical light fields section). Now we will address the question whether it is possible to actually do these reconstructions in combination with demonstrating possible ways to visualize them.

2.2.3. RECONSTRUCTION AND VISUALIZATION OF THE VISUAL LIGHT FIELD

Light field visualization is difficult due to the high dimensionality of the data. As the light field is a function of location (x, y, z) and direction (θ, ϕ), we need to project five dimensions into two for its representation in a flat image. The task is even more challenging because flat images inherently contain ambiguities. Mury et al. (2009) demonstrated several methods for visualizations of (certain properties of) the physical light field, such as contour plots of its components' strength distributions, collections of panoramic projections, fields of projected light vectors, and light tubes.

One way to visualize the visual light field is to simply superpose the adjusted probe objects on the scene (see Figure 2.4, top three rows). The white spheres represent the observer's fits in straightforward manner. Using this method, we can get an impression of the settings that is highly visual. This method, unlike others, allows display of the ambient component. However, the direction and diffuseness of the light on a smooth white sphere have been shown to interact perceptually (Pont & Koenderink, 2007). Additionally, such representation is discrete; it needs integration and interpolation to infer the global structure of the visual light field.

The light vector representation (see Figure 2.4, fourth row) consists of arrows depicting adjusted directions and relative intensities of the directed light. These vectors are taken to be the perceptual equivalent of the physical light vector. The directional components are perhaps more clear than in the sphere images, but still it is difficult to see the global structure. The last method we demonstrate is the light tubes visualization method (see Figure 2.4 bottom row; Gershun, 1939; Mury et al., 2009). The light tubes are locally tangential to the light vector and their width is inversely proportional to its strength. One can think about the tube as an enclosure of a part of the light flow: the amount of light passing through the crosssection is constant over the length of the tube. In physical light fields the tubes usually diverge from a light source and end on light absorbing surfaces. Such representations give an impression of the so-called light flow (Cuttle, 1973) through a space at first glance, and concern the global structure of the light field.

We calculated the light tubes for the visual light fields using interpolation of the light vectors parameters (direction, intensity) between neighboring measurement points. In their reconstructions of physical light fields, Mury et al. (2009) started the tubes from the top, since all the light sources were on the ceiling. Our algorithm for the tubes visualization started from the light absorbing surfaces because we had a condition in which the light source was located within the volume of the scene. The recursive algorithm created a matrix of tubes components: points constituting the tube path through the volume plus the tube widths. At initialization, the algorithm calculated the starting co-

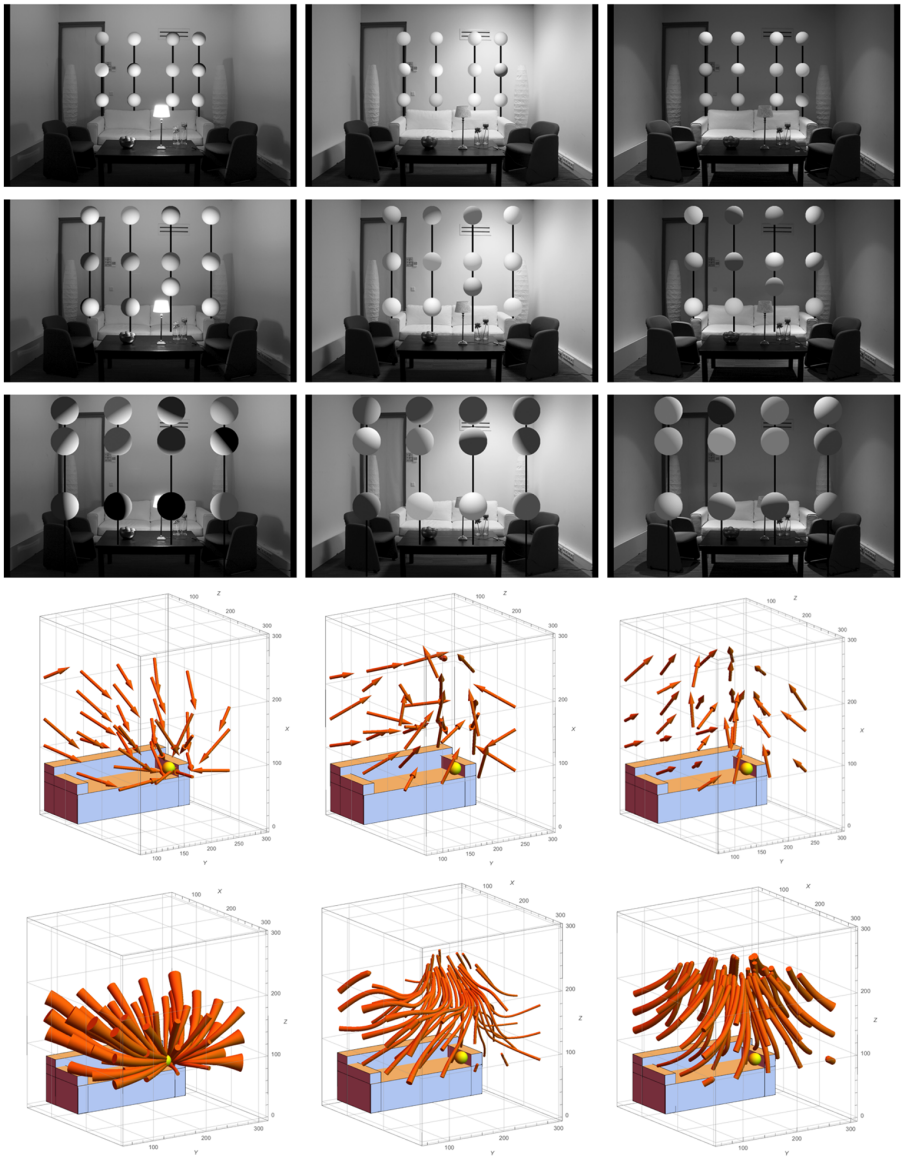

Figure 2.4: Subjective light source(s) position(s), where red dots represent single sources, and color dots represent pairs of sources. The actual positions of the light sources are shown using dotted lines. For (A) LAMP, all observers pointed at the lamp; for (B) DIFFUSE, the points were more spread out; and for (C) SPOTLIGHTS, most observers drew single sources, red dots and a transparent line for a single elongated source. The source next to the table lamp "is standing in front of the scene." Four observers drew a pair of sources.

ordinates such that the tubes origins were evenly distributed over the outer bounds of the visualization volume. The tubes' initial widths and light vector directions were then interpolated from these coordinates using linear interpolation functions for the visualized light condition (Mury et al., 2009). For each tube, the algorithm made a step in the interpolated light vector direction on the next iterations. The stopping condition for each tube was either reaching the predefined limit of steps, the tube leaving the volume of the scene, or the tube fluctuating in a small area (which would mean that the tube reached a light source in the visualized volume). The initial width, number of steps, and number of tubes were adjusted manually to optimize the imaged light flow and avoid cluttering.

It is important to note that the light fields presented in Figure 2.4 are examples of the individual visual light fields. We provided visualizations of all individual visual light fields in the supplementary material with the original paper (https://jov.arvojournals.org/ article.aspx?articleid=2545818) . Although the intersubjective angular spreads were quite small (see subsection Local settings above), some of the reconstructed individual visual light fields for the DIFFUSE and SPOTLIGHTS look quite different. This is probably due to global differences in the settings, which have a minor influence on the intersubjective spreads because those were based on local settings, but clearly change the overall reconstruction's appearance. We found that our experimental method provides sufficiently robust data to reconstruct the individual visual light fields for our scenes. Mury et al. (2009) tested how good their reconstructions were by comparing several interpolated values in between initially measured points with extra measurements at those points, concluding that, although the local values were not exactly identical, the global structure could be measured robustly. In order to avoid increasing the number of measurements, we used the existing points only. First, we excluded a point from the grid, then ran the interpolation on this grid, and finally calculated the angular and intensity differences between the excluded point values (measured vector) and interpolated ones (approximated vector on the basis of the other points of the grid). We repeated this for each point in each individual light field reconstruction and found that the median values for the angular differences were fairly small, 19, 23, and 23 degrees for LAMP, DIFFUSE,

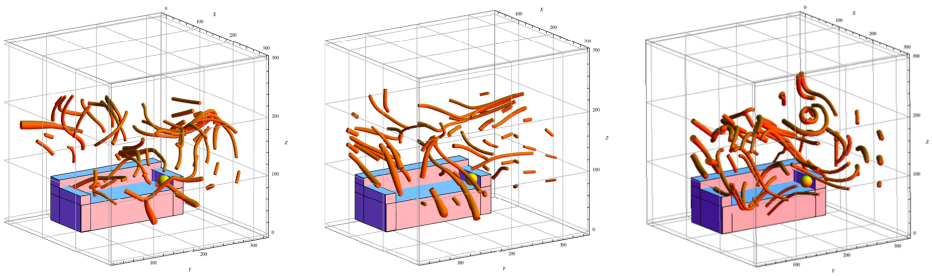

Figure 2.5: Examples of tubes created on the basis of randomly oriented vectors, which we made in order to check how coherent the interpolated flow patterns would be for locally random settings. It is obvious that these light flows do not represent a coherent "field."

and SPOTLIGHTS conditions, respectively.

We also ran the light flow reconstruction algorithm using randomly directed vectors with randomly appointed intensities. The angular differences were then found to be around 908 after running the algorithm on 100 sets of random vectors. To obtain the difference in intensities, we took the median of the absolute difference between the values, and it constituted 0.15, 0.12, 0.13, and 0.28 for LAMP, DIFFUSE, SPOTLIGHTS, and random conditions, respectively. To illustrate the contrast between the visual light fields and the models based on random values, Figure 2.5 presents examples of the outcome when running the interpolation and visualization algorithm on sets of random vectors. We can see that the reconstruction method breaks down for random data. Thus, our reconstructions of the global visual light field do represent its structure and are not an artifact of the interpolation method.

2.3. THE PHYSICAL LIGHT FIELD

2.3.1. MEASUREMENTS

In order to compare the visual light fields with the corresponding physical light fields, we first had to reconstruct the global structure of the physical light fields for the same scene and light conditions as in the psychophysical experiment. Mury et al. (2009) captured physical light fields for the same light lab as we used, though it was empty at that time. They measured over a grid of 3x5x3 points with a step size of 1 m using a plenopter, a custom-made illuminance meter with 12 measuring heads, to be able to reconstruct the light field up to its second order spherical harmonics representation, which can be described by nine coefficients, making the 12 measured values sufficient for its estimation. We took this approach and tuned it to our purposes.

The measurements were done over 49 points: a grid of three in height, five in width and three in depth of the scene, and four additional points (Figure 2.6, left). Unfortunately, the furniture disposition in the scene did not allow making the grid perfectly regular. The positions of the measurements can be seen in Figure 2.7. The heights of the measurements were 80, 145, and 210 cm, except for the lowest row behind the sofa, which was measured at the height of 122 cm. The heights of the four additional points are all 145 cm.

In our study we limited ourselves to the ambient and light vector components, which correspond to the zero and first order components in the spherical harmonics representation. Consequently, we did not need 12 measurements at each position as Mury et al. (2009) needed to include the second order spherical harmonics, so a substantially lower number of measurements were included, which were just enough to be able to estimate the four coefficients describing the zero and first order spherical harmonics representation. A cube was the closest approximation of a sphere having a regular shape with four or more faces.

We used a custom-made device (for details, see Xia et al., 2016b) for cubic illuminance measurements (Cuttle, 2013) on the basis of a Konica Minolta T- 10MA illumi-

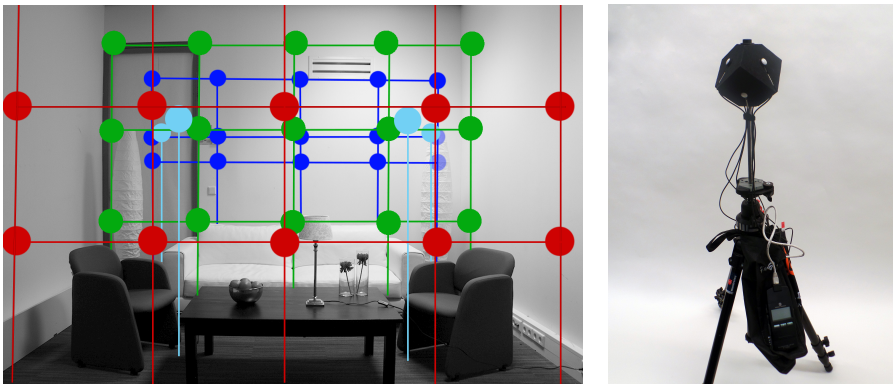

Figure 2.6: Left, scheme of measurement positions for the physical light measurements. Colored lines connect measurement positions at the same depth and denote where the cubical light meter was standing. The top row of the closest measurements is above the field of view of the camera. Right, cubic meter.

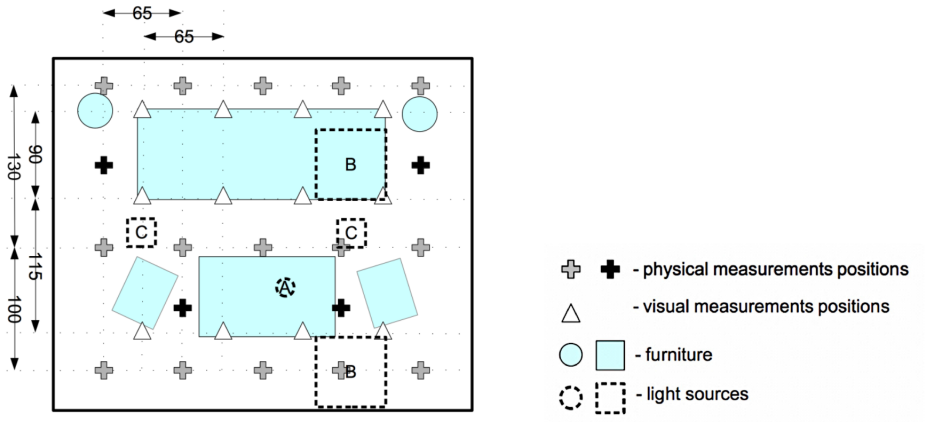

Figure 2.7: Scene scheme. Blue rectangles and circles define furniture positions; gray crosses represent the physical measurement positions and black crosses show four additional measurement positions. Triangles represent the psychophysical measurement positions, and dashed shapes define the light sources positions: A — lamp on the table, B — diffused light sources in the ceiling, and C — directed light sources in the ceiling.

nance meter (Konica Minolta, Inc., Tokyo, Japan), plus extra heads (Figure 2.6 , right). The main part of the device is a cube, covered by black velvety paper, with a sensor on each surface. The cube was fixed on a stick and tilted such that its long corner-to-corner diagonal was vertical, and the stick was fixed on a tripod. Our construction allowed the lowest measurement to be 50 cm from the ground and the highest about 2.5 m. On the top of the cube there was a bubble level and on the tripod there were protractors, which allowed adjusting the cube orientation horizontally. All six sensors were connected to a laptop through the luminance meter's main body. In this way, we could make simultaneous illuminance measurements from all six sensors. Following Cuttle's (2013) procedure,

we could then derive the local light field parameters from these six records and finally reconstruct the global structure of the light field by interpolation. The cubic illuminance measurements satisfied us in almost all respects. Yet, for one point close to the light source in the LAMP light condition, the resulting vector did not point to the lamp, due to known limitations of the cubic measurements whenever individual sensors record (close to) zero illuminance, as discussed by Xia et al. (2016b). This point was excluded from the analysis.

The procedure of the measurements was the following: set the tripod to the position, check the orientation of the cube, then make measurement and photograph (for reference) for each light condition. The minimum values of the sensors measurements were 3.97, 45.4, and 19.22 lux and the maximum values were 173.9, 2040, and 1493 lux for LAMP, DIFFUSE, and SPOTLIGHTS conditions, respectively.

2.3.2. DATA PROCESSING AND VISUALIZATION

The resulting measurement data constituted the six measurements per position and light condition. We translated the measurements to light vectors (a) via the method introduced by Cuttle (2013) and (b) via spherical harmonics approximations as introduced by Mury et al. (2007, 2009). These two methods are based on the same concepts, but framed within different mathematical approaches. In Xia et al. (2016b) an extensive comparison of these two methods is given, which leads to the conclusion that they give very similar results under natural circumstances.

Cuttle's (2013) method has a straightforward approach. The components of the resulting light vector are calculated by subtraction of the measurements of opposing faces, and rotation of the results to align with standard axes, taking into account that, initially, measurements were done with a tilted cube (see above).

In a spherical harmonics representation of the light field, the zero order component corresponds to the ambient component of the light (Cuttle's "density of light") and the first order component to the light vector. In order to calculate the coefficients, we used the system of equations proposed by Mury et al. (2009) and adapted it for 6 measurements instead of 12, since we were interested in the zero and first orders only. To use this system we had to define the sensitivity profile of the sensors, which we retrieved from the documentation of the sensors. The difference between the resulting vectors from the two methods was negligible so we used Cuttle's (2013) method for the calculations.

We applied the same interpolation and visualization algorithm for the physical light fields as for the visual light fields (see the section, Reconstruction and visualization of the visual light field). Diffuseness was calculated according to Cuttle's (2003, 2013) method using a cubic illuminance meter:

$$\mathbf{E}_{(x)} = \mathbf{E}_{x+} - \mathbf{E}_{x-} \tag{2.1}$$

$$|\mathbf{E}| = \sqrt{\mathbf{E}_{(x)}^2 + \mathbf{E}_{(y)}^2 + \mathbf{E}_{(z)}^2} \tag{2.2}$$

$$\sim E_X = \frac{\mathbf{E}_{x+} + \mathbf{E}_{x-} - |\mathbf{E}_{(x)}|}{2} \tag{2.3}$$

$$\sim E = \frac{\sim E_X + \sim E_Y + \sim E_Z}{3} \tag{2.4}$$

$$E_{scalar} = \frac{|\mathbf{E}|}{4} + \sim E \tag{2.5}$$

$$D = 1 - \frac{|\mathbf{E}|}{4E_{scalar}} \tag{2.6}$$

$\mathbf{E}_{x+}$, $\mathbf{E}_{x-}$ are the measurements in the positive and negative directions along the X axis (analogous for Y and Z). $\mathbf{E}_{(x)}$ is the light vector component (analogous for $\mathbf{E}_{(y)}$ and $\mathbf{E}_{(z)}$). $\mathbf{E}_{(x)}$, $\mathbf{E}_{(y)}$ and $\mathbf{E}_{(z)}$ constitute the light direction. $|\mathbf{E}|$ is the light vector magnitude.
$\sim$ E is the symmetric illuminance. E_{scalar} is the scalar illuminance or the mean illuminance in a point, which we took as measure of light intensity. The diffuseness D ranges from 0 (fully collimated light) to 1 (fully diffuse light).

2.4. COMPARISON OF VISUAL AND PHYSICAL LIGHT FIELDS

As was already stated, light fields have a complex structure, which makes the visualization, but also the quantitative analysis, difficult. To compare the light fields we chose to analyze the light vectors' directions first. Figure 2.8(a), top row, shows three-dimensional illustrations of the physical and observers' averaged vectors in the LAMP, DIFFUSE, and SPOTLIGHTS conditions. We analyzed these data by calculating for each position, observer, and light condition the angular difference between the visual and physical light vectors in three dimensions, as well as between their projections on the picture plane. We took into account the projected vectors comparisons (two-dimensional; i.e., taking into account the azimuthal angle settings and neglecting the polar angle settings) because polar angle settings of lighting on a sphere were proven to suffer from the bas-relief ambiguity (Belhumeur, Kriegman, & Yuille, 1999; Koenderink, van Doorn, Kappers, te Pas, & Pont, 2003; Koenderink et al., 2007).

The resulting angular differences for all positions and all observers were summarized in smoothed histograms (see Figure 2.8(b)). First, we took the unsigned differences of the observers' settings and the physical measurements results (PHYSICAL vs. OBSERVER). For each light condition, the two-dimensional results showed a maximum around 108 difference, which is rather small for this probing method but typical for azimuth settings in illuminance flow inferences (Koenderink et al., 2007;Xia et al., 2016d). The distributions are broad, however, resulting in medians of 54, 22, and 35 degrees. The three-dimensional results had maxima, as expected, at higher angular differences, namely between 40 and 60 degrees, and medians of 52, 42, and 47 degrees. Next, we used the same approach to compare the observers' settings and a model (SRC POINTERS vs. OBSERVER), based on the physical light source positions. The SRC POINTERS model

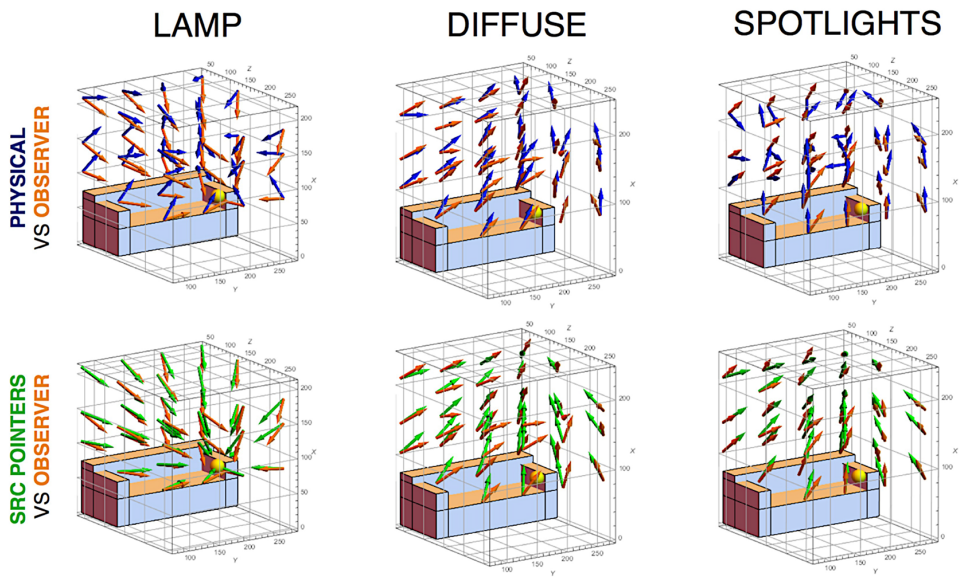

(a)

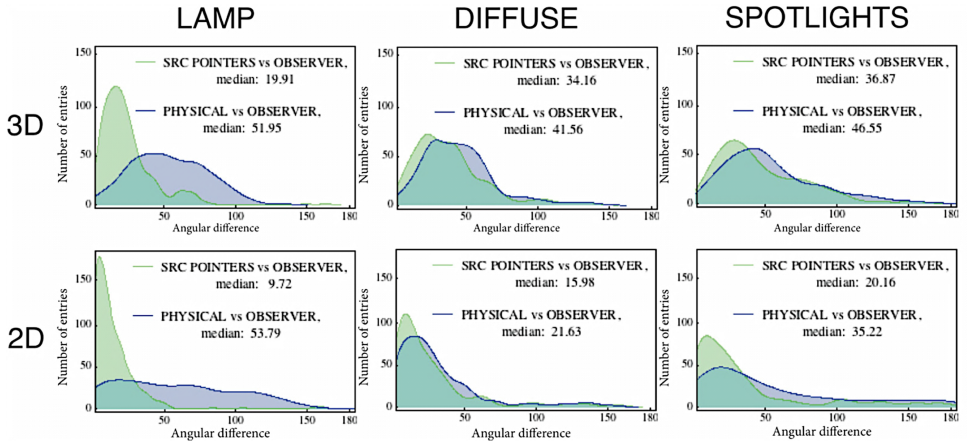

(b)

Figure 2.8: Light direction comparisons. (a) Three-dimensional illustrations of (normalized) light vectors for each light condition, with the blue arrows representing the PHYSICAL vectors, the orange representing (averaged) OBSERVER vectors, and green the SRC POINTERS vectors. (b) Histograms of angular differences between physical light vectors and observers' directional components (PHYSICAL vs. OBSERVER — blue histograms), and between vectors pointing at the subjective light sources and observers' directional components (SRC POINTERS vs. OBSERVER — green histograms) in three-dimensional representations (top row) and two-dimensional representations (bottom row).

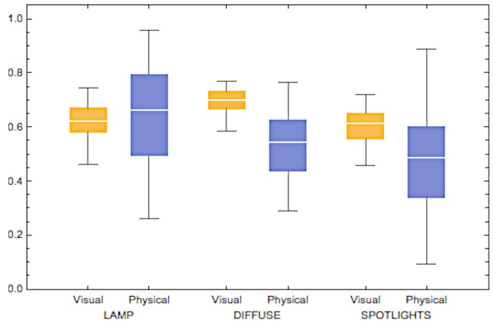

Figure 2.9: Box-and-whisker chart of normalized visual and physical light diffuseness as a function of light condition, ranging between 0 (fully collimated) and 1 (fully diffused light). The boxes represent the range between 25% and 75% (first and third quartile) and the bars represent the full range.

represents essentially a simple divergent field, which would occur if observers would be simply pointing to light sources, and in physics, if there would be a light source in empty space. We obtained the positions of the light sources from the scene measurements for each light condition and pointed all the vectors to these positions (see Figure 2.8(a), second row). For the DIFFUSE and SPOTLIGHTS conditions with two light sources, the directions of the vectors were calculated using linear superposition and the inverse square law of the distances to the sources. The histograms of comparisons between the observers' settings and the SRC POINTERS model moved noticeably to lower values, with respect to those for the PHYSICAL vs. OBSERVER histograms, resulting in lower medians for all three lighting conditions: 108, 168, and 208 for the two-dimensional analysis and 20, 34, and 37 degrees for the three-dimensional analysis. Pairwise Kolmogorov-Smirnov tests on the cumulative raw data confirmed this shift by showing that the shapes of the PHYSICAL vs. OBSERVER histograms are significantly different from the SRC POINTERS vs. OBSERVER for all two-dimensional and three- dimensional comparisons (for p = 0.05). Thus, human observers' settings were closer to the predictions of the diverging field models than to the physical values.

In Figure 2.9 we show the averaged data for the diffuseness values. Perhaps surprisingly, the spreads of the diffuseness settings of the observers were always smaller than the spreads of the physical diffuseness values. The overall means were different for physical and visual light fields. Specifically, human observers considered the DIFFUSE light condition the most diffuse (as did the authors, judging on the visual appearance), whereas physically the overall most diffuse condition turned out to be the LAMP condition. The ranges of the diffuseness values showed the same relation between conditions: for both physical and perceptual measurements, the DIFFUSE condition showed the smallest range, and the SPOTLIGHTS condition showed the biggest range.

We present the three-dimensional visualizations of the physical light fields and (averaged between observers) visual light fields in Figure 2.10. The physical light field for the LAMP light condition shows curved tubes at the top, due to the scattering of the light from the ceiling and inter-reflections in the corners. Towards the back of the scene, the

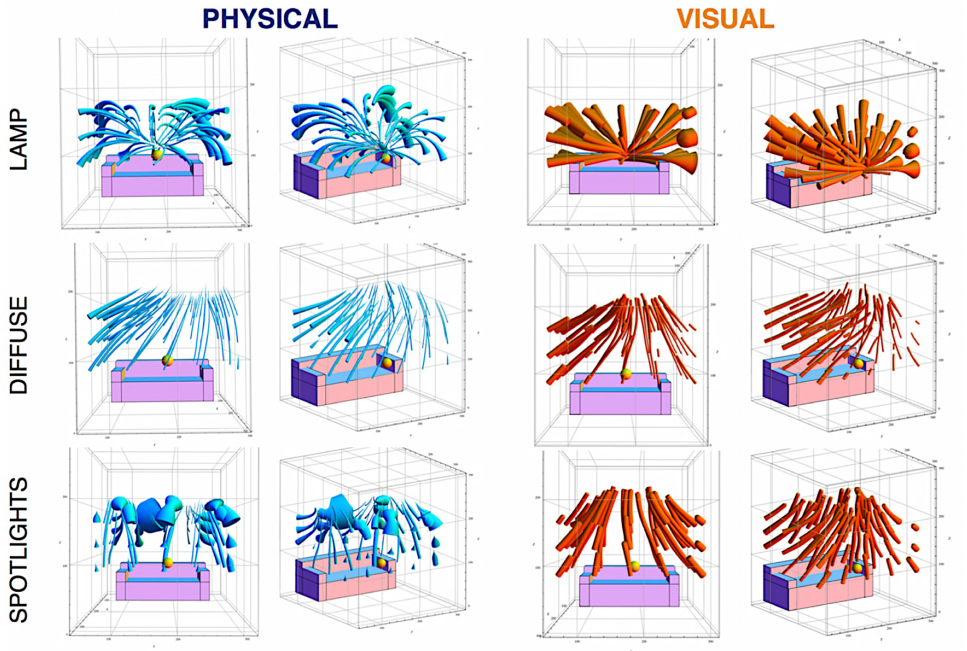

Figure 2.10: Physical and visual light fields. Blue shows reconstructions via light tubes of the physical measurements and orange shows reconstructions of the averaged observers' settings. Two different perspectives are shown for each condition.

light is more diffuse due to reflections from the ceiling and walls and dimmer because of the distance to the lamp. This causes a change of direction over the tube's length and thus, its curvy shape. None of the observers took these changes in the local average light direction into account for the LAMP condition, so their averaged settings form rather straight tubes diverging away from the light. The results of the physical and visual light field reconstructions were found to be most similar for the DIFFUSE light condition: the tubes seem to have the same origin, in the top left part of the ceiling, and spread out from there. In this condition, the physical tubes are also rather straight. In the SPOTLIGHTS condition, the physical reconstructions show slim, almost vertical, tubes under the lamps, where the light is highly directed. In other parts of the scene, the light is primarily due to scattering, causing the tubes to be thick and odd-shaped. The visual light field for this light condition shows tubes converging to the ceiling, and no odd-shaped tubes.

2.5. DISCUSSION

Measuring visual light fields is a novel technique that reveals how human observers make inferences about the structure of the physical light field. We developed this method by merging existing approaches of measuring the physical light field (Mury et al., 2009)

and the local visual light field (Koenderink et al., 2007). We have shown that the data obtained by this method is sufficient to reconstruct and visualize individual visual light fields. In addition to the psychophysical measurements, we did physical measurements and compared the visual and physical light fields for three light conditions.

The goal of this study was to examine the structure of the visual light field. One way to assess it is to make multiple local measurements and interpolate them in order to provide values of the light properties in an arbitrary point within the measured volume. For the local measurements we used Koenderink et al.'s (2007) method of visual fit for illumination probing, which proved its reliability already in their and others' studies (Pont & Koenderink, 2007; Pont et al., 2010; Xia et al., 2014). Additionally, we took into account that Mury et al. (2009) demonstrated that the grid of 45 (3 x 5 x 3) points was sufficient to reconstruct a physical light field in the light lab where we also did our measurements. We did our measurements in only part (about half) of the room, but with a similar number of measurement points in the grid, so that the sampling density was about a factor of two higher. This was done because the living room scene is more complex than Mury et al.'s (2009) empty room.

Our first result was the finding that observers' settings on a probe are indeed reliable enough to reconstruct the visual light field for real scenes. In Koenderink et al.'s (2007) experiment, quartile deviations between repetitions were within 48 and 128 for the polar angle ("slant" in their terms) and 1.68 and 138 for azimuth ("tilt"). Since we did not do repetitions of trials, it is not possible to make direct comparisons of the spreads with their study. Additionally, it was stated that all observers reproduced azimuth (tilt) within 58 and 108, which is more accurate than our results. We connect it to the fact that the light fields in our experiment were more complex than theirs. The striking difference between the interpolations of the visual measurements (Figures 2.4 and 2.10) and of the random vector grids (Figure 2.5) demonstrates that the data was regular enough to reconstruct visual light fields.

We discovered that the structure of the visual light field can be quite different from the physical one. The analysis of the light flows (see illustration via light tubes in Figure 2.10) shows that the participants' settings seem to grasp the basic structure of the physical light field and converge at light sources, but ignore subtle changes due to (inter)reflections. Van Doorn, Koenderink, and Wagemans (2011) and van Doorn et al. (2012) revealed that human observers are able to infer convergent and divergent two-dimensional light flows but not more complex ones, such as rotational and deformation two- dimensional flows. Our findings confirm their conclu- sions also for three-dimensional global structures of light fields. More specifically, the observers' results correlated better with the models containing almost straight tubes diverging out from the sources, than with the physical, more complicated truth. This was particularly evident in the LAMP condition with its strong reflections from the ceiling and walls. Figure 2.3 shows that observers were actually not able to infer where the sources were unless the lamp was visible. Altogether, these results suggest that what the observers do is far from "inverse optics" and that instead, a diverging field is a template for the visual light field.

An important remaining question is: is the inferred global visual light field something that is represented perceptually? In other words, do observers only make local

settings on the basis of object appearance and are the reconstructed visual fields mere mathematical inferences by the authors, or do the observers have a fairly good internal representation of the light field? The consistencies within and between the findings in Koenderink et al. (2007), van Doorn et al., (2011, 2012), Schirillo (2013), and our study perhaps suggest that observers have such representations, though they concern strongly simplified (convergent/divergent light flow structures with fairly straight flow lines/tubes) compared to natural light flows. However, further research is needed to provide conclusive research on the internal representation of the luminous environment.

Our results revealed some dependencies of the visual light field on the features of the scenes, which is especially apparent in the similarities between the settings on the spheres and light location estimates. Specifically, in the scene with a single visible light source in the image, the LAMP condition, the observers seemed to simply have pointed at the source both in the probe settings and in the light source position estimations. For this condition, the settings on the spheres showed the highest consistency between subjects. In the DIFFUSE light condition, the light source was not visible but the physical light field had a relatively simple structure and observers inferred it fairly well. In the SPOTLIGHTS condition, both the settings on the probe and the source estimations were the least consistent overall. The dependencies between the complexity of the stimulus scene and lighting need further investigation. The approach demonstrated in this paper could be used in studies answering questions such as whether perception of the luminous environment is dependent on the scene being empty or full of objects, and how different scene geometries and materials affect the structure of the perceived light field. On the basis of earlier results — plus the basic fact that the optical structure entering the eye confounds geometry, material, and light — we expect interactions between shape/space, material, and light perception (Anderson, 2011; Fleming, 2014; Pont & te Pas, 2006; Zhang, de Ridder, & Pont, 2015).

Currently there is a rise of interest into the topic of light diffuseness (Koenderink et al., 2007; Pont et al., 2010; Morgenstern et al., 2014; Xia et al., 2014, 2015, 2016a, 2016b). As expected on the basis of these studies, we found that the physical diffuseness varied in a much wider range over the scenes than the visual diffuseness. In the LAMP light condition, a lampshade scattered the light in all directions except for the light exiting in the direction of the ceiling. The white ceiling and walls function as big diffusers. In the DIFFUSE light condition, the light sources themselves are rather diffuse, but they were directed downward to the dark floor, which functioned as a light absorber. This result, namely that the scene with physically the most diffuse light turned out not to be the DIFFUSE condition as the authors and observers thought but, instead, the LAMP condition, is perhaps surprising. The resultant light (field) is thus determined by the relation between the light source positions and the scene geometry and materials, and not primarily by the illuminants. Koenderink and van Doorn (1983), Mury et al. (2007), and Xia et al. (2016d) confirm and give insights into such optical mechanisms.

We found that human observers have a robust impression of the light field that is simplified with respect to the physical light field and that corresponds rather well with a model based on simple divergent fields from the light sources. These results have high practical interest. For example, the understanding of observers' inferences of light

propagation through spaces can be used in lighting design for architecture or computer graphics. Moreover, the experiment setup itself might be used as a tool for visual light probing, exempting a designer or other lighting professional from physical measurements, if he or she is only interested in perceived light qualities. The method allows us to obtain the spatial structure of a visual light field from a single experimental session. Having such a tool, it is possible to construct the inferences that observers make about the light propagation through a scene and the variation of its qualities along the flow. We think that this fast and cheap tool has a big potential in perception studies, lighting, and computer graphics industries.

2.6. CONCLUSIONS

In this study, we focused on the global structure of the visual light field. Our main questions were whether the global visual light field can be measured, and if so, how similar it is to the physical light field. Our method for constructing the visual light field and its visualization via interpolation of regularized local measurements is shown to be robust even for individual light fields. Additionally, our comparisons of the visual and physical measurements results suggest that human observers have consistent impressions of the light field, though not exactly corresponding to the physical truth; specifically, they tend to neglect subtle spatial variations in the physical light fields.

BIBLIOGRAPHY

Adelson, E., & Bergen, J. (1991). The plenoptic function and the elements of early vision. In M. Landy & J. A. Movshon (Eds.), Computational models of visual processing (pp. 3—20). Cambridge, MA: MIT Press.

Anderson, B. L. (2011). Visual perception of materials and surfaces. Current Biology, 21, R978—R983.

Belhumeur, P. N., Kriegman, D. J., & Yuille, A. L. (1999). The bas-relief ambiguity. International Journal of Computer Vision, 35, 33—44.

Berbaum, K., Bever, T., & Chung, C. S. (1983). Light source position in the perception of object shape. Perception, 12, 411—416.

Boyce, P. (1981). Human factors in lighting. London, UK: Applied Science Publishers. Brainard, D. H. (1997). The psychophysics toolbox. Spatial Vision, 10, 433—436.

Cuttle, C., & Ilium, M. (1973). The sharpness and the flow of light. In R. Kuller (Ed.), Architectural psychology. Proceedings of the conference held at Lund University (pp. 12—22). Lund, Sweden: Lund University.

Cuttle, C. (2003). Lighting by design. Oxford, UK: Architectural Press.

Cuttle, C. (2013). Research note: A practical approach to cubic illuminance measurement. Lighting Re- search & Technology, 46(1), 31—34.

Doerschner, K., Boyaci, H., & Maloney, L. T. (2007). Testing limits on matte surface color perception in three-dimensional scenes with complex light fields. Vision Research, 47, 3409—3423.

Dror, R. O., Willsky, A. S., & Adelson, E. H. (2004). Statistical characterization of real-world illumina- tion. Journal of Vision, 4(9):11, 821—837, doi:10. 1167/4.9.11.

Fleming, R. W., Dror, R. O., & Adelson, E. H. (2003). Real-world illumination and the perception of surface reflectance properties. Journal of Vision, 3(5):3, 347—368, doi:10.1167/3.5.3.

Fleming, R. W. (2014). Visual perception of materials and their properties. Vision Research, 94, 62—75.

Ganslandt, R., & Hofmann, H. (1992). Handbook of lighting design. Ludenscheid, Germany: Vieweg, ERCO Edition.

Gerhard, H., & Maloney, L. (2010). Estimating changes in lighting direction in binocularly viewed three-dimensional scenes. Journal of Vision, 10(9): 14, 1—22, doi:10.1167/10.9.14.

Gershun, A. (1939). The light field [Translated by P. Moon & G. Timoshenko]. Journal of Mathematics and Physics, 18, 51—151.

Gilchrist, A. L., & Radonjic, A. (2009). Functional frameworks of illumination revealed by probe disk technique. Journal of Vision, 10(5):6, 1—12, doi:10. 1167/10.5.6.

Ho, Y.-X., Landy, M. S., & Maloney, L. T. (2006). How direction of illumination affects visually perceived surface roughness. Journal of Vision, 6(5): 8, 634—648, doi:10.1167/6.5.8.

Hunter, F., Biver, S., & Fuqua, P. (2007). Light science and magic. Oxford, UK: Elsevier.

Koenderink, J. J., Pont, S. C., van Doorn, A. J., Kappers, A. M. L., & Todd, J. T. (2007). The visual light field. Perception, 36, 1595—1610. doi:10.1068/ p5672.

Koenderink, J. J., & van Doorn, A. J. (1983). Geometrical modes as a general method to treat diffuse interreflections in radiometry. Journal of the Optical Society of America, 73, 843—850.

Koenderink, J. J., & van Doorn, A. J. (2006). Shape from shading. In N. Paragios, Y. Chen, & O. D. Faugeras (Eds.), Handbook of mathematical models in computer vision (pp. 375—388). New York: Springer US.

Koenderink, J. J., van Doorn, A. J., Kappers, A. M. L., te Pas, S. F., & Pont, S. C. (2003). Illumination direction from texture shading. Journal of the Optical Society of America A, Optics, Image Science, and Vision, 20, 987—995.

Madsen, M. (2007). Light-zones(s): As concept and tool. ARCC Journal, 4(1), 50—59.

Maloney, L. T., Gerhard, H. E., Boyaci, H., & Doerschner, K. (2010). Surface color perception and light field estimation in 3D scenes. In L. Harris & M. Jenkin (Eds.), Vision in 3D environments (pp. 65—88). New York: Cambridge University Press.

Marlow, P. J., Kim, J., & Anderson, B. L. (2012). The perception and misperception of specular surface reflectance. Current Biology, 22, 1909—1913. doi:10. 1016/j.cub.2012.08.009.
Moon, P., & Spencer, D. E. (1981). The photic field. Cambridge, MA: MIT Press.

Morgenstern, Y., Geisler, W. S., & Murray, R. F. (2014). Human vision is attuned to the diffuseness of natural light. Journal of Vision, 14(9):15, 1—18, doi:10.1167/14.9.15.

Mury, A., Pont, S. C., & Koenderink, J. J. (2007). Light field constancy within natural scenes. Applied Optics, 46, 7308—7316.

Mury, A., Pont, S. C., & Koenderink, J. J. (2009). Representing the light field in finite three-dimen- sional spaces from sparse discrete samples. Applied Optics, 48, 450—457.

O'Shea, J., Agrawala, M., & Banks, M. S. (2010). The influence of shape cues on the perception of lighting direction. Journal of Vision, 10(12):21, 1—21, doi:10. 1167/10.12.21.

Ostrovsky, Y., Cavanagh, P., & Sinha, P. (2005). Perceiving illumination inconsistencies in scenes. Perception, 34, 1301—1314. doi:10.1068/p5418.

Pentland, A. P. (1982). Finding the illuminant direc- tion. Journal of Optical Society of America, 72(4), 448—455.

Pont, S. (2011). An ecologically valid description of the light field. Journal of Vision, 11(11):, 345, doi:10. 1167/11.11.345. [Abstract]

Pont, S. C. (2013). Spatial and form-giving qualities of light. Handbook of Experimental Phenomenology: Visual Perception of Shape, Space, and Appearance (pp. 205—222). New York: Wiley.

Pont, S. C., & Koenderink, J. J. (2007). Matching illumination of solid objects. Perception & Psycho- physics, 69, 459—468.

Pont, S. C., & te Pas, S. F. (2006). Material— Illumination ambiguities and the perception of solid objects. Perception, 35, 1331—1350.

Pont, S. C., van Doorn, A., de Ridder, H., & Koenderink, J. J. (2010). The visual light field in the in- and outside. Perception, 39, ECVP Abstract Supplement, 104.

Schirillo, J. A. (2013). We infer light in space. Psychonomic Bulletin & Review, 20, 905—915. doi: 10.3758/s13423-013-0408-1.

van Doorn, A. J., Koenderink, J. J., Todd, J. T., & Wagemans, J. (2012). Awareness of the light field: The case of deformation. I-Perception, 3, 467—480.

van Doorn, A. J., Koenderink, J. J., & Wagemans, J. (2011). Light fields and shape from shading. Journal of Vision, 11(3):21, 1—21, doi:10.1167/11.3. 21.

Wijntjes, M. W. A., & Pont, S. C. (2010). Pointing in pictorial space: Quantifying the perceived relative depth structure in mono and stereo images of natural scenes. ACM Transactions on Applied Perception, 7(4), 1—8.

Xia, L., Pont, S. C., & Heynderickx, I. (2014). The visual light field in real scenes. i-Perception, 5(7), 613—629. doi:10.1068/i0654.

Xia, L., Pont, S. C., & Heynderickx, I. (2015). Simultaneous measurement and visualization of light flow and diffuseness in 3D spaces. Proceedings of 28th CIE Session (pp. 556— 563). City, ST: Publisher.

Xia, L., Pont, S. C., & Heynderickx, I. (2016a). Light diffuseness metric Part 1: Theory. Lighting Research & Technology.

Xia, L., Pont, S. C., & Heynderickx, I. (2016b). Light diffuseness metric Part 2: describing measuring and visualizing the light flow and diffuseness in 3D spaces. Lighting Research & Technology.

Xia, L., Pont, S. C., & Heynderickx, I. (2016c). Probing the sensitivity of observers for light qualities in real scenes. Manuscript in preparation.

Xia, L., Pont, S. C., & Heynderickx, I. (2016d). Effects of scene content and layout on the perceived light direction in 3D spaces. Manuscript in preparation.

Yamauchi, R., Ikeda, M., & Shinoda, H. (2003). Walls surrounding a space work more efficiently construct a recognized visual space of illumination than do scattered objects. Optical Review, 10, 166— 173.

Zhang, F., de Ridder, H., & Pont, S. C. (2015). The influence of lighting on visual perception of material qualities. In Proceedings of SPIE 9394, Human Vision and Electronic Imaging XX, 93940Q, doi:10.1117/12.2085021.

3

The Visual Light Field in Paintings

Abstract

The aim of this study was to investigate whether inferences of light in the empty space of a painting and on objects in that painting are congruent with each other. We conducted an experiment in which we tested the perception of light qualities (direction, intensity of directed and ambient components) for two conditions: a) for a position in empty space in a painting and b) on the convex object that was replaced by the probe in the first condition. We found that the consistency of directional settings both between conditions and within paintings is highly dependent on painting content, specifically on the number of qualitatively different light zones (Madsen, 2007) in a scene. For uniform lighting observers are very consistent, but when there are two or more light zones present in a painting the individual differences become prominent. We discuss several possible explanations of such results, the most plausible of which is that human observers are blind to complex features of a light field (van Doorn et al., 2012).

Published as: Kartashova, T., de Ridder, H., te Pas, S. F., Schoemaker, M., & Pont, S. C. (2015). The visual light field in paintings of Museum Prinsenhof: comparing settings in empty space and on objects. Proceedings of SPIE 9394, Human Vision and Electronic Imaging XX, 9394, 93941M.

3.1. INTRODUCTION

To convey an image, a painting does not have to be photorealistic. However, such a straightforward approach captures a scene closest to an original. Lighting in natural environments is demonstrated to be rather constant (Mury et al., 2007), so in order to fit "the original", lighting consistency within objects of a pictured scene should be one of the biggest concerns of an artist. Therefore, artists probably were the first explorers of light qualities. Passing successful techniques from generation to generation, they achieved splendid results. This drove our attention to lighting in paintings: faithful at first glance, is it accurate and consistent in details? Wijntjes and de Ridder (2014) have already approached the topic with his study of objects' shadows and shading in Canaletto paintings, in which he points out that the artist probably rendered the shading inconsistently with the shadowing. In our research we shift the focus from object lighting to a comparison between local and global light structure in paintings.

One of the first systematical study on light structure was performed by Gershun (1939). He described the light field as the radiance arriving at a point (x,y,z) from all directions. Adelson & Bergen (1991) extended Gershun's physicomathematical description into the psychophysical domain, introducing the plenoptic function, which specifies the structure of light as a function of position, time, wavelength and parallax; and suggested a systematical approach for exploration of human sensitivity to its elemental properties. In recent experimental psychology papers Koenderink et al. (2007) demonstrated that human observers are sensitive to various parameters of the physical light field and Schirillo (2013) summarized previous studies and concluded that humans infer light in empty space. Certainly, that space is not completely empty — it is a space between reference objects. The perception of light in space also forms the basis of lighting design (Cuttle, 2010; Frandsen, 1987). Practical insights from lighting professionals refer to this issue. We cite from conversations: "light is about light, not about lamps".

As was said, objects are needed to scatter light and we usually infer the light in space from the scattering by objects instead of looking at sources directly. There are multiple studies on objects' lighting (Pont et al, 2007), mostly focusing on objects' surfaces properties (Fleming et al., 2003; Maloney et al., 2010). However, we did not encounter any comparisons between lighting in empty space and on objects. It is interesting to study whether light inferences in empty space and on objects are congruent with each other. This interest, combined with an interest in how we see (and can learn to see) the light in the paintings of the "Masters in innovation" department of museum Prinsenhof resulted

in the experiment that we describe in this paper.

Intending to investigate light perception in empty space and on objects, we made measurements in two conditions: by putting a light probe in a position in empty space and by putting a probe next to an object cutout from that space. Therefore, we selected paintings that fulfilled two requirements: they represented realistic paintings of spatial scenes and they contained multiple volumetric objects, which could be replaced and compared to a probe. The observers' task was either to set the light on a probe as it belongs to a pictured scene or in the same manner as on an object.

3.2. METHODS

3.2.1. STIMULI

PAINTINGS AND CUTOUTS

The stimuli were obtained from photographs of five paintings of the museum Prinsenhof Delft from the "Masters of Innovation" exhibition (see Figure 3.1):

- The Quarrel between Ajax and Odysseus, De twist tussen Ajax en Odysseus (Leonaert Bramer, 1629 - 1631), further "Ajax";
- Fruits on a marble table with a blue cloth, Vruchten op een marmeren tafel met een blauw kleed (Willem van Aelst, 1649), further "Fruits";
- The Art of Painting, De Schilderkunst (Mary Waters, copy of a fragment of "The Art of Painting" by Johannes Vermeer, 1996), further "Girl";
- Woman with cat in interior, Vrouw met kat in interieur (Cornelis de Man, 1666), further "Cat";
- Woman with child at a window, Vrouw met kind bij een raam (Hendrick van der Burgh, circa 1650), further "Window".

The "Ajax" painting was also used in its mirrored version to test for a possible bias in light direction perception. The "Girl" painting was shown only in its mirrored version to obtain more variety of lighting directions in the stimuli, since the majority of the originals showed light coming from left above.

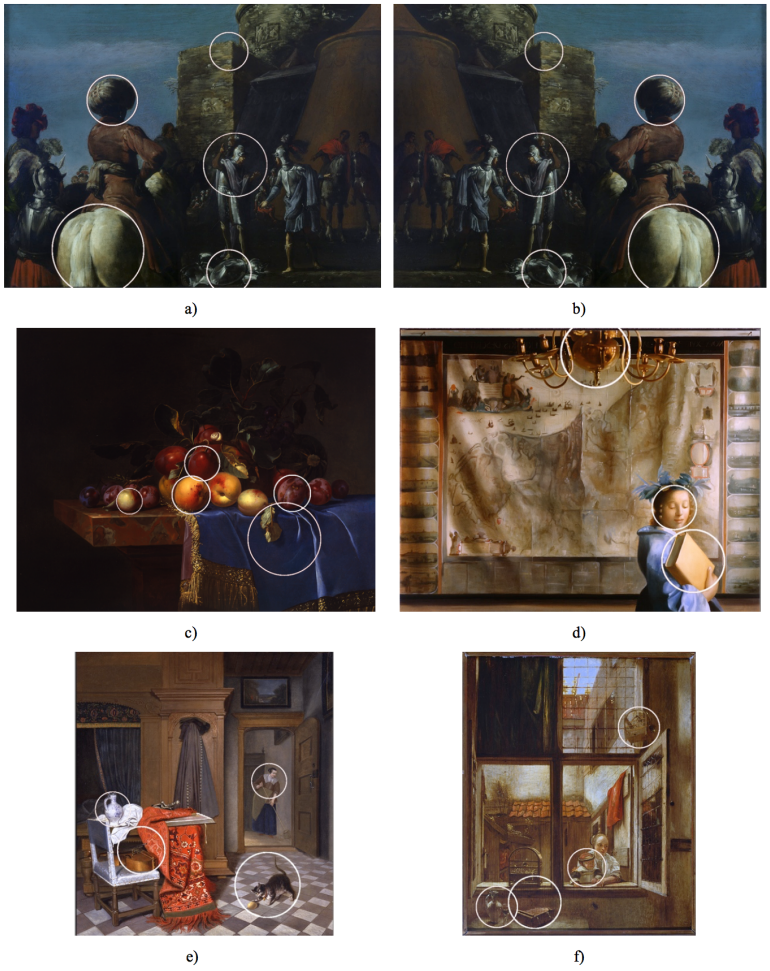

Figure 3.1: The images of the paintings that were used in the experiment, with white circles denoting the selected objects (the sizes of circles represent the sizes of the probes): a) "The Quarrel between Ajax and Odysseus" ("Ajax"), b) "The Quarrel between Ajax and Odysseus" mirrored ("AjaxMir"), c) "Fruits on a marble table with a blue cloth" ("Fruits"), d) "The Art of Painting" ("Girl"), e) "Woman with cat in interior" ("Cat"), f) "Woman with child at a window" ("Window").

In each painting we selected objects, which could be used by observers to infer the light conditions in the painting. The objects were selected on the basis of shape, specifically the objects had to present something roughly convex or at least clearly voluminous. Examples are the turban in "Ajax" or the book in "Girl", a complete overview can be seen in figure 3.1. For the paintings, which had visible color distortions we made white point corrections using the algorithm described in the appendix.

PROBE

As a probe we used a white Lambertian sphere of which the observers could control the lighting as to make it fit into the painting or fit with the lighting conditions of the object next to it. The sphere was rendered under a combination of collimated and ambient light. The observers could vary the collimated light direction using a touchpad, the collimated light intensity with the arrows Up and Down keys of a keyboard, and the ambient light intensity with the arrows Left and Right keys. All software was written with PsychToolbox14,15.

In the first condition, the "full image condition", we presented the paintings with a probe located in the position of the selected objects. The probe was sized to cover the object, which it was replacing. In the second one, the "cut-out condition", we presented circular cutouts of the objects next to the probe, see Figure 3.2. The cutouts corresponded exactly to the image part that was covered by the sphere in the paintings of the full image condition. Stimuli were presented on a mid-gray background.

In the full image condition the probe was either shown on a black monopod, which end was always grounded on a surface, or "laying" on the surface in the locations of the cutout objects, or "stuck" to the closest object, for example in the top position in the "Ajax" painting it is "stuck" to the wall.

The directional settings of the lighting of the sphere were quantified as two angles, polar angle and azimuth. The polar angle is the angle between a line from the eye (or cyclopean eye) to the center of the object and a vector from the center of the object to the light, it ranges from 0 (light source behind the observer), to 180 degrees (light source is behind the object). The azimuth is the angle between the horizontal axis and

Figure 3.2: Examples of the interface in the full image condition (left) and cutout condition (right). In the experiment, observers were asked to adjust the lighting of the probe such that it fitted the scene. Here in the cutout condition it obviously does not.

the projection of the lighting direction onto the frontal plane, it ranges from 0 to 360 degrees. If both angles are 90 degrees the source is strictly above the object in the plane of the image. The ranges of directed and ambient light intensities are both from 0 to 1, where 0 means an absence of that component of light and 1 means maximal intensity for that component. For example, in Figure 3.2, the intensity settings for (directed, ambient) are (0.6645, 0.3402) on the left and (1, 0) on the right respectively.

3.2.2. OBSERVERS

Sixteen observers (10 male, 6 female) participated in the experiment, including one of the authors (SP). Observers ranged in age from early twenties to late forties. Nine participants were experienced observers, and seven did not participate in light study experiments before, of which three never participated in a psychophysical experiment of any kind. All had normal or corrected-to-normal vision. All observers gave written, informed consent. Experiments were done in agreement with local ethical guidelines, Dutch Law, and the Declaration of Helsinki; and approved by the TUDelft Human Research Ethical Committee.

3.2.3. PROCEDURE

The experiment was performed in a dark room on a computer screen. The observer's task was to change the parameters of the probe's lighting (direction, intensities of directed and ambient components) in order to make it appear like it fitted the scene or the lighting of the cut out object next to it. Observers were shown 26 stimuli per condition ("full painting" and "cutout"), which were blocked per condition. Half of the observers first measured the full images block and then the cutouts one, and the other half of the observers vice versa. On average the experiment took about half an hour.

After the experiment we asked observers to rate the difficulty and satisfaction of the settings, both for the full images and for the cutouts.

3.3. RESULTS

To compare the directional settings between the "full painting" and "cutout" conditions, we translated the directional settings to 3D unit vectors and calculated the dot product between the vectors for the two conditions for each stimulus. The dot product of these unit vectors represents the cosine of the angle between them and is, in that sense, a

measure of how similar the directions are. The average dot product reached 0.7, i.e. the average angular difference was about 45 degrees. However, we found that the results largely depend on the painting content. Specifically, for the paintings "Ajax", "AjaxMir", "Fruits", and "Girl" (which we will name group 1) the averages were between 0.75 and 0.83, whereas for "Cat" and "Window" (which we will call group 2) they were 0.47 and 0.5 respectively. We transformed the inner product values to angles and plotted those results in Figure 3.3. In the histogram in Figure 3.3 you can see that the angular differences between the two conditions peak between 10 and 30 degrees, and that the results for the

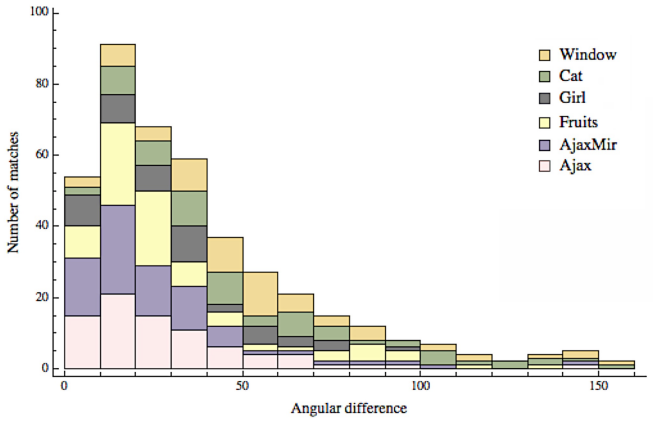

Figure 3.3: Histogram of angular differences between "full painting" and "cutout" vectors obtained from light direction settings for all trials.

group 1 paintings show maxima in that range, whereas, the results for the group 2 paintings spread out to higher values.

In addition, the paintings "Cat" and "Window" have the largest inconsistencies for directional settings (the azimuthal and polar angles, respectively) between conditions, which are illustrated by the differences between the means for the two conditions in Figure 3.4, the upper row. There was no clear influence on directed light intensity settings. For all paintings the ambient settings in the "cutout" condition were slightly higher than in the "full painting" condition. To test if this might be an effect of the mid-gray background in the cut-out interface, we calculated the average brightness level of the paintings and opposed it to the differences between the means for the two conditions. There was no clear correlation between the compared results.

In Figure 3.5 we show average settings of the light direction per location. Here it can

be clearly seen that for the group 1 paintings the directional settings are very consistent between observers within a painting (see Figure 3.6). Interestingly the arrows representing the orientations in the image plane or azimuths are either parallel ("Ajax", "AjaxMir", "Fruits") or converging ("Girl"). For paintings of group 2 observers have multiple interpretations, which was partially reflected in the variation of the averages. Results of the light direction azimuths for "Ajax" and its mirrored version are almost symmetrically reflected, and the corresponding polar angles are roughly identical, as expected.

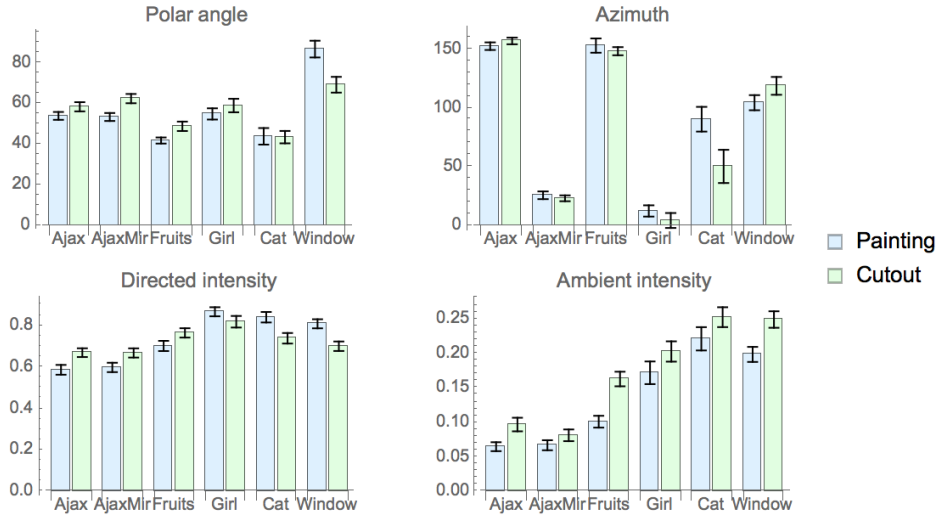

Figure 3.4: Comparisons of conditions: means of parameter settings per painting.

3.4. DISCUSSION

After comparing the results for the two conditions we found that the observers are highly consistent in directed and ambient light intensity settings for all paintings (on average the difference is less than 10%). For directional settings the striking result was the strong relation between the content of the painting and the consistency of results. More specific, the average angular difference between the conditions for paintings group 1 (see examples of settings in Figure 3.6) was 36 degrees, while for group 2 (see examples of settings in Figure 3.7 and 3.8) it was about 60 degrees.

However we consider the most likely explanation for the inconsistencies in the paintings "Cat" and "Window" to be the complexity of the light field in these two paintings.

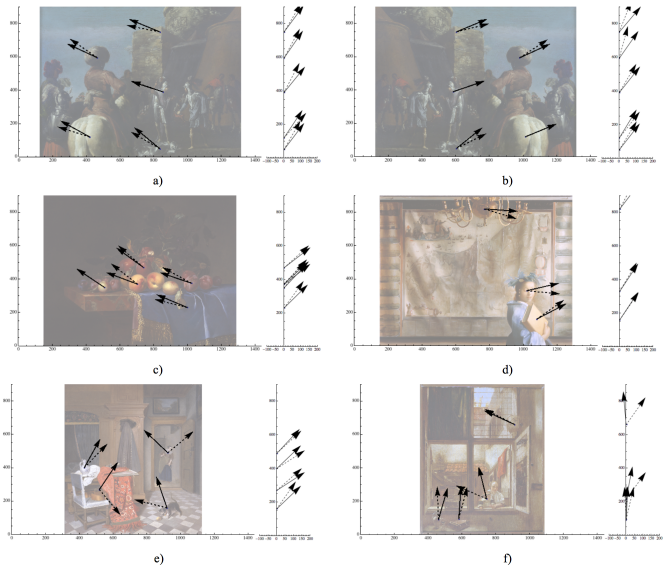

Figure 3.5: Average directional settings per location, with the azimuth depicted on the painting and the polar angle next to it in a side view (the x-axis is perpendicular to the picture plane, directed to the observer). The dashed arrows are the cutout results and the drawn arrows the full painting results. a), b), c), d) depict group 1, in which settings were consistent between observers, and e), f) depict group 2, for which observers have multiple interpretations.

Figure 3.6: Examples of representative observers' settings for the paintings of group 1, demonstrating consistent settings between the conditions: a) "Ajax" painting, b) "Girl" painting. The top row shows the settings for the "full painting" condition, the bottom row for the "cutout" condition.

Figure 3.7: Examples of representative observers' settings for the "Cat" painting. The top row shows the settings for the "full painting" condition, the bottom row for the "cutout" condition.

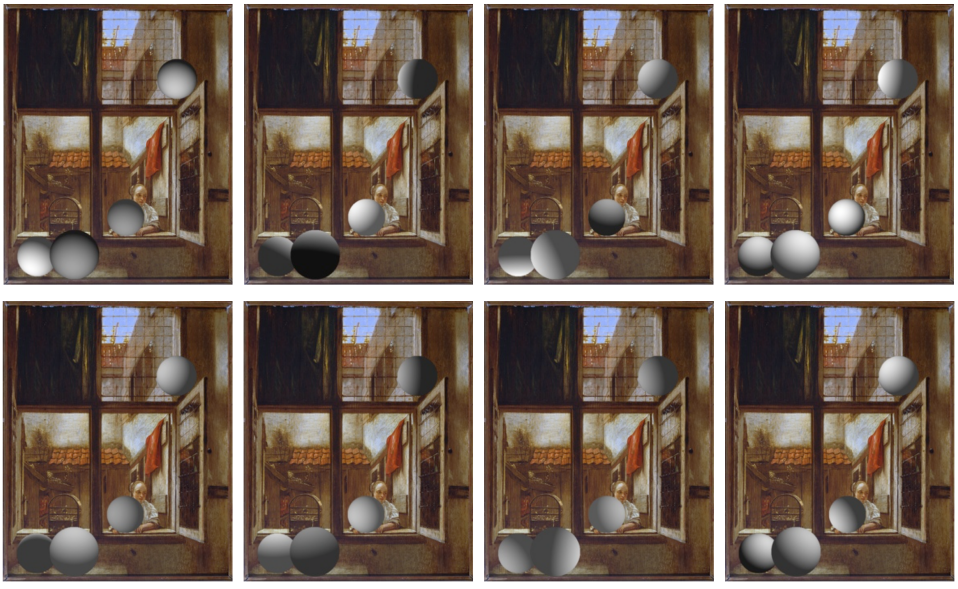

Figure 3.8: Examples of representative observers' settings for the "Window" painting. The top row shows the settings for the "full painting" condition, the bottom row for the "cutout" condition.

Van Doorn et al. (2012) showed that human observers can perceive uniform, diverging, and converging light fields, but are blind to light field deformation patterns, i.e. in complex lighting the observers are not able to group cues in order to draw a conclusion about the overall lighting. In the paintings of group 1 the lighting is uniform or slightly diverging over the scene, so there is almost no confusion about the primary light direction. Examples of the individual settings for this group can be seen in Figure 3.6, and clearly show consistent settings over the entire scene. In "Cat" and "Window", on the other hand, there are two zones with qualitatively different lighting and for observers it seems not always clear which object was under which lighting. Without uniform lighting observers might try to determine the light zones (spatial groupings of the light qualities, which are significant to the spatial and form-giving characteristics of light1) in the painting, but their interpretation varies from one individual to another, as can be clearly seen in Figures 3.7 and 3.8. In the "full painting" condition of the "Cat" painting some observers made the settings on the spheres as if the light comes primarily from the front of the painting and some as if it comes primarily from the back room (see Figure 3.7, a) and b) respectively), while others made settings that varied much more wildly (see Figure 3.7, c) and d)). The same story applies to the results for the "Window" painting, see Figure 3.8.

3.5. CONCLUSION

This study was focused on the perception of lighting in empty space and on objects. We carried out an experiment in which we probed the visual qualities of light in paintings and on cutouts with objects of those paintings. The results suggest that human observers infer the light in space ("full painting" condition) and on objects ("cutout condition") in a similar manner. However, the judgments turned out to be very dependent on the paintings' contents. Specifically, for a group of paintings with uniform or slightly diverging lighting the directional settings are highly consistent between conditions and also within the paintings, whereas for a group with more than one qualitatively different light zone the interpretations varied wildly from individual to individual. We believe that the most credible reason of our results is that in complex lighting the observers are not able to group cues in order to draw a conclusion about the overall lighting2. The demonstrated experimental interaction design allows developing new insights about light perception as well as a novel manner of experiencing paintings. It made our observers aware of the paintings' details ("The shadows here are wrong!") and in that sense may provide a tool

to learn museum visitors to see the paintings' light.

3.6. APPENDIX

3.6.1. COLOR CORRECTION METHOD

The algorithm (Langendijk & Klompenhouwer, 2004) reads an image in raw RGB-format, assuming its reproduction on a monitor with given color coordinates for the primaries, a given whitepoint and a given gamma. It then transfers the RGB-coordinates (per pixel) in xyz- coordinates using a transformation matrix An based on the new (corrected) white-point. This results in xyz-coordinates (per pixel) that are corrected for the new white-point. To reproduce this new image on the above assumed monitor, the xyz-coordinates need to be transferred back to RGB-coordinates (per pixel) with the inverse of the matrix A0, using now the original white point of the monitor. It may happen that this operation results in R-, G- or B-coordinates that are smaller than 0 or larger than 1 (the latter being equivalent to 256 in the 8-bits format), and so, cannot be reproduced on the monitor. In that case, we applied clipping. Coordinates smaller than 0 were simply replaced by 0, whereas for coordinates larger than one (i.e., this may be either the R-, G- or B-coordinate of a pixel) the three corresponding pixel coordinates (so the R-, G- and B-coordinates) were scaled down with the maximum value of these three coordinates.

BIBLIOGRAPHY

Adelson, E., & Bergen, J.. (1991) The plenoptic function and the elements of early vision. Computational Models of Visual Processing 3—20.

Brainard, D. H. (1997). The psychophysics toolbox. Spatial Vision 10, 433—436.

Cuttle, C. (2010). Towards the third stage of the lighting profession. Lighting Research and Technology, 42 (1), 73—93.

Fleming, R. W., Dror, R. O., & Adelson, E. H. (2003). Real-world illumination and the perception of surface reflectance properties. Journal of Vision, 3, 347—368.

Frandsen, S. (2007). Light Scale,. International Lighting Review, 3, 108-112 (1987). [11] Pont, S. C., & Koenderink, J. J., Matching illumination of solid objects. Perception & Psychophysics, 69(3), 459—468.

Gershun A. (1939) The light field. J. Math. Phys., 18, 51151 (translated by P. Moon and

G. Timoshenko)

Koenderink, Pont, S. C., van Doorn, A. J., Kappers, A. M. L., & Todd, J. T. (2007). The visual light field. Perception, 36(11), 1595—1610.

Langendijk, E. H. A., & Klompenhouwer, M. A.(2004). 43.2: More Realistic Colors from Small-Gamut Mobile Displays. SID Symposium Digest of Technical Papers, 35(1), 1258—1261.

Madsen, M. (2012). Light-zones(s): as Concept and Tool. ARCC Journal, 4(1), 50—59 (2007).

Maloney, L., Gerhard, H., Boyaci, H., & Doerschner, K. (2010). Surface color perception and light field estimation in 3D scenes. Vision in 3D environments, 65—88.

Mury, A. A., Pont, S. C., & Koenderink, J. J.. (2007). Light field constancy within natural scenes. Applied Optics, 46(29), 7308—7316.

Pelli, D. G. (1997). The videotoolbox software for visual psychophysics: Transforming numbers into movies. Spatial Vision 10, 437-442.

Schirillo, J. A. (2013). We infer light in space. Psychonomic Bulletin & Review, 20(5), 905—15.

Van Doorn, A. J., Koenderink, J. J., Todd, J. T., & Wagemans, J.. (2012). Awareness of the light field: the case of deformation. I-Perception, 3(7), 467—480.

Wijntjes M.W.A., Doerschner K., Kucukoglu G., & Pont S.C. (2012). Relative flattening between velvet and matte 3D shapes: evidence for similar shape-from-shading computations. Journal of Vision, 12(1), 1-11.

Wijntjes, M. W. A., & de Ridder, H.. (2014). Shading and shadowing on Canaletto's Piazza San Marco. Proc. SPIE 9014, 901415.

4

Visual Light Zones

Abstract

In this paper, we studied perception of a particular case of light fields which is characterized by a difference in its consistent structure between parts of a scene. In architectural lighting design, such a consistent structure in a part of a light field is called a light zone (Madsen, 2007). First, we explored whether human observers are sensitive to light zones, that is, zones determined primarily by light flow differences, for a natural-looking scene. We found that observers were able to distinguish the light conditions between the zones. The results suggested an effect of light zones orientation. Therefore, in Experiment 2 we systematically examined how the orientation of light zones (left-right or front-back) with respect to a viewer influences light inferences in symmetric scenes. We found that observers are quite sensitive to the difference in the light flow of the light zones. Additionally, we found that participants showed idiosyncratic behavior, especially for front-back oriented light zones. Our findings show that observers are sensitive to differences in light field structure between two parts of a scene, which we call visual light zones.

Published as: Kartashova, T., de Ridder, H., Pas, S. F., & Pont, S. C. (2018) Visual light zones. i-Perception, 9(3), 1-20.

4.1. INTRODUCTION

Can one make visual estimations of something that can not be seen? Yes, human observers are sensitive to the light field in empty space (Koenderink et al., 2007; Xia et al., 2014, Schirillo, 2013). They can visually fit the intensity, direction and diffuseness of light on a matte white sphere to a scene basing on appearance of objects in that scene. This sensitivity was named the visual light field (Koenderink et al., 2007). Moreover, observers can robustly estimate these light properties throughout an empty space (Kartashova et al., 2016) and their inferences agree with homogeneous, converging or diverging superpatterns (van Doorn et al., 2012). The human ability to infer light in (empty!) space is an interesting scientific topic in itself and also relates to questions about interdependency of light, shape and material perceptions. In this paper, we further explore visual light fields by investigating inferences on spatially varying superpatterns, created by variation in illumination over scenes.

Light fields in natural scenes can contain uniform, convergent, divergent, rotational, and deformation patterns (Mury, 2009). A uniform pattern is formed by perfectly collimated light (having parallel light rays), e.g. direct sunlight. Convergent and divergent patterns are formed by light which focuses in a point or spread out from a point, respectively. A rotational pattern is formed by light that cycles around a point. Finally, a deformation pattern has a complex flow structure, for example a saddle. Van Doorn et al. (2012) showed that observers group local shading patterns into global super-patterns that appear to be illuminated in some unitary fashion. They found that observers can perceive uniform, convergent and divergent patterns, but that they are blind to rotational and deformation patterns. The question we address here is whether observers are able to perceive such global super-patterns if a single scene contains two of such patterns.

In the architecture field, such patterns or consistent structures within complex light fields were named light zones by Madsen (2007). She introduced the concept of light zones, provided several practical examples and defined them as "(spatial) groupings of the lighting variables (intensity, direction, distribution and colour), which are significant to the space and form-giving characteristics of light". We note that light zones or the zone system were also introduced in photography by Adams (1948), yet those zones concern luminance ranges of photographed scenes used for determining optimal film exposure. This is of course closely related to lightness perception and spatial grouping on the basis of intensity, which was already intensely studied, see below. We here study

light zones in Madsen's (2007) sense of spatially segmented parts of a scene that can be grouped on the basis of the structure of the light flow, or, in van Doorn et al.'s words, "global super-patterns that appear to be illuminated in some unitary fashion". As van Doorn et al., we consider primarily the directional properties of the light field structure, the light flow, for this segmentation. Moreover, we will restrict our light zones to flow structures that are uniform / divergent / convergent. Please note that the super-patterns that van Doorn et al. studied were defined in a plane, but that they can be easily extrapolated to 3-dimensional spaces especially for these simple structures.

Although under different names, the concept of light zones can be found in a number of perceptual studies. The first prominent example is Gilchrist's (1977) experiment on the perceived lightness of a patch, which depended on its perceived position. Stimuli consisted of two empty spaces, a dark one in the front and a bright one in the back, which were connected with a door opening. When a patch was thought to be in the brightly lit back space (one light zone), its matched lightness was much lower than when it appeared to be in the dim front space (another light zone). Snyder et al. (2005) changed the apparent depth of a probe sphere by manipulating retinal disparity. The sphere could appear to be placed either in a far bright room or in a close dark room, along the observer's line of sight. Hence, retinal disparity moved the probe between different light zones. This manipulation affected the perceived lightness of the probe. Schirillo (2013) discussed this and other examples in which the lightness and chromaticity of patches were judged in depth planes with different illuminations. He concluded that human observers are able to infer the light in empty space (between illuminated objects). This was tested and confirmed in Koenderink et al.'s (2007) visual light field study.

Toscani et al. (2017) studied the difference in perception of illumination in #thedress scene between observers who see the dress white and gold and those who see it blue and black. The light was probed in front of the dress and in the background. It was found that in the background there were no differences in chromaticity settings between different perceivers. However, in the foreground the white-perceivers made bluer settings than blue-perceivers, making the chromatic difference between the front and back of the scene more pronounced. The foreground and background in this case represent two zones with different illuminations. The question remains whether observers are able to spatially segment parts of a scene on the basis of the structure of the light flow, that is, the directional properties of the light.

The study presented in this paper was inspired by an experiment using seventeenth

Century Dutch paintings (Kartashova et al., 2015), results of which showed a relation between settings consistency and the complexity of light fields in painted scenes. In that experiment, we tested the perception of light on objects and in empty space. Observers were asked to infer light either on volumetric objects cut-out from images of six painted scenes, or in empty space in positions of those cut-out objects in the scenes. The consistency of observers' settings varied greatly between paintings. Four paintings contained seemingly consistently structured light fields (uniform or diverging), or a single light zone. For those paintings, the observers' settings were rather consistent between conditions (comparing settings for the cutout object with those for the probe in the painting) and within a scene. However, for the other two paintings the observers' inferences varied greatly. One of those paintings showed an interior and exterior through a window opening, and the other an interior and back room through a door, thus, both paintings seemed to present two spaces with different light qualities — including its directional properties. The most likely explanation of the inconsistencies in the observers' settings was the presence of two light zones in both paintings. The observers seemed to interpret the border between the zones idiosyncratically, some inferred two different illuminations in the two parts of the scene, while others made settings as if there was only one light zone. It was an interesting finding, yet we could not compare the settings of observers to the veridical values in those scenes, since they were painted hundreds of years ago.

Our goal in the current study is to investigate the perception of light properties in scenes with two light (direction) zones. We performed two experiments. Experiment 1 (see Section 2) had an explorative nature and was done to test whether we could repeat the finding of our former study and to analyze how it is related to the physical light field. We built a model of a natural scene and illuminated it with two configurations of light sources, both creating two light zones. The two configurations were designed to have different orientations with respect to the viewing direction. The visual light field was measured over a grid of points, analyzed, visualized and compared to the physical light field. In experiment 2 (see Section 3) we focused on the specific question whether the orientation of the light zones (in the picture plane versus in depth) influences the light inferences. In experiment 2 we used less probes per scene to allow probing more illumination configurations, and we used a controlled environment. Finally, we discuss the obtained results and propose further directions for research on light zones perception (see Section 4).

4.2. EXPERIMENT 1

The aim of the first experiment was to investigate whether human observers are able to distinguish differences in light properties between physical light zones that were designed to have prominent differences in light directions. We created a scene with two illumination conditions. One condition produced different light zones in the left and in the right part of the scene, another condition created different light zones in the front and in the back parts of the scene. We obtained visual light fields for both illumination conditions by sampling the observers' light inferences over a grid of positions (for method see Kartashova et al., 2016).

4.2.1. METHODS

STIMULI

We created a model of a scene resembling a living room and illuminated it using two sets of light sources (see Figure 4.1). In both illumination conditions the light sources were placed such that approximately half of the scene was in one light zone, and approximately half in another. The main difference between the light zones was the light direction. In the first condition the illumination direction differed between the left and right sides of the scene, creating a left-right (LR) light zones condition. The left side of the scene was illuminated from top left, with the lamps on the ceiling of the room, and the right part from top-right with the sun shining through the window. The second, front-back (FB) condition had the front part illuminated from the top-front, via lamps above the viewer (not visible in the image), and the back part was illuminated from the left with the light coming through the door in the back of the room. The light of the lamps was simulated by small spherical light sources producing diverging light. The sun- and sky-light was simulated by small luminous planes. We rendered images of 1200x900 pixels size with the following settings: linear gamma, mental ray renderer (built-in software for rendering of images and light measurements), minimum one sample per pixel, maximum 128 samples per pixel.

SETUP

In order to measure the visual light field in the scenes, we used a light probing approach (Kartashova et al., 2016; Koenderink et al., 2007). During the actual measurements, a white matte sphere on a black monopod was superimposed on an image of the scene.

Figure 4.1: Scenes of experiment 1. Left is the left-right (LR) condition, right is the front-back (FB) condition.

Observers could control the direction of the light on the sphere via mouse movements and the intensities of the directed and ambient lights using keyboard buttons. From the observers' settings, we also extracted the diffuseness of the light, parameterized as 1 minus the ratio between the directed and ambient intensities (Xia et al., 2016b). The diffuseness can range from fully collimated light (e.g. sunlight) to fully diffuse or Ganzfeld illumination (e.g., light in the mist on a snowy field).

To define the positions and sizes of the sphere and pole, we created a grid of spheres standing on poles in the model, five spheres in width, five in depth and three in height. The grid was positioned in the scene such that for both illumination conditions the vertical middle planes of the grid were on the borders between the light zones (see Figure 4.2 and Figure 4.4). The grid was also adjusted such that the poles were always standing on non-occluded objects in order to clearly define the spheres positions. For Figure 4 the probes were rendered in the scenes.

For the experiment, we used a high-resolution 15 inch computer screen (2880 x 1800 pixels, Retina Display, luminance range from 0.4 cd/m2 to 330.8 cd/ m2). The experiment sequence and controls were developed using the Psychtoolbox library (Brainard, 1997; Pelli, 1997). The light in the room was switched off to avoid illumination interference on the screen. The viewing distance of the observers was fixed at 27 cm from the screen with a chin rest to keep the viewing angle the same as that of the virtual camera used for rendering. The images and probe were presented in grayscale, since we wanted primarily to test the influence of the distribution of light. The images, probe and screen were calibrated linearly.

PROCEDURE

At each trial of the experiment observers were asked to set the illumination on the probe to make it appear as if it belongs to the scene. The experiment consisted of two blocks for the two conditions LR and FB. Half of the observers started with the LR scene and half with the FB scene to balance the order. In each condition observers made one setting for each grid position and two additional settings for probes corresponding to the red spheres in Figure 4.2. Having three repetitions in these points allowed us to compare the spread of the settings within observers across light zones and illumination conditions. Before the experiment, we explained the procedure, task and probe controls to the observers. We did not explain the concept of light zones to the observers. In order to explain the task, we showed a scene resembling a different room that was not used in the experiment, with spheres rendered in it. Then we performed three trials for training the use of the controls, after which the two parts of the experiment were conducted.

PARTICIPANTS

Ten observers participated in this experiment. The participants were naive with respect to the setup and purpose of this experiment. All participants had normal or corrected-to-normal vision. They all gave written, informed consent. All experiments were done in agreement with the Declaration of Helsinki, Dutch Law, local ethical guidelines, and approved by the TUDelft Human Research Ethics Committee.

IN-SCENE LIGHT MEASUREMENTS.

In addition to the psychophysical measurements we also performed measurements of the light in the modeled scene. For this purpose, we used the Lighting Analysis Assistant (LAA) tool of the Autodesk 3ds Max system, which allows virtual illuminance measuring. We created a grid of virtual cubic illuminance meters (six illuminance meters on a

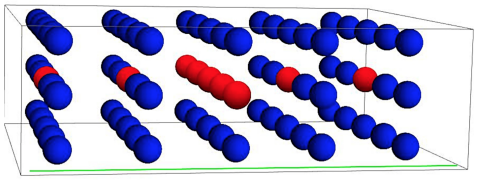

Figure 4.2: Schematic representation of the measurements positions. The positions of repeated measurements are marked with red. The viewing plane orientation is denoted as a green line.

cube, which allows to measure a first order approximation to the light field, see Xia et al, 2016a and 2016b) using a script. We set the measurement cubes to be in the same positions as the probes. The script placed all six meters in the same position, with the sensors facing the positive and negative directions of each axis (see details in Kartashova et al., under review). Then, for each cube, we extracted from the resulting six luminance measurements the intensity, diffuseness and direction of the light using Cuttle's (2003, 2013) formulas and interpolated them to obtain a representation of the mathematical first order structure of the "physical" light field in the scene (Kartashova et al., 2016). Alternative could be estimating the properties from for instance local spherical panoramic images. They are easy to use in rendered scenes, yet would require a spherical harmonics decomposition to compute the properties. Xia et al. (2017ab) showed that the cubic approach forms a computationally easier approach. Moreover, it can easily be used in real scenes too.

We visualized the light fields as light tubes (see Figure 4.3). A tube is aligned to the light vectors along its length. A tube's path is calculated via interpolation methods (see Kartashova et al. (2016) and Mury et al., (2009) for the details). The thickness of a tube is inversely proportional to the light intensity. The physical light field in the LR condition contains curved tubes. This happens because in the middle of the measured volume there is a space that is occluded from all direct light sources, where light arrives mostly through scattering from the floor. Therefore, it is dim (the tubes are rather thick) and the light vector is directed downwards (to the floor, a secondary light source). It is clear that the light direction in the left side of the measured volume is very different from the middle and the right side of the volume. There is less curvature in the light field topology for the FB condition, because there is almost no space occluded from the direct light sources. As a result, there is a clear division between the light zones, one being in the volume of the light from the door, and the other in the volume of the light from the lamps.

4.2.2. RESULTS

From the observers' settings on the spheres, we obtained psychophysical measurements of the direction, intensities (directed and ambient) and diffuseness of light in the two illumination conditions. The diffuseness D was calculated in accordance to the following formulas (Cuttle, 2003, 2013; Kartashova et al.,2016; Xia et al.,2016a,b):

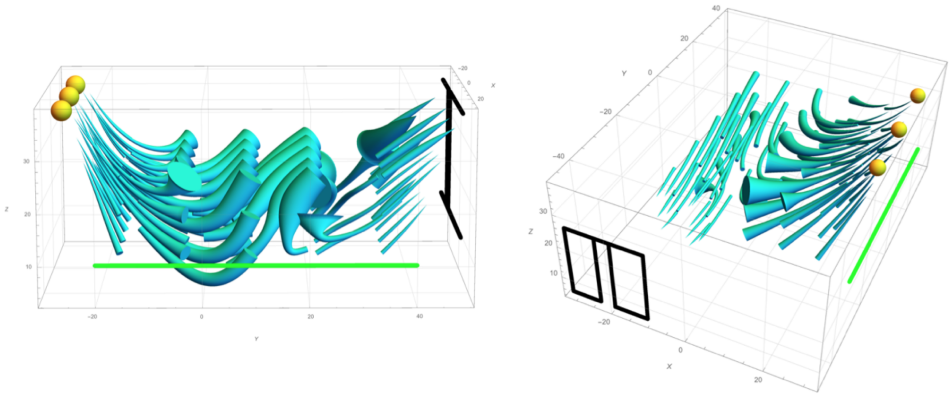

Figure 4.3: The mathematical first order structure of the physical light fields for the stimuli used in experiment 1. Left is LR orientation, right FB orientation.

$$\mathbf{E}_{(x)} = \mathbf{E}_{x+} - \mathbf{E}_{x-} \tag{4.1}$$

$$|\mathbf{E}| = \sqrt{\mathbf{E}^2_{(x)} + \mathbf{E}^2_{(y)} + \mathbf{E}^2_{(z)}} \tag{4.2}$$

$$\sim E_X = \frac{\mathbf{E}_{x+} + \mathbf{E}_{x-} - |\mathbf{E}_{(x)}|}{2} \tag{4.3}$$

$$\sim E = \frac{\sim E_X + \sim E_Y + \sim E_Z}{3} \tag{4.4}$$

$$E_{scalar} = \frac{|\mathbf{E}|}{4} + \sim E \tag{4.5}$$

$$D = 1 - \frac{|\mathbf{E}|}{4E_{scalar}} \tag{4.6}$$

$\mathbf{E}_{x+}$, $\mathbf{E}_{x-}$ are the illuminance measurements on opposite sides of the cube. $\mathbf{E}_{(x)}$, $\mathbf{E}_{(y)}$ and $\mathbf{E}_{(z)}$ are the light vector component. $|\mathbf{E}|$ is the light vector magnitude. $\sim$ E is the symmetric illuminance. E_{scalar} is the mean illuminance in a point, which we took as measure of light intensity. For the observers' settings, directed and ambient light were taken as the magnitudes of $\mathbf{E}$ and $\sim$ E, respectively, after correction for the clipping of

intensities on the probe. The diffuseness D ranges from 0 (fully collimated light) to 1 (fully diffuse light).

In order to analyze the results quantitatively, we grouped the settings according to the positions of the probes. The grid was "sliced" into planes parallel to the border between the light zones (see Figure 4.4). In the LR condition the probes were grouped parallel to the viewing direction and in the FB condition parallel to the picture plane.

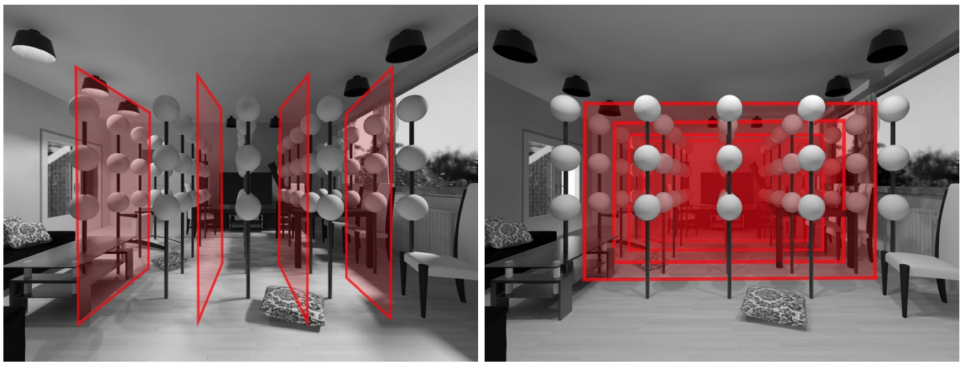

Figure 4.4: Slicing of the resulting settings. Left the LR condition sliced parallel to the viewing direction, right the FB condition sliced across the viewing direction.

Thus, each of the five groups of data points contained the directional settings of all observers (including the repetitions) on all probes of a slice.

Figure 4.5 shows the distribution of the directional settings on spheres, with the mean direction represented by a red dot and one standard deviation by red ellipses, for each plane and both conditions. The ellipses' short and long axes were determined by projecting the data on a plane and calculating standard deviations of the resulting bivariate distributions. It is clear that the settings on the two left spheres in Figure 4.5 (left light zone for LR, and back light zone for FB) are dramatically different from the settings on the two right spheres (right light zone for LR, and front light zone for FB). The angular differences between the means of the different light zones are large: from 82 to 111 degrees for LR and from 49 to 61 degrees for FB. In contrast, the differences for planes in the same light zones are small: 24 and 12 degrees for LR, and 4 and 8 degrees for FB. This suggests that observers were on average able to distinguish the light zones. However, the data show quite some variation and therefore we will now analyse individual results in detail.

Having the observers' settings for a grid of points allowed us to reconstruct the visual

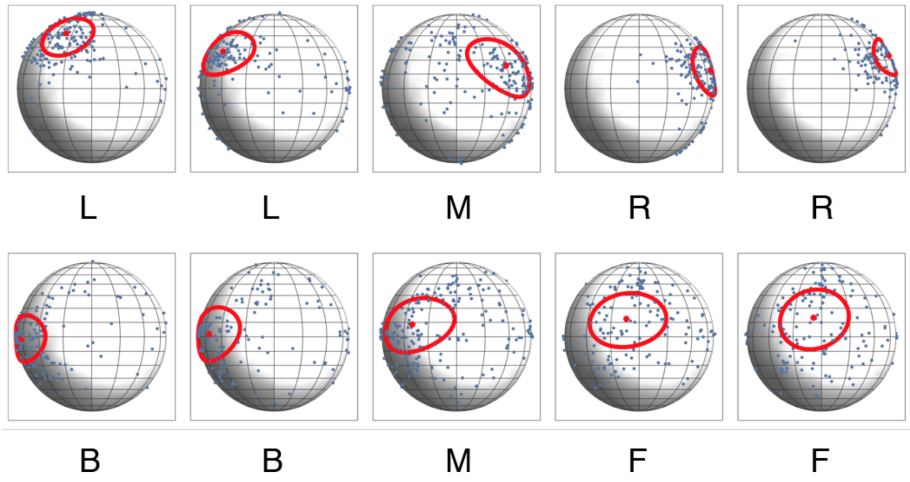

Figure 4.5: Distribution of settings per slice. The first row shows the results for the LR condition, the second row for the FB condition. Each sphere represents all the directional settings of all observers on all the spheres of a corresponding slice. The red dots represent the mean directions, the red ellipses represent one standard deviation.

light fields via interpolation (Kartashova et al., 2016; Mury et al., 2009), see Figure 4.6 for three representative cases per condition. Generally, in the LR condition, there is an apparent distinction between the light zones with the border slightly varying from one observer to another, but roughly in the middle of the measured volume (see Figure 4.6, top row). For none of the observers we found curved light tubes in the center of the scene, as in the physical light field (see Figure 4.3). This confirms our previous finding that human observers ignore subtle variations in physical light fields (Kartashova et al., 2016). The visual light fields in the FB condition differed from one observer to another, see Figure 4.6, bottom row. In the left visualization, the tubes in the back of the room seem to flow to the door, whereas the tubes in the rest of the room point to the lamps in front; in the second figure, all the tubes point to the lamps, and in the third, most of the tubes point to the door.

We analyzed the spreads of the data between and within observers (see Figure 4.7). As a measure of the spread of the directional settings we took the dispersion 1/R, where R was the length of the vector summation of the settings represented as unit vectors divided by the number of measurements (Leong & Carlile, 1998). R has the highest value (namely 1) when all the vectors point in the same direction, it decreases with increasing spread, and it is smallest (namely 0) for data that is uniformly spread over all directions.

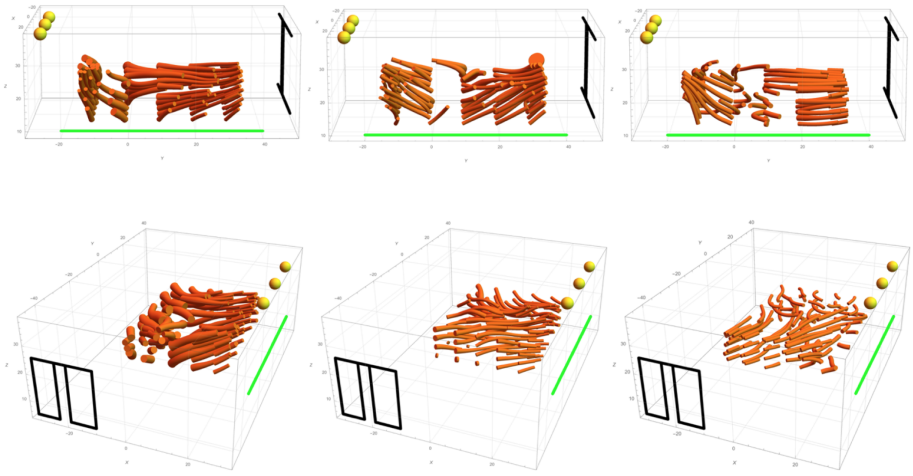

Figure 4.6: Pairs of visual light fields of three representative observers. The first row represents results for the LR condition, the second row for the FB condition. The green line denotes the picture plane. Yellow spheres represent the lamps. Black lines show the positions of the window and the door. The visualizations of the LR conditions have a rather clear border between the light zones, whereas for the FB conditions the visual light fields vary idiosyncratically.

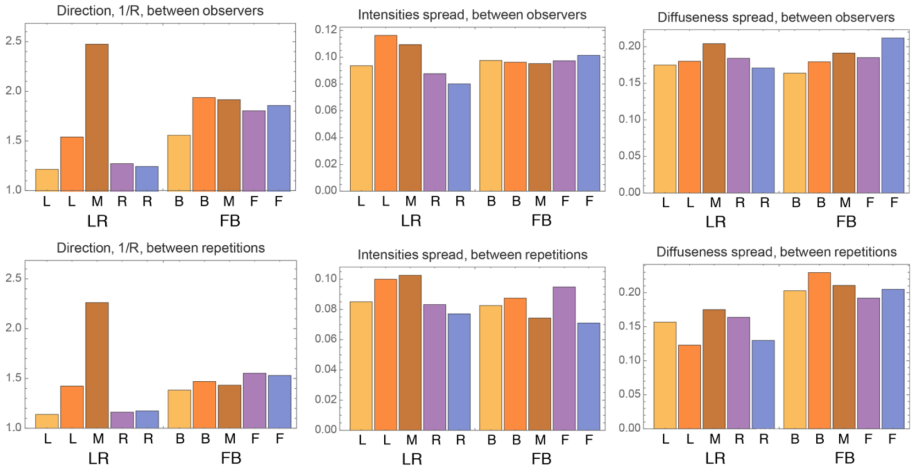

Figure 4.7: Spreads of settings between observers in the first row and between repetitions in the second row. The first column concerns the spread in the directional settings, the second column in the intensity settings, and the third column in the diffuseness settings. For the bar charts between observers, each bar represents the spread between all observers' settings in one slice of the grid. For the bar charts between repetitions each bar represents an average of the spreads between observers' repetitions for each probe.

So, 1/R ranges from 1 to infinity. The motivation of using such method is that the data has a spherical nature, and therefore such a spherical analysis is better suited than splitting the data into two angles. For the inter-observer spread of the directional settings, represented in the first column and row of Figure 4.7, we calculated the dispersion 1/R for all settings of all observers on all spheres of a slice, including the repetitions (thus the same data as we grouped in Figure 4.5 for calculating means and ellipses). For the LR light condition (left half of the graph) the dispersion peaks on the middle plane, and otherwise is relatively low. The dispersions in the FB condition (right half of the graph) seem more uniform across the slices than in the LR condition and on average higher. We did not calculate the significance of the differences between the data for the slices, because we did not have a tool at hand for the analysis of such spherical data. The dispersion between repetitions (within observers) was calculated using the repeated settings data for five probes. The five probes were selected from the nine repetition probes such that two of the probes lay in one light zone, two in the other light zone and one in the center of the grid. The dispersions between repetitions showed a similar pattern as those between observers. Moreover, the values of 1/R between repetitions or within observers seemed, overall, somewhat smaller than between observers.

In order to compare the intensity settings, we calculated the scalar illuminance, see Equation 5. For diffuseness, we used the normalized diffuseness formula of Xia (Cuttle, 2003; Xia et al., 2016a), see Equation 6. We took the standard deviation as a measure of the spread of the intensity and diffuseness (see Figure 4.7). We find that the spreads for the intensities (ranging from 0 to 1) are always between 0.07 and 0.12 and for the diffuseness (ranging from 0 to 1) between 0.10 and 0.25, and we did not find significant differences for these data. Moreover, again the values between repetitions or within observers seem overall somewhat smaller than between observers.

Summarizing the results, the observers were able to distinguish the illumination differences between the light zones. Additionally, we found trends in the data indicating that there might be idiosyncratic differences as well as differences between the light conditions: in the LR condition the results seemed to be consistent, except the plane between the light zones, whereas in the FB condition the spread values seemed on average higher than in the LR condition. The question remains whether these differences between the conditions were genuine or that they were evoked by other stimulus properties. The light sources positions were different between the conditions, with respect to the scene geometry. Specifically, in the LR condition the light sources were on two oppo-

site sides of the scene, and in the FB condition on two perpendicular sides. Additionally, in the LR condition the observers could see the lamps and not in the FB condition. Finally, the scene was not symmetric. We performed a second experiment in order to study if the trends in the findings were indeed caused by the light zones orientations. In Experiment 2 we eliminated all the listed interfering differences between conditions.

4.3. EXPERIMENT 2

The goal of this experiment was to systematically investigate light perception for LR and FB orientations of light zones. A rotationally symmetric scene was illuminated with three configurations of light sources, creating physical light zones. Viewing each illumination condition from two perpendicular directions allowed us to test left-right (LR) and front-back (FB) orientations of the light zones while keeping the actual light and geometry in the scene constant.

4.3.1. METHODS

STIMULI

The constructed scene contained a set of simple shapes that were placed and adjusted such that the scene was geometrically symmetric with respect to 90-degrees rotations (see Figure 4.8 and Figure 4.9). The objects of the scene were chosen to induce a variety of light cues: shading, shadows, highlights, interreflections. All objects were white, and most of the objects, except four spinners, were matte. The spinners were glossy. The ground plane was mid-gray and the background was black. The scene was created and rendered in the same software as in Experiment 1.

For each illumination condition the light sources were positioned at a 45-degrees elevation with respect to the center of the scene and the ground plane. For the first three conditions, we illuminated the scene with two identical small spherical light sources (see Figure 4.8 and Figure 4.9). The conditions were viewed from two directions, such that from one viewpoint the light zones were on the left and on the right side of the scene (1LR, 2LR and 3LR), and from the other viewpoint in the front and in the back of the scene (1FB, 2FB and 3FB). We modulated the positions of the light sources and shades to create light zones differing in average light direction. Conditions 1 and 2 both have identical positions of the light sources at opposite sides of the scene (see Figure 4.8, first row). In condition 1 the shades partially occluded the light, so that the light source illu-

minated only the closer half of the scene. In condition 2 the shades completely occluded the light on half of the scene. The placing and orientation of shades in these two conditions create light zones with complementary directions. As a result, in 1LR the scene is illuminated from the left and the right (similarly to LR condition of experiment 1), whereas in 2LR from the front and back. Condition 3 was selected to test a condition that is similar to the FB condition of experiment 1. In this condition, we used the combination of the shades used in conditions 1 and 2. The fourth condition contained a single light source, identical to the sources of previous conditions, creating a quite homogeneous single light zone. This single light zone condition was created in order to have baseline settings for each light direction. It was viewed from each side of the scene (Front, Right, Back, Left). Thus, altogether we created ten test images, six with two light zones and four with a single light zone (see Figure 4.9).

SETUP AND PROCEDURE

The setup in Experiment 2 was the same as in Experiment 1. Each test image contained five probes, one in each quadrant of the scene and one in the center (see Figure 4.10) — but during the experiment only one probe was shown per trial. Five probes do not suffice to model the global light field, but allowed us to include more scenes in the experiment and systematically test the effects of light directions and viewing directions. The adjustments were repeated three times for each probe and each test image. Thus, 10 test images x 5 probes x 3 repetitions constituted 150 trials, of which we randomized the order of presentation.

Before the experiment, we explained the procedure, task and probe controls to the observers. We did not explain the concept light zones to the observers. To explain the task, we showed two illuminations of the scene, which were not used in the experiment, with spheres rendered in it. Then we performed three trials for training the use of the controls and the experiment trials.

As in Experiment 1, we also conducted "physical" light measurements in the scene at the positions of the probes for each illumination condition.

PARTICIPANTS

Ten observers (different observers than who participated in Experiment 1) participated in this experiment. The participants were naive with respect to the setup and purpose of this experiment. All participants had normal or corrected-to-normal vision. They all

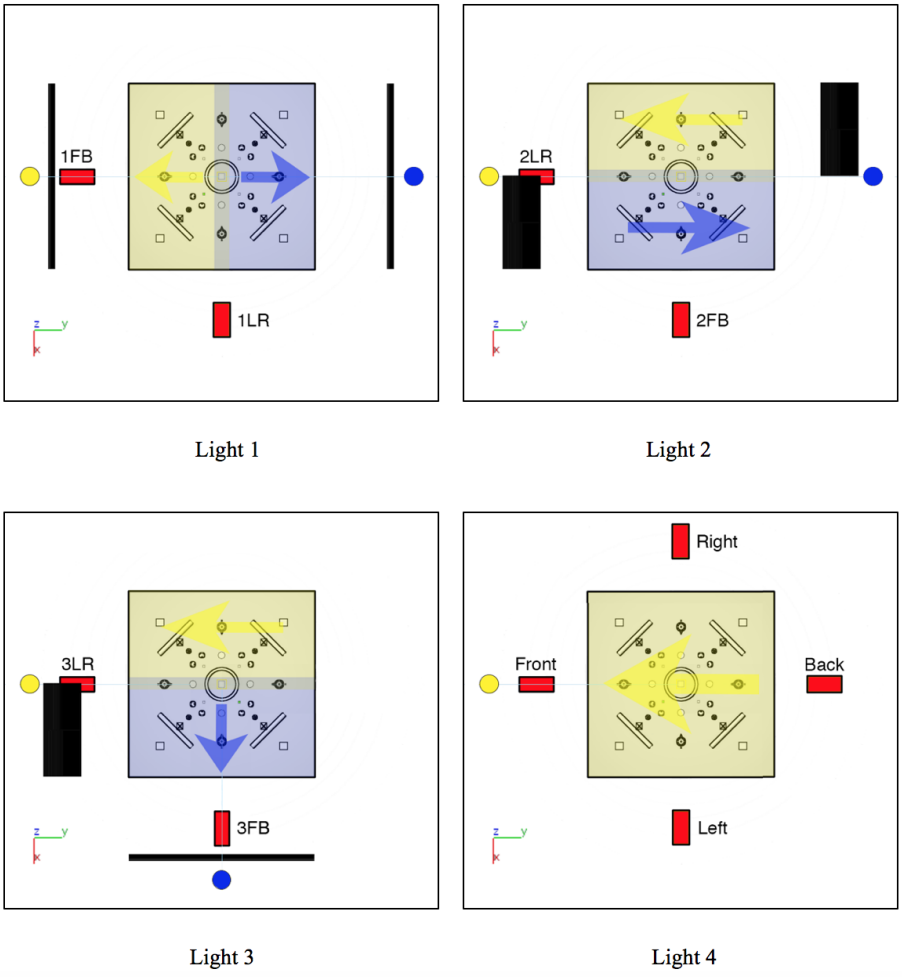

Figure 4.8: Schematic representation of the tested conditions and views. Each image represents the top view of the scene and light sources (the distances to light sources and shades are not proportional). Red rectangles represent the cameras, labeled according to the resulting scene image. Yellow and blue circles represent the light sources. Black bars show the shades, which partially occluded the light, so that the light source illuminated only the closest half of the scene. Black rectangles show the shades that completely occluded the light on a half of the scene. Yellow and blue arrows show the approximate light orientation (as a vector, pointing towards the source) in the zones of corresponding colors.

gave written, informed consent. All experiments were done in agreement with the Declaration of Helsinki, Dutch Law, local ethical guidelines, and approved by the TUDelft Human Research Ethics Committee.

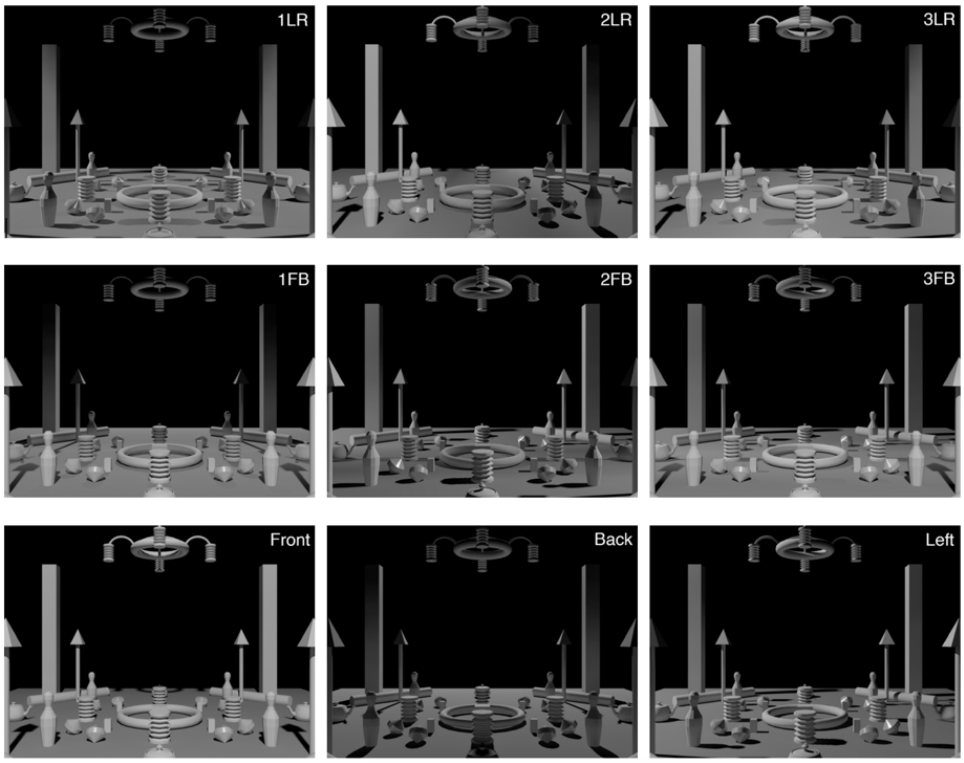

Figure 4.9: Test images. The first two rows contain the conditions with two light zones. The first row shows the LR orientations, the second row the FB orientations. The third row shows the single light zone condition from the Left, Front and Back (the Right is not shown here, because that is exactly mirrored to the Left case).

4.3.2. RESULTS

The results of Experiment 2 consisted of observers' repeated settings on the five probes for the ten test images, six of which were pairs of light zones conditions, and the remaining four considered the single light source condition. We made several comparisons of the results for the direction settings. We arranged the results for each test image in three groups, with the first group representing the settings on the two probes of the first light zone (L for LR and F for FB), the second group of the single middle probe, and the third group of the two probes of the second light zone (R for LR and B for FB). For the single light source condition the data were grouped into left, middle probe, and right parts of the scene with regard to the viewing direction.

We parameterized the directional variability via the dispersion 1/R as described in

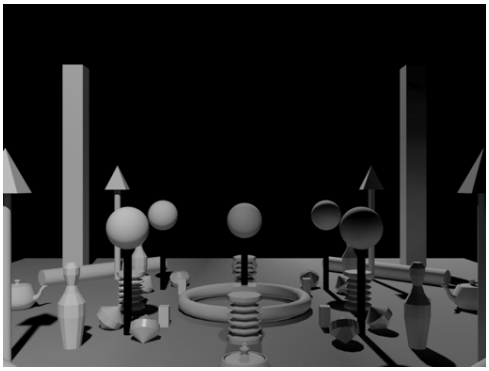

Figure 4.10: White spheres illustrating the probes positions (for 2LR, with veridical probe illuminations). Each scene contained five probes, four in each quadrant of the scene and one in the center of the scene. Only one probe was shown at a time. A probe did not produce a shadow in the trials.

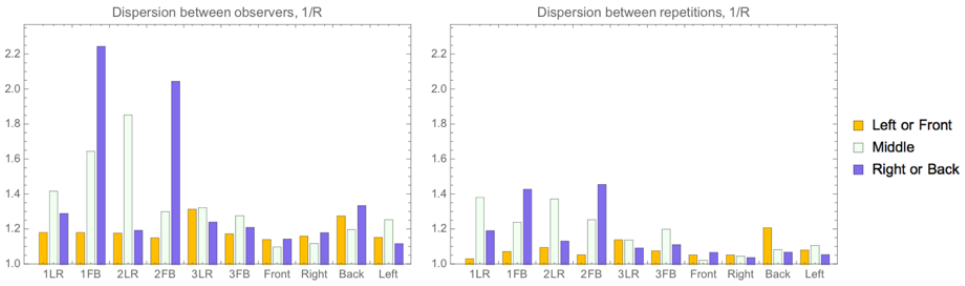

Figure 4.11: Inter- and intra-observers' variability of the directions of the settings (parameterized via the dispersion).

Experiment 1. Figure 4.11 shows that the dispersions are overall quite low, and that they are significantly lower between repetitions than between observers (paired t-test, n = 30: t = 3.04, p = 0.002<0.05). There are clear peaks for the B zones of 1FB and 2FB, both between observers and between repetitions. The peaks are even higher than on the middle sphere, where high dispersion could be expected because this probe is on the border between the light zones.

For comparison with the physical light directions for each probe, we calculated the mean angular differences between the veridical and the observers' inferred light directions (see Figure 4.12). These deviations from veridical again showed peaks for the B zones of 1FB and 2FB. We tested if deviations from the veridical values for back light zones are significantly different from deviations from the veridical values for front light zones. We made paired t-tests (n=60) of these groups for 1FB and 2FB. The differences

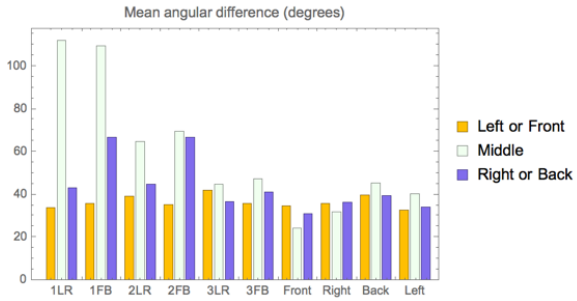

Figure 4.12: Deviations with respect to the veridical average light direction (light vector) as a function of condition.

are significant (1FB t= -4.91, p = 2.4x10^{-6}; 2FB t=4.46, p=0.000013). The large deviation from veridical that we find for the middle sphere of Condition 1 is due to the physical light direction being from below (light vector pointing down), while the observers inferred it to be from above.

We also analyzed the distributions of the directional settings. Since all the light sources were positioned on the same height (specifically, making a 45-degrees angle between light source, middle of the scene and the scene floor plane), the differences in their positions could be specified in the XY-plane / a top view. Figure 4.13 shows the circular histograms of the settings for the data of all test images, with the data grouped in three clusters as above. The red lines in the centres of the circles show the veridical light directions (red dots instead of lines mean that the veridical light vector points straight up or straight down). First, it is evident that the majority of the settings are close to the veridical directions. Thus, observers are well able to distinguish the light zones. If we take a closer look we can see that for the back light zone of 1FB and 2FB there is a number of settings in the direction opposite to the veridical, whereas this is not the case for the LR conditions. It appears from the plots that observers often made settings on the probe in the back light zone opposite to the actual illumination in that light zone, but in accordance to the illumination in the front light zone. Additionally, for these images the middle probe settings appear the same as those of the front probe, which is not the case for the LR conditions.

As we explained in the methods section, the two test images of the same light condition differed only in the direction of view. Thus, if the settings would only depend on light condition and not on viewing direction, the settings for the LR and FB cases should

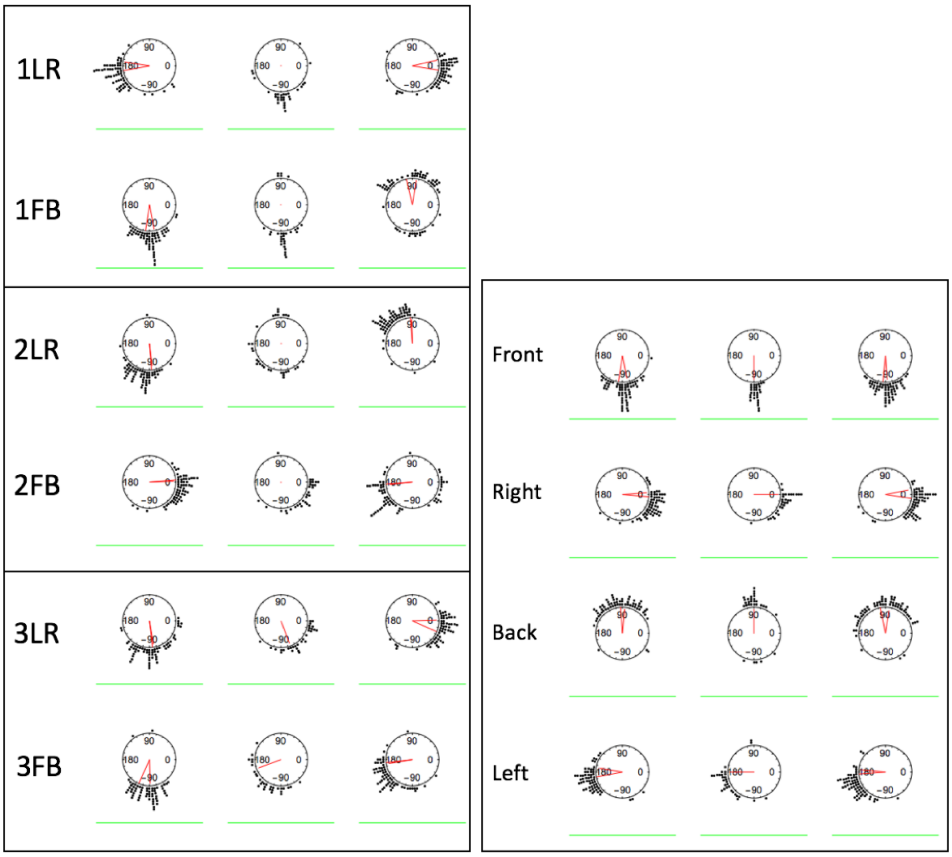

Figure 4.13: Top view circular histograms of direction settings. Settings are grouped such that the left histogram of a test image shows the settings made on the two probes in the left or front light zone (for LR or FB respectively), the middle histogram shows the settings on the middle sphere, and the right histogram shows the settings made on the two probes in the right or back light zone (for LR or FB respectively). The red lines in the center of the circles show the veridical light directions (red dots instead of lines mean that veridical light vector points straight up or straight down). The green line represents the picture plane.

be the same up to a 90 degrees rotation. For example, the settings in the L light zone of 1LR should be the same as in the F light zone of 1FB, after a 90 degrees correction. We tested the significance of the differences between pairs of directional settings (top view, as presented in Figure 4.13) after 90 degrees corrections. To this aim we used Watson's $U\hat{2}$ test (code by Megevand (`https://github.com/pierremegevand/watsons_u2`) based on equations by Zar (1999)) for circular distributions. First, we compared the settings between the couples of light zones under the same illumination (see Table 6.1). For example, L of 1LR vs. F of 1FB, and L of 2LR vs. B of 2FB. We found, see Table 1, that the front

Table 4.1: Examples of naming light properties in different fields

Comparison of settings between light zones	Front vs (rotated) corresponding zone	Back vs (rotated) corresponding zone
Light 1	0.067 (non-significant)	< 0.001 (significant)
Light 2	< 0.001 (significant)	< 0.001 (significant)
Light 3	0.433 (non-significant)	< 0.001 (significant)
Single light source settings: 4R and (mirrored) 4L; p = 0.117 (not significantly different), 4F and (mirrored) 4B; p < 0.001 (significantly different).		

light zones of all FB conditions were not significantly different from the corresponding zones of the LR conditions, except for light condition 2. However, the back light zones of all FB conditions were significantly different from the corresponding zones of the LR conditions. For the single light source condition the settings were compared for the pairs 4L vs. 4R and 4F vs. 4B. We compared the pairs after flipping. The settings of 4L did not differ significantly from the (mirrored) settings of 4R. There was a significant difference between settings 4F and (mirrored) settings for 4B.

4.4. DISCUSSION AND CONCLUSION

We investigated whether human observers can distinguish light zones that are determined by a difference in overall light direction. In the first experiment, we measured and analyzed visual light fields for two illumination conditions. In the second experiment, we created highly controlled stimuli to systematically investigate the influence of light zones' orientations. Specifically, we tested illumination perception in left-right and front-back orientations of light zones.

The distributions, spreads and visualizations of the first experiment's settings show that observers were able to distinguish the illumination differences between the light zones. This sensitivity we call visual light zones. There seemed to be a trend suggest-

ing that inter-observer spreads were larger than intra-observer spreads, especially for the front-back (FB) condition. The results of the second experiment confirmed the existence of visual light zones. In experiment 2 we again found that inter-observer spreads were larger than intra-observer spreads, indicating idiosyncratic behavior. Additionally, we found a difference between LR and FB orientations of light zones. In particular, the observers often made the settings in the back light zone of the FB conditions in accordance to the illumination in the front light zone of those conditions.

One of the reasons of the differences in the settings between the light zones orientations might be the visibility of light cues, e.g. shadows, shading and highlights (Boyaci et al., 2006, Koenderink et al., 2003; O'Shea et al., 2010; Ripamonti et al., 2004; Xia et al., 2014, 2017). In the left-right orientation each light zone took half of the picture plane, and therefore it was likely that in both light zones the cues were approximately equally well visible. In the front-back condition light cues in the back part might be less obvious than those in the front, because of occlusions and perspective / scaling. Boyaci et al. (2006) and Xia et al. (2017) demonstrated how in the presence of less (articulated) cues the veridicality of participants' settings declined. There are still many unanswered questions about light zones. One of the concerns is how the grouping of such patterns happens. Illuminance flow patterns (Pont et al., 2015) are a probable candidate as a cue for direction-based zones. The exact mechanisms are subject of further studies. Additionally, it needs to be studied how intensity, direction, diffuseness, and color interact in the perception of light zones. Furthermore, grouping light zones can be done at different scales of analysis. This scale (the dimensions of the light zones with respect to the scene) determines the relative size and the number of light zones in natural (usually complex) light fields. It determines for instance whether relatively small parts of a scene are determined to be a separate light zone or part of a larger one. In Koenderink et al's (2007) visual light field study we find an interesting example. They tested a position in their spotlight condition where the probe was in a relatively small shadow volume that was cast by one of the objects (penguins). Only one of eight observers inferred the probe to be in the shadow, but others adjusted the illumination on the probe as if it was in the spotlight. It might well be the case that visual light zones concern a rather coarse-scale analysis which neglects such fine-scale light variations. Further studies are needed to fully understand these mechanisms.

Our findings might help to understand the structure of the visual light field, which can contribute to several applied areas. In computer graphics volume zoning was intro-

duced for the case of participating media, e.g. dust or fog (Rushmeier & Torrance, 1987). We believe that research on light zones could be useful for automated creation of light probes (Chajdas et al., 2011). It would be also interesting to test the veridicality of perception of light on objects moving through light zones, extending the existing studies of lightness estimations of an object moving though differently illuminated areas (Toscani et al., 2016; Zdravkovic, 2008). Would observers notice it if a change of illumination on a moving object does not match the variations of the light in a space through which it is moving? How (in)sensitive are we to such changes? Can we simplify implementations by modelling complex natural light fields in a segmented model containing only a few zones with simple uniform / divergent / convergent light flows? Light zones are regularly used in architecture and light design. Madsen (2007) coined the concept and provided a number of practical architectural examples. There is a continuing interest in the topic from researchers in the field of architecture and lighting (Lindh, 2013; Trisha & Imran, 2014). We sharpened the definition of light zones, and provided an approach for measuring and evaluating their perception. Finally, our results confirmed the existence of visual light zones.

BIBLIOGRAPHY

Adams, A. 1948. The Negative: Exposure and Development. Ansel Adams Basic Photography Series/Book 2. Boston: New York Graphic Society. ISBN 0-8212-0717-2

Boyaci, H., Doerschner, K., & Maloney, L. T. (2006). Cues to an equivalent lighting model. Journal of Vision, 6(2), 106-118. https://doi.org/10.1167/6.2.2

Brainard, D. H. (1997). The psychophysics toolbox. Spatial Vision, 10, 433-436.

Chajdas, M. G., Weis, A., & Westermann, R. (2011). Assisted Environment Map Probe Placement. Proceedings of SIGRAD 2011.

Cuttle, C. (2003). Lighting by Design. Oxford: Architectural Press.

Cuttle, C. (2013). Research Note: A practical approach to cubic illuminance measurement. Lighting Research and Technology, 46(1), 31-34.

Gershun A. (1939) The light field. J. Math. Phys., 18, 51151 (translated by P. Moon and G. Timoshenko)

Gilchrist, A. (1977). Perceived lightness depends on perceived spatial arrangement. Science (New York, N.Y.), 195(4274), 185-187.

Hecht, H., van Doorn, a, & Koenderink, J. J. (1999). Compression of visual space in natural scenes and in their photographic counterparts. Perception & Psychophysics, 61(7), 1269-1286.

Kartashova, T., de Ridder, H., te Pas, S. F., Schoemaker, M., & Pont, S. C. (2015). The visual light field in paintings of Museum Prinsenhof: comparing settings in empty space and on objects. Proceedings of SPIE 9394, Human Vision and Electronic Imaging XX, 9394, 93941M.

Kartashova, T., Sekulovksi, D., de Ridder, H., te Pas, S. F., & Pont, S. C. (2016). The global structure of the visual light field and its relation to the physical light field. Journal of Vision, 16(9).

Kartashova, T., de Ridder, H., te Pas, S. F., & Pont, S. C. (under review) Light shapes: Perception-Based Visualizations of the Global Light Transport.

Koenderink, van Doorn, A. J., Kappers, A. M. L., te Pas, S. F., & Pont, S. C. (2003). Illumination direction from texture shading. Journal of the Optical Society of America. A, Optics, Image Science, and Vision, 20(6), 987-995.

Koenderink, Pont, S. C., van Doorn, A. J., Kappers, A. M. L., & Todd, J. T. (2007). The visual light field. Perception, 36(11), 1595-1610.

Leong, P., & Carlile, S. (1998). Methods for spherical data analysis and visualization. Journal of Neuroscience Methods, 80, 191-200.

Lindh, U. W. (2013). Distribution of light and atmosphere in an urban environment. J. of Design Research, 11(2), 126.

Lopez-Moreno, J., Sundstedt, V., Sangorrin, F., & Gutierrez, D. (2010). Measuring the perception of light inconsistencies. Proceedings of the 7th Symposium on Applied Perception in Graphics and Visualization - APGV '10, 1(212), 25.

Madsen, M. (2007) Light-zones(s): as Concept and Tool. ARCC Journal, 4(1), 50-59.

Mury, A. A, Pont, S. C., & Koenderink, J. J. (2007). Light field constancy within natural scenes. Applied Optics, 46(29), 7308-7316.

Mury, A. A, Pont, S. C., & Koenderink, J. J. (2009). Representing the light field in finite three-dimensional spaces from sparse discrete samples. Applied Optics, 48(3), 450-457.

Mury, A. A. (2009). The light field in natural scenes. Thesis (PhD). Technical University of Delft, Delft, The Netherlands.

O'Shea, J., Agrawala, M., & Banks, M. S. (2010). The influence of shape cues on the perception of lighting direction. Journal of Vision, 10(12), 21.

Ostrovsky, Y., Cavanagh, P., & Sinha, P. (2005). Perceiving illumination inconsistencies in scenes. Perception, 34, 1301-1314.

Pas, S. F., Pont, S. C., Dalmaijer, E. S., & Hooge, I. T. C. (2017). Perception of object illumination depends on highlights and shadows , not shading. Journal of Vision, 17(8), 1-15.

Pelli, D. G. (1997) The videotoolbox software for visual psychophysics: Transforming numbers into movies, Spatial Vision 10, 437-442.

Pont, S. C. (2009). Ecological optics of natural materials and light fields. Human Vision and Electronic Imaging XIV, Edited by Bernice E. Rogowitz, 7240, 724009-724009-12. Pont, S. C., Nefs, H. T., van Doorn, A. J., Wijntjes, M. W. A., te Pas, S. F., de Ridder, H., & Koenderink, J. J. (2012). Depth in Box Spaces. Seeing and Perceiving, 25, 339-349. https://

Pont, S. C., van Doorn, A. J., Wijntjes, M. W. A., & Koenderink, J. J. (2015). Texture, illumination, and material perception. Proc. of SPIE, 9394, 93940E.

Ripamonti, C., Bloj, M., Hauck, R., Mitha, K., Greenwald, S., Maloney, S. I., & Brainard, D. H. (2004). Measurements of the effect of surface slant on perceived lightness. Journal of Vision, 4(9), 747-763.

Rushmeier, H. E., & Torrance, K. E. (1987). The zonal presence of a participating medium. ACM SIGGRAPH Computer Graphics, 21(4), 293-302.

Schirillo, J. a. (2013). We infer light in space. Psychonomic Bulletin & Review, 20(5), 905-15.

Snyder, J. L., Doerschner, K., & Maloney, L. T. (2005). Illumination estimation in three-dimensional scenes with and without specular cues. Journal of Vision, 5(10), 863-877.

Toscani, M., Gegenfurtner, K. R., & Doerschner, K. (2017). Differences in illumination estimation in #thedress. Journal of Vision, 17(1), 22.

Toscani, M., Zdravkovic, S., & Gegenfurtner, K. R. (2016). Lightness perception for surfaces moving through different illumination levels. Journal of vision, 16(15), 1-18.

Trisha, S. H., & Imran, M. M. S. (2014). Light Zone: An Assessment Tool of Spatial

Depth and Aperture Height Relationship for Tall Office Buildings of Dhaka. Asian Journal of Applied Science and Engineering, 3(9), 72-87.

van Doorn, A. J., Koenderink, J. J., Todd, J. T., & Wagemans, J. (2012). Awareness of the light field: the case of deformation. I-Perception, 3(7), 467-480.

Xia, L., Pont, S. C., & Heynderickx, I. (2014). The visual light field in real scenes. i-Perception, 5(7), 613-629.

Xia, L., Pont, S. C., & Heynderickx, I. (2016a). Light diffuseness metric Part 1 : Theory. Lighting Res. Technol., 49(4), 411-427.

Xia, L., Pont, S. C., & Heynderickx, I. (2016b). Light diffuseness metric, Part 2 : Describing , measuring and visualising the light flow and diffuseness in three-dimensional spaces. Lighting Res. Technol., 49(4), 428-445.

Xia, L., Pont, S. C., & Heynderickx, I. (2017). Effects of scene content and layout on the perceived light direction in 3D spaces. Journal of Vision, 16(10), 1-13.

Zar, J. H. (1999). Biostatistical analysis. Pearson Education India.

Zdravkovic, S. (2008). Lightness constancy: Object identity and temporal integration. Psihologija, 41(1), 5-20.

5

Perception-Based Visualizations of the Global Light Transport

Abstract

In computer graphics, illuminating a scene is a complex task, typically consisting of cycles of adjusting and rendering the scene to see the effects. We propose a technique for visualization of light as a tensor field via extracting its properties (i.e. intensity, direction, diffuseness) from (virtual) radiance measurements and showing these properties as a grid of shapes over a volume of a scene. Presented in the viewport, our visualizations give an understanding of the illumination conditions in the measured volume for both the local values and the global variations of light properties. Additionally, they allow quick inferences of the resulting visual appearance of (objects in) scenes without the need to render them. In our evaluation, observers performed at least as well using visualizations as using renderings when they were comparing illumination between parts of a scene and inferring the final appearance of objects in the measured volume. Therefore, the proposed visualizations are expected to help lighting artists by providing perceptually relevant information about the structure of the light field and flow in a scene.

In print as: Kartashova, T., Pas, S. F., de Ridder, H., & Pont, S. C. (2018) Light shapes: Perception-Based Visualizations of the Global Light Transport. Transactions on Applied Perception, xx(x).

5.1. INTRODUCTION

Complex sceneries are ever-present in computer graphics either as a context of primary action (e.g. cinematography and game design) or as the main focus (e.g. architecture and interior design). Lighting plays a crucial role in modeling virtual scenes because of its strong influence on the appearance of objects, materials, and spaces. In turn, objects, materials and spaces influence the resulting light in a scene. For example, both the appearance of objects and the physically measured properties of the light differ in a room with white walls from that in a room with black walls (Xia et al. 2016a). Therefore, in order to consciously manage the looks of a scene, one should keep in mind the intricate model of all light interactions, a sheer impossible task. Common practice in computer graphics is the use of preview renderings to see the results of scene manipulations. A disadvantage of this approach is that inferring the illumination from a resulting image suffers from ambiguities of interactions between light, material and shape perception (Belhumeur et al. 1999; Marlow et al. 2012; Pont and te Pas 2006; Zhang et al. 2015) and consequently might be insufficient to understand how a certain light effect was achieved. Besides, a repetitive rendering wastes a significant portion of working time. Thus, an explicit visualization of light in a scene can be a powerful tool to help in the design of its appearance.

Conventional light visualizations for lighting designers, i.e. false-color plots of the luminance, show luminance distribution over the scene surfaces or planar cross-sections (e.g. Dialux, Lighting Analysis Assistant of Autodesk 3ds Max, LiteVis (Sorger et al. 2016)). This approach provides little more information than a simple rendering and is not enough to explain how light affects appearance including shading, shadowing, 3D texture, highlight contrast etcetera. In a recent review of artistic appearance, lighting and material editing approaches, Schmidt et al.(2016) recognised the necessity of methods conveying more information about lighting than preview renderings, while they also acknowledge the difficulty of light visualization because of its high dimensionality.

The visualization of light transport, which shows the propagation of light through a known 3D environment, is gaining attention in the computer graphics field. Many researchers (Reiner et al. 2012; Schmidt et al. 2013, 2016; Zirr et al. 2015) acknowledge the difficulty of light transport analysis and visualization because light travels in every possible direction through any point in an empty space and interacts in complicated manners with the environment. There is a number of studies on volumetric light visualization (see Section 2.1), yet many of those provide analyses that are too complex for many users in

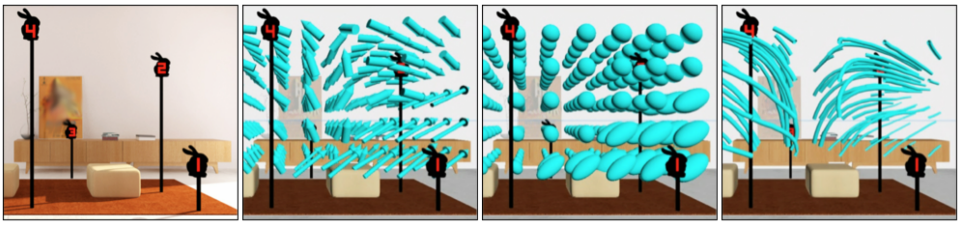

Figure 5.1: Fragment of a scene and three types of light visualizations. Left to right: scene rendering, arrows visualization, ellipsoids visualization, tubes visualization. Note that the visualizations were presented in a viewport, in which the default shading is incongruent with the actual light field and thus the visualizations provide the only cue to the light field. For the formal evaluations of our proposed methods we placed five bunnies' silhouettes (four shown) for comparison of light properties in each image.

the lighting design realm. Moreover, a lighting designer might not need to see all the light interactions in order to manipulate illumination in a scene. Most important is to judge the variations of light that have a strong influence on the human visual perception of objects/scenes. Our visualizations show perceptually relevant light properties, accessible to a user after a brief instruction.

We address light visualization from lighting design and perception perspectives, with a focus specifically on showing intensity (in our tool — mean spherical illuminance), direction and diffuseness of light. These three are the basic properties that underlie our visual experience of light, which are perceptually meaningful and make sense to anyone — in contradistinction to, for instance, the sixth order spherical harmonic component or number of photons in a specific direction. Moreover, these components are used as the basic building blocks to compose a light "atmosphere" in architectural perception-based lighting design (see Section 2.2). Consideration of only these parameters turns our light transport visualization problem into one of tensor field visualization, along with the concept of "light flow" that is well known and used in architectural lighting design (Ashdown, 1998; Cuttle, 1973; Cuttle, 2003). A tensor field can be visualized via a wide range of primitives that allow simultaneous representation of the three parameters. We chose three types of shapes: arrows, ellipsoids or tubes as presented in Figure 5.1.

Our main contribution is thus a new approach to light visualization inspired by insights from architectural lighting design and perception. The principal feature of our approach is visualizing perceptually relevant properties of light as a tensor field — in a manner that can be easily understood also by lighting artists without a computational background.

5.2. RELATED WORK

5.2.1. LIGHT TRANSPORT VISUALIZATION

In recent years, the visualization of light transport was addressed for several goals. Some researchers use light visualization to demonstrate the working of their computation methods or to study the optical mechanisms behind the light transport. Such representations often require a high level of technical expertise to understand them and are less suitable for practical purposes of light artists. For example, Durand et al. (2005) presented a signal-processing framework for analysis and visualization of space-angle frequency spectra of the radiance function. This framework was extended by Ramamoorthi et al. (2007) to gradient analysis of the basic shading steps, showing the relationship between spatial and angular effects on appearance. The technique of Zirr et al. (2015) provides information about the amount of light scattering in the neighborhood of a given point. Although they provide visualizations of light throughout the whole scene, their approach seems to be hard to grasp without understanding vector field topology and also quite time consuming, since stated computation time ranges from one to five hours. In contrast to the studies listed above, our goal is to visualize light in an intuitive way even for novice users.

One of the most straightforward methods of light transport visualization is showing it as rays or in the form of ray trees, light paths or light beams (Gribble et al. 2012; Nowrouzezahrai et al., 2011; Simons et al. 2016). In the field of optics, relevant studies have been done on capturing and visualizing physical light as traces of light through fluorescent liquids or frame-wise propagation of light (Hullin et al. 2008; Velten et al. 2013). However, such representations might be cluttered due to the presence of too many rays/paths and provide only directional information. Moreover, one should mentally integrate all rays to infer the final effect on the appearance of the scene. Schmidt et al. (2013) in their light-paths clustered the paths and contracted them towards the paths' medial axis within a user-specified region of interest. This approach reduces clutter, but still only tells about light paths' directions. Impressively, the authors also provided a possibility to manipulate the visualized light paths in physics based rendering contexts, and for example move shadows and caustics.

Another approach is to visualize certain properties of light transport in a volume of a scene. Reiner et al. (2012) proposed a set of light transport visualization tools for interactive exploration of scenes. Two of them translated a single probe measurement to a

spherical plot or a particle flow. To explore the whole scene a user needed to manually move the probe over the volume, seeing the results in each point separately, and then integrate them mentally. Their "light path inspection" tool recursively clustered measurements from other probes to show from which direction is a point illuminated and their "volumetric control" tool showed rasterized light paths in a volume. Chajdas et al. (2011), in their paper about environment map probe placement, selected probes' positions in sinks of irradiance gradient fields, which was visualized as a grid of arrows. Their illustrations give a clear impression of the irradiance gradient field (directional component) in a space. Jacobs (2014) proposed a similar technique in the Radiance lighting simulation software (Ward 1989). For multiple points in a grid, Jacobs showed the direction of light via an arrow direction and intensity (illuminance) as both arrow length and color. Mury et al. (2009) visualized the physical light (radiant flux transfer) using tubes. The light tubes are tangential to the light vector (net flux transfer) and their thickness is inversely proportional to the strength of the light vector (see section 3.1). Xia et al. (2016b) extended the tubes visualization by adding color saturation and brightness to represent the diffuseness and the light density, respectively.

In this paper we bring together the advantages of volumetric light visualizations listed above with knowledge of human perception (see Section 2.2) and apply that in visualizations that represent the variation of three perceptually meaningful light properties throughout a scene, underlying our visual experience of the light and basic components in lighting design. As representation shapes we chose arrows and tubes, because their suitability for light visualization was already demonstrated by Mury (2009) and Jacobs (2014), and ellipsoids, because we found their variation of proportions an interesting alternative to arrows.

5.2.2. PERCEPTUALLY RELEVANT LIGHT PROPERTIES

A professional involved in scene or image creation must know how to use light as a tool to change the appearance of that scene or image. Typically, lighting artists are guided by their own knowledge and trial and error procedures (Gershbein & Hanrahan, 2000; Kim & Noh, 2009). By repetitive adjusting, rendering and viewing a resulting scene they experiment until they are satisfied, judged via their visual perception of the result. Would there be a more efficient, scientifically informed manner to find what combination of light properties reveals their scene best?

The importance of intensity, direction and diffuseness of light for designing illumi-

Table 5.1: Examples of naming light properties in different fields

Field	Intensity	Direction	Diffuseness	Other
lighting design (Kelly 1952)	intensity and brightness	direction	diffusion	spectral color
photography (Hunter et al. 2007)	brightness	direction	contrast	color
perception (Koenderink et al., 2007)	intensity	direction	diffuseness	
computer graphics (Birn, 2013)	brightness	angle	softness	color temperature, throw pattern

nation are pointed out in multiple fields: architectural lighting design (Cuttle 2003; Descottes and Ramos 2013; Innes 2012; Kelly 1952; Livingston, 2014; Russell 2008), photography and drawing (Hunter et al. 2007; Yot, 2001), and, of course, computer graphics (Birn 2013; Brooker 2006). There is no universal terminology adopted by all fields, and authors describe the same (or very similar) properties in different terms, see the examples in Table 5.1. These light properties determine scene appearance for a large part (Ramamoorthi & Hanrahan, 2001a), for instance the modeling (how well 3D shape is brought out), material attributes (for instance 3D roughness textures or softness, Zhang et al., 2015), and spatial perception (for instance how wide or high a space looks). Here it should be noted that most natural materials show a major diffuse mode in their reflectance, and that the appearance of this mode is determined by these mathematically lower order light properties (the higher order ones are "diffused out", (Ramamoorthi & Hanrahan, 2001b)). Since we perceive light by its effects on objects and people in scenes, and not by looking directly at the sources, these properties also form the major part of our experience of light itself (Koenderink et al., 2007; Schirillo, 2013; Pont, 2013). In addition, the higher order angular frequencies of the spherical harmonic approach are important in a statistical sense, for instance for glossiness and atmosphere / gist perception.

Psychophysics provides a rich background for understanding how the human visual system processes interactions between light, shape and material (Fleming et al., 2003;

Fleming et al., 2004; Koenderink et al., 2003; Koenderink et al., 2006; Maloney & Brainard, 2010; Marlow et al., 2012; O'Shea et al., 2010; Pont & te Pas, 2006; Pont et al., 2015; Zhang et al., 2015). Perception of light properties was researched less extensively, yet there are multiple results that could be useful for computer graphics lighting artists.

Some studies focus on a single light property or a combination of two. For example, Lopez-Moreno et al. (2010) measured the accuracy of human vision in detecting lighting inconsistencies in images. Gerhard & Maloney (2010) investigated sensitivity to a change in light direction. Toscani et al. (2017) studied how changing the illumination intensity on a moving object influences the perception of the object's lightness. Morgenstern et al. (2014) found that performance on judging light direction is worse in diffuse light, largely because of intrinsic difficulty of lighting direction discrimination.

Koenderink et al. (2007) tested sensitivity of human observers to all three light properties in empty space. They created a binocularly viewed scene under three light conditions and placed a virtual white spherical probe on top of the scene images. Observers could control the lighting of the sphere. The task was to set the lighting of the sphere as if it was in the scene. They demonstrated that observers have robust expectations about a matte object's appearance in accordance to the illumination of a surrounding scene. Xia et al. (2015, 2017) confirmed these results for real scenes using a setup with two independently controlled scenes that were optically mixed via a semi-transparent mirror.

It is rather difficult to judge multiple light properties simultaneously and entirely in the observer's mind, because this task is complex due to their interactions and also because light is ungraspable and quite abstract "matter" to most people. If one needs to add spatial dimensions to the task, i.e. estimate the three light properties throughout a scene space, it becomes even harder. In an earlier study we (Kartashova et al., 2016) compared physical measurements of light fields in a scene under three illuminations and visual inferences on photographs of those conditions. We found that, although human observers have a robust impression of the light field, this impression is simplified with respect to the physical truth and agrees with homogeneous, converging and diverging superpatterns (van Doorn et al., 2012). In the current study we intended to visualize the light properties (intensity, direction and diffuseness) of which the influence on human perception of objects and space was confirmed by multiple studies and additionally, determine the global superpatterns in perception of light itself.

5.2.3. MEASURING AND VISUALIZING THE PHYSICAL LIGHT

Gershun (1939) first introduced the concepts light vector defined as the net transport of radiant power and light field describing the radiance arriving at a point x, y, z from direction θ, ϕ (thus, as a 5-dimensional function, usually called a "plenoptic function" in graphics). Ramamoorthi and Hanrahan (2001a) demonstrated that lighting for matte convex objects can be successfully approximated by the first three components of a spherical harmonics (SH) decomposition losing only about one percent of information. The SH components can be related to lighting design terms. The zeroth order component, a monopole, corresponds to ambient light, uniform light coming from all directions. The first order component is a dipole, the orientation of which matches the orientation of the light vector. The second order component is a quadrupole varying from a "clamp", illumination from opposite light poles (combined with a dark ring), to a "ring", illumination from a ring surrounding an object (combined with two dark poles). Consequently, the primary direction of light in a point can be derived from the orientation of the first order component. The diffuseness can be acquired from the ratio between the first and zeroth SH order components (Xia et al. 2016a) and intensity (mean spherical illuminance) can be acquired from the magnitude of the zeroth order component. Recently, Mury et al. (2007; 2009) demonstrated that the lower order SH components of physical light fields can be reconstructed for points in-between relatively few measurements using interpolation. This finding allows us to sample the light field using a limited amount of points in our measurement grids.

Mury et al. (2007; 2009) used a custom-made device called a "plenopter", with 12 sensors evenly distributed over a sphere to sample the second order SH approach to the light field. Note that the second order SH description has 9 coefficients, and therefore such a 12 sensors apparatus suffices to capture it. Xia et al. (2016b) showed how a cubic apparatus with only 6 sensors suffices to robustly measure the first order SH approach to the light field (having 4 coefficients) and that the ratio of the first and zeroth order determines the diffuseness. Moreover, they showed that the approach by Cuttle (2003; 2013), a researcher in the architectural light design field, comes down to the same measurements. Cuttle's formulas for the cubic meter are simpler to calculate than a SH approach (Xia et al. 2016b) and therefore we will use those.

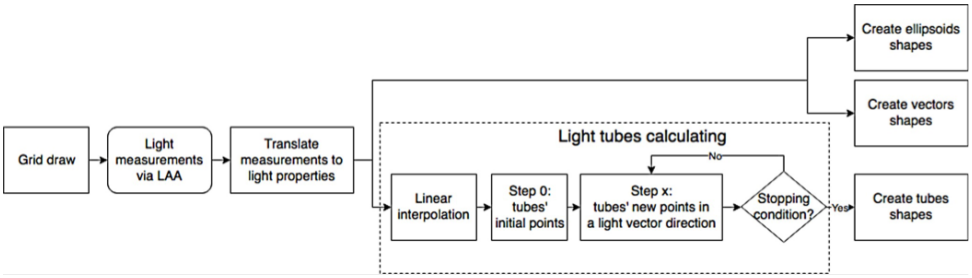

Figure 5.2: Workflow scheme of our prototype for visualizations creation. Light measurements are performed via the Lighting Analysis Assistant (LAA) tool of 3ds Max.

5.3. LIGHT VISUALIZATION FRAMEWORK

In this section, we describe the principles and the prototype of our light visualization tool. The objective of this paper was to visualize the light properties in such a way that observers are able to infer the light properties in a viewport preview as well as from a full rendering. Extracting just three perceptually relevant light properties from (virtual) measurements allows us to visualize light as tensor field via a grid of ellipsoids, arrows or tubes.

The workflow of our tool was as follows: the user specifies a volume in which the light should be visualized; our script creates a grid of sensors; the user makes and exports the measurements via the Lighting Analysis Assistant (LAA) tool of the Autodesk 3ds Max system; the resulting data is processed, imported back to the modelling environment (3ds Max in our case) and represented in the form of shapes (arrows, ellipsoids or tubes), which visualize the calculated light properties. The user can view the visualizations from an arbitrary viewing direction and manage the visualization shapes in a similar way as other objects in a scene (move, edit visibility, delete, etc.). Note that the objects in the viewport are typically "shaded" in a default manner that bears no relation to the actual scene illumination. So, in the viewport, the shapes of the visualizations are the only source of information about light.

It is important to note that our prototype is intended to merely demonstrate the potential of the proposed light visualization method. It consists of a script for placing the measurement grid, code for translating the measurements to light properties, calculating tubes and creating visualizations matrices, and a script for importing visualization matrices back into 3ds Max and creating the shapes in the volume of the scene in the viewport (see Figure 5.2). Each type of visualization represents the (variations of the)

light properties via (variations of) shapes' size, proportions and orientation.

Our prototype created a visualization about 2 to 10 times faster than it took to make a full rendering of the same scene. However, we will not focus on the performance times. The reason is that every component of the prototype might be brought to real-time performance using existing computer graphics algorithms. We did not explore the efficiency of the used algorithms because the focus of the paper was the perceptual rather than the computational efficiency. We overview possibilities of the prototype improvement in the discussion.

5.3.1. MEASUREMENTS

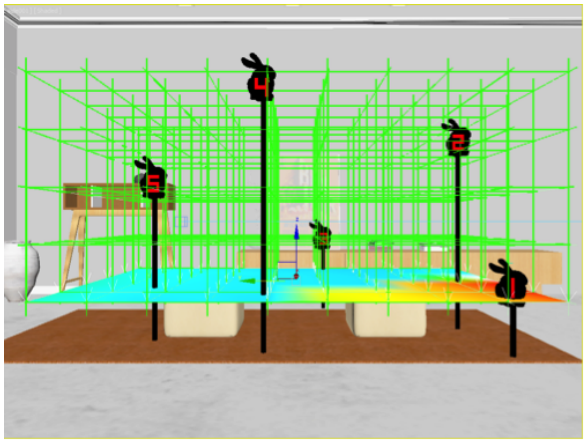

Figure 5.3: Measurements grid in one of the scenes. Measurement planes are shown as green lines. The lowest horizontal up-facing plane is colored according to its sensors measurements (for demonstration purposes) varying from red, high illuminance, to blue, low illuminance.

In our prototype of the visualizing tool, the (virtual) measurements are performed using the LAA, which allows creating planes with grids of sensors in arbitrary positions of modelled scenes (requires the use of the 3ds Max mental ray renderer). Our measurement script first needs the user-specified bounds of a volume for visualization and the number of measurements on each axis. Then it creates and places sensor planes evenly over that volume (see Figure 5.3). The grid of sensor planes is aligned such that in each measurement point there are six sensors, which face the positive and negative directions of each axis, as if they are on the six faces of a microscopic cube. Next, the user runs the measurements and batch-exports the results (a file for each plane) using LAA. The resulting data files contain the following (relevant for processing) information:

the position of each sensor, its orientation, and the amount of direct, indirect and total illumination arriving at the sensor. Then, our algorithm regroups the data from planes to points (sets of six measurements in each measurement point, forming a cubic illuminance measurement) and calculates the light properties according to Cuttle's (2003, 2013] formulas:

$$\mathbf{E}_{(x)} = \mathbf{E}_{x+} - \mathbf{E}_{x-} \tag{5.1}$$

$$|\mathbf{E}| = \sqrt{\mathbf{E}_{(x)}^2 + \mathbf{E}_{(y)}^2 + \mathbf{E}_{(z)}^2} \tag{5.2}$$

$$\sim E_X = \frac{\mathbf{E}_{x+} + \mathbf{E}_{x-} - |\mathbf{E}_{(x)}|}{2} \tag{5.3}$$

$$\sim E = \frac{\sim E_X + \sim E_Y + \sim E_Z}{3} \tag{5.4}$$

$$E_{scalar} = \frac{|\mathbf{E}|}{4} + \sim E \tag{5.5}$$

$$D = 1 - \frac{|\mathbf{E}|}{4E_{scalar}} \tag{5.6}$$

$\mathbf{E}_{x+}$, $\mathbf{E}_{x-}$ are the measurements in the positive and negative directions along the X axis (analogous for Y and Z). $\mathbf{E}_{(x)}$ is the light vector component (analogous for $\mathbf{E}_{(y)}$ and $\mathbf{E}_{(z)}$). $\mathbf{E}_{(x)}$, $\mathbf{E}_{(y)}$ and $\mathbf{E}_{(z)}$ constitute the light direction. $|\mathbf{E}|$ is the light vector magnitude.
$\sim$ E is the symmetric illuminance. E_{scalar} is the scalar illuminance or the mean illuminance in a point, which we took as measure of light intensity. The diffuseness D ranges from 0 (fully collimated light) to 1 (fully diffuse light).

5.3.2. VISUALIZATIONS

After converting the light measurements to light properties, the algorithm acts differently depending on the visualization type (arrow, ellipsoid, tube) as shown in Figure 5.2. For each visualization we describe the concepts behind it, and then explain how the light properties were processed and mapped to the geometrical properties of the shapes used.

Table 5.2: Demonstration of the visualizations' shapes' variations respective to variations of light conditions. The column Renderings contains images for varying light properties, the visualizations' columns contain shapes resulting from measurements in corresponding light conditions. In this table, the variations of the properties were achieved by changing lighting intensity, lighting direction and ground plane color in order to vary intensity (mean illuminance), direction and diffuseness, respectively.

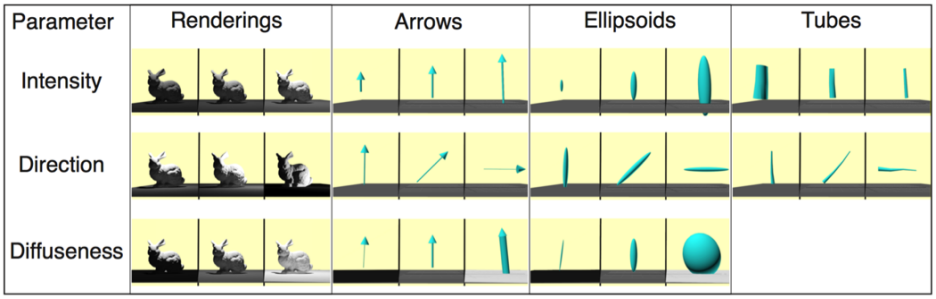

ARROWS

The arrows visualization is an extended version of Jacobs' (2014) representation of the set of light vectors pointing at the directions where, locally, on average, the light comes from. In his visualization Jacobs showed light intensity through both the size and colour of an arrow, whereas in our approach we visualize the mean illuminance through the arrow length, and the diffuseness through the width of the arrow shaft: the thicker shaft, the more diffuse (less directed) the light is (see Table 5.2). An arrow is a perfect visualization for the light direction, since it is the most reasonable representation of a vector. The arrowhead-shaft ratio is a suitable visualization for the diffuseness, because the arrowhead is always of the same size whereas the ratio with the shaft thickness differs, so the shaft thickness judgments do not suffer of perspective distortion.

Having the light properties calculated for each measurement point, the algorithm saves them as a matrix consisting of measurement coordinates and corresponding light properties. Then the user can run the script for the arrows which imports this matrix back into 3ds Max, and draws arrows at the measurement points. The script aligns the directions of the arrows with the directions of the light vectors using rotations. The lengths and widths of the arrows are initialized as a constant, which can be adjusted in the script to fit the arrows to the size of a scene, and then automatically scaled with respect to the light properties in each point.

ELLIPSOIDS

The concept behind the ellipsoids visualization is similar to that for the arrows, and is inspired by tensor visualization (Westin et al. 1999). Like arrows, ellipsoids were chosen for their ability to represent multiple properties through variation of proportions. The orientation of the long axis of the ellipsoid is aligned with the light vector. The length of the long axis of each ellipsoid corresponds to the mean illuminance. The proportion of the short and long axes corresponds to the diffuseness. Thus, the more spherical the ellipsoid is, the less pronounced the direction appears, and the higher the diffuseness is. Fully diffuse light does not have a dominant direction, and is thus represented by a sphere.

The ellipsoids show intensity variations via size differences. This visualization suffers from a 180 degrees direction ambiguity, because of the ellipsoid's symmetry. Additionally, the perspective affects the apparent size of the ellipsoids. The ellipsoids are generated in a very similar manner as the arrows. First, they are initialized as spheres in every measured point, then the long axes are stretched linearly with respect to their values of 1/diffuseness, and finally rotated to match the light vectors' directions.

TUBES

The light tubes visualization was first introduced by Gershun (1939) and first sampled and visualized throughout a real scene by Mury et al. (2009). A tube is always tangential to the light vector and in our visualizations its width is inversely proportional to the mean illuminance (in Gershun and Mury et al.'s approach width was inversely proportional to the strength of the light vector). The intuition behind this choice is derived from fluid flow representations: the smaller the tube, the stronger the flow.

In empirical studies it was found that usually a tube starts at a light source and finishes at a light absorbing surface while getting thicker — and that the set of tubes representing the "light flow" (Cuttle 1973) shows a structure diverging out from the source (Kartashova et al. 2016; Mury et al. 2009). An advantage of the tubes is that they show in one glance the "flow of light" through the scene. Thus, a user can see the global light flow structure without the need to "mentally interpolate" discrete measurements. The diffuseness could be represented on the tubes via color, brightness or pattern of texture (Xia et al. 2016b). However, in the current study we chose to restrict our visualizations to variations of shape, to allow fair comparisons in the user study.

The generation process of the tubes differs from that of the arrows and ellipsoids, because a tube represents (interpolated) values over several points. After calculating the light vectors and mean illuminances for all measurements, the linear interpolation function is calculated for both properties independently. In order to calculate the tubes, our algorithm iteratively calculates points constituting tube paths through the volume plus mean illuminances at those points for the widths of the tubes. Before running the algorithm, a user defines how many tubes should be visualized for each axis, plus the initial thickness of the tubes, and the number of iterations of the algorithm. These settings need to be manually adjusted to the size of the scene and the complexity of light properties' variations over the volume. For example, for more complex luminous environments it might be better to use many thin tubes instead of a few thicker ones, in order to show subtle and fine-grained variations of the light flow structure. The algorithm calculates the first values for the matrix by setting the starting points for the tubes paths, such that the tubes origins are evenly distributed over the visualization volume. The mean illuminances and light vectors' directions for the starting points are calculated using the linear interpolation functions. On the next and following iterations, the algorithm makes a step of user-defined step size in the light vector direction, saves the new coordinates, then calculates the light vector direction and mean illuminance of the new point. The ending condition for each tube is either reaching a predefined maximum number of steps, or the tube leaving the measured volume, or the tube fluctuating in a small area (which usually means that the tube reached a light source in the visualized volume). Finally, a separate script imports the resulting matrix into 3dsMax and visualizes the tubes using splines. At this point, the tubes' initial widths can be manually scaled with respect to the size of the scene. The paths of the tubes correspond to the points recorded in the matrix.

5.4. USER STUDY

We evaluate the performance of our visualizations through a user study, in which 14 participants perform two types of tasks, one related to comparison of light conditions between parts of the scenes and the other to inferring the appearance of objects.

5.4.1. GOAL

In renderings, inferences of light properties are made based on cues resulting from interactions of the light with the environment (shadows, shading, highlights etc.), while the arrows/ellipsoids/tubes visualizations (AET visualizations) directly represent the light

properties. So, the perceptual processes underlying these inferences are different. We performed a psychophysical user study in order to evaluate how informative the AET visualizations are for estimating the light properties in comparison with rendered images.

We set up an experiment investigating two typical actions in a 3D light designer workflow (Pellacini et al. 2007; Gershbein and Hanrahan 2000): 1) comparing light conditions between parts of a scene and 2) inferring what the appearance of an object would be if that object would be placed in a specific location in the scene, based on the light conditions in that location. The stimuli consisted of renderings of the scenes or one of the AET visualizations in the scenes. In the first part of the study participants were asked to rank order three positions in the scene with respect to a specific light property. In the second part of the experiment we showed several objects that were rendered in the scene and then presented in isolation, without a background, and asked observers to match those objects to locations in the scene.

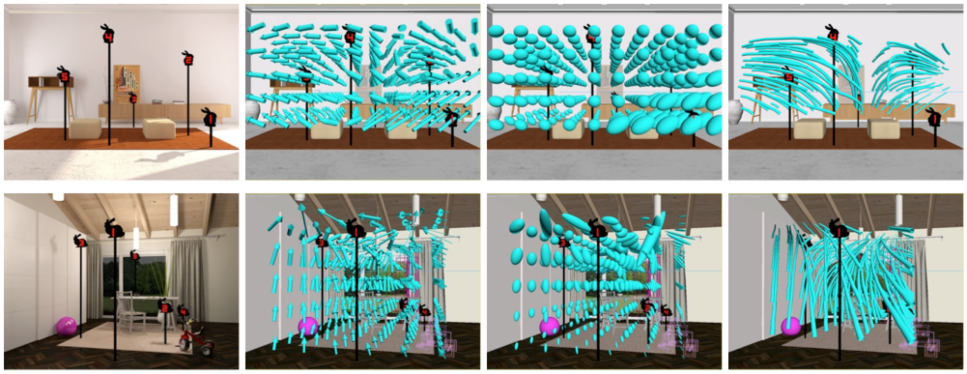

Figure 5.4: Examples of the renderings and light visualizations for two scenes (first row Room 1 Illumination 1, second row Room 2 Illumination 2). Left to right: scene rendering, arrows visualization, ellipsoids visualization, tubes visualization.

5.4.2. SCENES

We illuminated three models of rooms, each in two ways, so that observers could not match one-to-one scene geometry and illumination. For each of the resulting 6 scenes we created renderings and visualizations (see examples in Figures 5.1, 5.4, 5.5, 5.6). The AET visualizations were placed in most of the scenes' empty volume, in grids of 6x10x5 shapes for the arrows and ellipsoids and a corresponding starting positions' grid for the tubes. The renderings were done for output images sized 800x600 pixels and the follow-

ing renderer setup: mental ray, minimum one sample per pixel, maximum 128 samples per pixel, maximum 500 photons per sample. The majority of the objects in the scenes were matte. We used area light sources (flat or spherical).

In order to refer to specific positions we added five (Stanford) bunnies in the measured volumes of every scene. Each bunny was attached to a pole standing on the floor or another horizontal surface to depict the position of the bunny in the scene. We placed the bunnies such that the light properties in their locations differed widely between bunnies. As the processing speed of our prototype is not real-time, we captured the viewport and renderings of the scenes in advance, and then demonstrated the resulting images in the experiment interface.

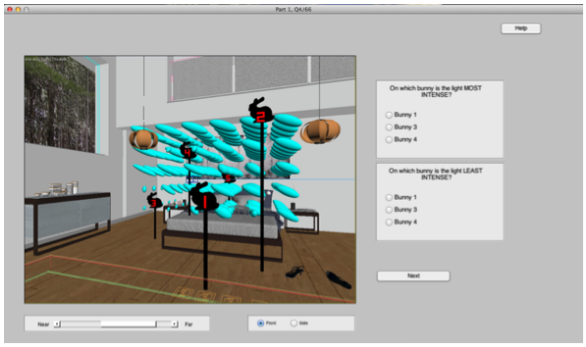

Figure 5.5: Experiment interface, part 1. The stimulus is at top left (Room 3, Illumination 1); the view control block is below the stimulus; the help button is at the top right; the Q&A block asking to compare a property value between the bunnies is at bottom right.

5.4.3. INTERFACE AND TASKS

The user interface of both parts of the experiment consisted of a scene block, question and answer (Q&A) block, view control block and help button. In each trial a scene rendering or visualization was presented in the scene block. Each scene contained bunnies presented as silhouettes. All bunnies were rotated such that they had the same silhouettes, independent of their position in the scene. The view control block had radio buttons for selecting the frontal or the side viewing direction, and a slider for stepping through the visualizations in depth (four layers, not active for the renderings). Moving the slider made closer shapes invisible, in order to see the further ones without occlusions. The help button opened a window with a short explanation of the visualizations and examples of them for a scene not used in the experiment.

In part 1 of the experiment (see Figure 5.5) participants rank ordered three bunnies according to one light property. Specifically, in each trial we asked two questions, one to pick the bunny with the highest, and one to pick the bunny with the lowest value of the property:

- On which bunny is the light most intense? / On which bunny is the light least intense?
- On which bunny is the light direction closest to straight from above? / On which bunny is the light direction furthest from straight from above?
- On which bunny is the light most diffuse? / On which bunny is the light least diffuse?

In part 2 (see Figure 5.6) we asked observers to match five white, Lambertian shaded bunnies in the Q&A block to five bunnies' silhouettes in the scene according to the expected appearance of the bunnies at the positions of the silhouettes. The order of the images of the bunnies in the Q&A block was randomized. When the observer changed the viewing direction of the scene, the images of the shaded bunnies also changed accordingly. The interfaces did not allow picking the same answers for both questions in part 1 and for picking the same number for two shaded bunnies in part 2.

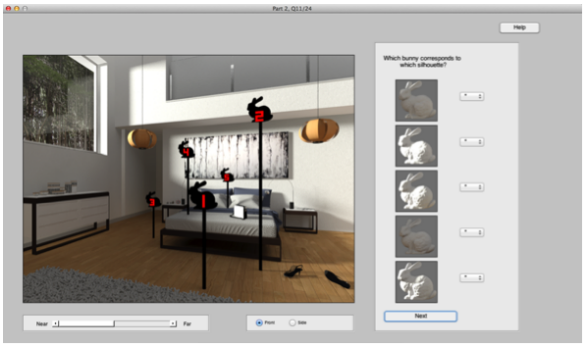

Figure 5.6: Experiment interface, part 2. The stimulus is at top left (Room 3, Illumination 1); the view control block is below the stimulus; the help button is at the top right; Q&A block, asking to match the bunnies to their positions in the scene is at the bottom right.

Before the start of the experiment all observers did a training session, in which we checked whether they understood the interface, tasks, and visualizations (e.g., how a shape variation reflects a light property). It was not possible to pass a trial of the training

session without picking the correct answers. After this, a participant first went through part 1 of the experiment, then through part 2. Part 1 consisted of tests for 6 scenes for three properties (two for the tubes where diffuseness was excluded) and four conditions (renderings, arrows, ellipsoids and tubes), making 6x3x3+6x2x1=66 trials. Part 2 consisted of six scenes and four conditions (renderings, arrows, ellipsoids and tubes), so 24 trials in total. The order of trials in both parts was randomized.

5.4.4. PARTICIPANTS

Two groups of seven participants took part in this experiment. The first group consisted of observers who took part in many visual perception experiments, but did not have experience in computer graphics; the second group consisted of participants with expertise in computer graphics, but did not have experience with visual perception experiments. All participants had normal or corrected-to-normal vision. They all gave written, informed consent. All experiments were done in agreement with the Declaration of Helsinki, Dutch Law, local ethical guidelines, and were approved by the TUDelft Human Research Ethics Committee.

5.4.5. RESULTS

As a metric of performance we took the percentage of correct answers over all participants and scenes. We compared the results between the two groups of participants (p-value and 95% confidence interval), the experienced observers and the computer graphics professionals, and did not find a significant difference in their results. There was some variation of results between tasks (scenes), but the reason was in the difficulty of the task. For example, in the scene in Figures 5.5 and 5.6, bunny number 4 was in the cast shadow of the lamp, which was not noted by most observers in the renderings, and hardly, but more, noted in the visualizations conditions. For both Part 1 and Part 2 of the experiment results over all scenes and all observers were above chance levels. The chance levels for part 1 were 0.5 and 0.167 (expressed as fraction correct) for at least one correct and all correct answers, respectively. The chance levels for part 2 were 0.633, 0.258, 0.0917, and 0.008 for at least one, two, three and five (i.e. all) correct answers, respectively. We present the results as bar charts, which show the fractions of correct answers for each condition over all scenes and all observers (see Figure 5.7).

For part 1 we found the largest fraction of correct answers for the ellipsoids for intensity (mean illuminance), for the arrows and tubes for direction, and for the arrows

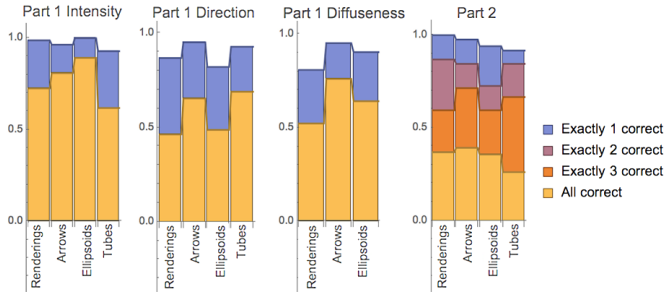

Figure 5.7: Experiment results, left to right: Part 1 fractions correct for intensity (mean illuminance), direction, diffuseness, Part 2. The boxplot shows the fractions of fully or partially correct answers. The results are stacked bottom-up, so that all correct answers bars are on the bottom. Thus, to know the fraction of at least N correct, one should sum up bars from all correct to exactly N correct. For example, in Part 2 the fraction of trials, in which observers made at least three correct answers using renderings, is around 0.6.

5

for diffuseness (see Figure 5.7). For part 2 (see Figure 5.7, last graph) the results show different patterns depending on how many bunnies were matched correctly. For example, renderings are the best for matching at least one bunny correctly, but the the arrows show the best results for matching all and at least three bunnies correctly.

We evaluated the significance of the differences between renderings and each of the visualizations via z-tests (two-sided p-value<0.017 after Bonferroni correction) and confidence intervals (CI, 95%). In part 1 (for All correct results), results for ellipsoids were significantly better than for renderings for interpreting intensity, whereas the results for arrows and tubes were not significantly different from those for renderings. For direction, arrows and tubes were significantly better than renderings, and results for ellipsoids were the same as for renderings. For diffuseness, arrows were significantly better than the renderings, and ellipsoids were not different. For part 2, the fractions correct did not differ significantly between renderings and visualizations.

In summary, we found that in both parts using visualizations lead to the same or better performance as using renderings. These results show that the visualizations indeed help to compare light conditions in parts of a scene volume and to infer the resulting appearance of objects placed in a visualized volume. Depending on the specific property of light one wants to judge (intensity, direction, diffuseness), ellipsoids, tubes or arrows give the most optimal visualization.

5.5. DISCUSSION AND FUTURE WORK

The user study results demonstrate that for our comparison task (part 1) the visualizations, overall, resulted in more correct answers than the renderings. For the matching task (part 2) the visualizations performed as good as the renderings. Comparing the visualizations with each other was not the main purpose of this user study. We believe, and an informal survey with our participants confirmed, that the choice of shape type here was probably a matter of personal preference. The main result is that all of them showed better or not significantly different performance compared to renderings. We consider the experiment outcomes promising, taking into account that the visualizations were demonstrated in the viewport, and thus their shapes provided the only information about the light in the scene.

It might appear surprising that using a schematic geometric representation of light properties resulted in equal performance to a fully-developed rendering. The reason for such a result might be that, as shown by multiple psychophysical studies, the human visual system cannot veridically extract illumination information from light cues (Kartashova et al. 2016; Koenderink et al. 2007; Lopez-Moreno et al. 2010; Marlow et al. 2012; Ostrovsky et al. 2005; Xia et al. 2014). Therefore, it will be difficult for an observer to estimate light properties throughout the empty space of a complex scene. Our visualizations show the light properties explicitly and veridically, which makes them equipotential to renderings for both inferring the variations of the light properties over the scenes and predicting the appearance of objects under the visualized illumination. One could argue that since our visualizations represent light properties and thus what an object would look like in a certain point in space, an alternative could be rendering a grid of simple probe objects in the empty space of a scene. However, such method would require the rendering of every probe object separately, because otherwise the objects would disturb the scene and each others' illumination (e.g. casting shadows on each other). Additionally, visual guesstimation of light direction and diffuseness from probe appearances suffers from the direction-diffuseness and other ambiguities (Pont & te Pas, 2006, Pont & Koenderink, 2007).

In comparison with existing light visualization approaches, our tool has a number of advantages. As Reiner et al. (2012) stated, many of the existing methods are very complex and allow only experts to analyze the light transport (Durand et al., 2005; Ramamoorthi et al., 2007; Zirr et al., 2015). Contrarily, we convert measurement results of complex natural light into three perceptually meaningful parameters that are intuitive also to non-

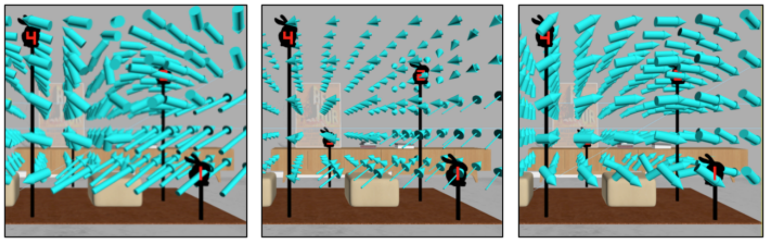

Figure 5.8: Example of visualizations in which we show from left to right: visualizations of the light (as in the rest of this paper), only the direct light, only the indirect light.

expert-users. Unlike light rays or paths visualizations (Hullin et al. 2008; Gribble et al. 2012; Nowrouzezahrai et al., 2011; Schmidt et al., 2013; Simons et al. 2016 Velten et al. 2013), we show pre-processed information that allows users "to see the forest through the trees," i.e. to understand the structure of the light field and its properties variations in one glance. Finally, different to the most common light visualization tool — the false color plot — our visualizations represent light in a volume, giving much more information about how scene appearance is related to the potential origins of light effects and its interactions with the materials and geometry in the scene.

The inherent characteristics of the proposed tool imply some limitations. First, the concept of reducing visualized information to three light properties eliminates all finer angular features of the light distribution. For example, if a point would be illuminated by two light sources, the visualization would show the average light direction between those sources. A solution for this issue could be adding the so-called squash tensor (Mury et al., 2007), second order of spherical harmonics is neglected in our visualizations, while it is also important for the appearance of matte objects (Ramamoorthi & Hanrahan, 2001a). Mury et al. (2007) showed how this property can be visualized. Moreover, addition of a summary metric of the higher (> 2) orders could show the remaining "light texture" or "brilliance" (Pont, 2018). Using our visualizations one would also not be fully able to predict the reflections on a specular object. Perceptually, the specularly reflected higher order structure of the light field is assumed to be relevant in a statistical sense only, as a "light texture" or what architectural lighting designers call "the play of brilliance" (Kelly, 1952; Mury et al., 2007; Pont, 2013). In the future we will study how this light property can be described and visualized.

We see several possible ways to improve and expand the proposed approach. In terms of processing speed, the technique could be significantly improved by implement-

ing a different tool for the light measurements instead of LAA, for example capturing the full irradiance distribution function (Reiner et al. 2012). We could apply flow visualization techniques for making the visualizations clearer, for example using streamline seeding techniques for placing the measurement points. Other variables to consider in this regard are the grids' density, shapes' size, and transparency. Moreover, the scaling of the shapes could be adjusted in various ways, depending on the scene environment and goals of the user. One option would be using logarithmic scaling for scenes with large intensity ranges. Adding texture to the shapes might provide more information, for example to show the light diffuseness. Texturing ellipsoids to imitate shading congruent with the light properties would closely approximate an object's appearance. Furthermore, the color of the shapes can represent the color of the measured light, considering that color is also a common property to describe light. This, however, will require extending the measurement method. Superquadrics (Kindlmann, 2004, Schultz et al., 2010) might be an alternative to the ellipsoids shapes. Splitting the direct and indirect contributions of the light also might produce interesting and useful results. In Figure 5.8 we show an example of such split arrows visualizations and it is insightful to see how the directions and diffuseness differ for the two contributions while both contributions show very systematic global structures. Finally, it might be possible, though very challenging, to find a method of editing light transport via editing the visualizations, similarly to what was done in work by Schmidt et al. (2013).

5.6. CONCLUSION

In this paper, we introduced a new approach to visualizing the light in modeled scenes via translating radiance measurements into three light properties which can be visualized as tensor fields. A distinctive feature of our approach is visualizing light in the whole volume of a scene. Zirr et al. (2015) commented that many of the recent visualization techniques focus on local regions only, therefore in order to understand the global picture a user should manually place a visualization tool around a scene to explore it. The main idea of this paper is to extract important properties of light and visualize them as a 3D flow. We proposed three perceptually-relevant properties, because they strongly influence the visual appearance of the surrounding world and are widely used in light design in various fields. With our technique, the global changes of light properties can be seen at a glance and from arbitrary viewpoints. Finally, it is rather simple and straightforward in implementation. Measurements can be performed by virtual sensors or even

a grid of cameras (or in a real scene, allowing architectural applications). The light properties extracting formulas do not require complex calculations. Shape creation is done using basic shapes and splines. Thus, our visualization technique is a promising tool, which, at the same time, is easy to replicate using the presented methods. The work of a digital light artist/designer is often described as a tedious process of hundreds repeated adjustments and renderings guided mainly by the artist's intuition (Gershbein and Hanrahan 2000; Kim & Noh 2009; Pellacini et al. 2007). Our visualization approach strives to increase their work efficiency by providing quick and qualitative representation of the light conditions. Using such tool, a light artist can see the changes of light intensity, direction and diffuseness over a scene and after modifications.

BIBLIOGRAPHY

Ashdown, I. (1998). The Virtual Photometer - Modeling the Flow of Light. 1998 IESNA Conference Proceedings, (October), 437-452.

Belhumeur, P. N., Kriegman, D. J., & Yuille, A. L. (1999). The bas-relief ambiguity. International Journal of Computer Vision, 35(1), 33-44.

Birn, J.. 2013. Digital Lighting and Rendering (3rd Edition).New Riders.

Brooker, D.. 2006. Essential CG Lighting Techniques with 3ds Max. Focal Press.

Chajdas, M. G., Weis, A., & Westermann, R. (2011). Assisted Environment Map Probe Placement. Proceedings of SIGRAD 2011.

Cuttle, C. 1973. The sharpness and the flow of light.

Cuttle, C. 2003. Lighting by Design. Architectural Press, Oxford.

Cuttle, C. 2013. Research Note: A practical approach to cubic illuminance measurement. Lighting Research and Technology 46, 1 (aug 2013), 31-34.

Descottes, H. and Ramos, C. E. 2013. Architectural Lighting: Designing with Light and Space. Princeton Architectural Press.

Durand, F., Holzschuch, N., Soler, C., Chan, E., & Sillion, F. X. (2005). A frequency analysis of light transport. ACM Transactions on Graphics, 24(3), 1115.

Fleming, R. W., Dror, R. O., & Adelson, E. H. (2003). Real-world illumination and the perception of surface reflectance properties. Journal of Vision, 3, 347-368.

Fleming, R. W., Torralba, A., & Adelson, E. H. (2004). Specular reflections and the

perception of shape. Journal of Vision, 4(9), 798-820.

Gerhard, H. E., & Maloney, L. T. (2010). Estimating changes in lighting direction in binocularly viewed three-dimensional scenes. Journal of Vision, 10, 14.

Gershbein, R., & Hanrahan, P. (2000). A fast relighting engine for interactive cinematic lighting design. Proceedings of the 27th Annual Conference on Computer Graphics and Interactive Techniques, 353-358.

Gershun, A. (1939). The Light Field (Translated by Moon P. and Timoshenko G.). Journal Of Mathematics And Physics, 18(2), 51-151.

Gribble, C., Fisher, J., Eby, D., Quigley, E., & Ludwig, G. (2012). Ray tracing visualization toolkit. Proceedings of the ACM SIGGRAPH Symposium on Interactive 3D Graphics and Games - I3D '12, 1(212), 71.

Hullin, M. B., Seidel, H., & Lensch, H. P. A. (2008). Direct Visualization of Real-World Light Transport.

Hunter, F., Biver, S., & Fuqua, P. (2007). Light Science and magic. Burlington: Focal Press, Elsevier Inc.

Innes, M. (2012) Lighting for interior design. Laurence King Publishing Ltd.

Jacobs, A. (2014) Radiance Cookbook. http://www.jaloxa.eu/.

Kartashova, T., Sekulovksi, D., de Ridder, H., Pas, S. F., & Pont, S. C. (2016). The global structure of the visual light field and its relation to the physical light field. Journal of Vision, 16(9).

Kelly, R. (1952). Lighting as an Integral Part of Architecture. College Art Journal, 12(1), 24-30.

Kindlmann, G. (2004). Superquadric Tensor Glyphs. Joint Eurographics - IEEE TCVG Symposium on Visualization, 1-8.

Kim, Y., & Noh, J. (2009). LightShop: An interactive lighting system incorporating the 2D image editing paradigm. In Advances in Visual Computing (pp. 59-70). Berlin: Springer Berlin Heidelberg.

Koenderink J., van Doorn, A. J., Kappers, A. M. L., te Pas, S. F., & Pont, S. C. (2003). Illumination direction from texture shading. Journal of the Optical Society of America. A, Optics, Image Science, and Vision, 20(6), 987-995.

Koenderink, J. & van Doorn A. J. (2006). Shape from Shading. In: Paragios N., Chen

Y., Faugeras O. (eds) Handbook of Mathematical Models in Computer Vision. Springer, Boston, MA.

Koenderink, Pont, S. C., van Doorn, A. J., Kappers, A. M. L., & Todd, J. T. (2007). The visual light field. Perception, 36(11), 1595-1610.

Livingston, J. (2014) Designing with light: the art,science, and practice of architectural lighting design. Hoboken: John Wiley & Sons.

Maloney, L. T., & Brainard, D. H. (2010). Color and material perception: achievements and challenges. Journal of Vision, 10.

Morgenstern, Y., Geisler, W. S., & Murray, R. F. (2014). Human vision is attuned to the diffuseness of natural light. Journal of Vision, 14(2014), 1-18.

Lopez-Moreno, J., Sundstedt, V., Sangorrin, F., & Gutierrez, D. (2010). Measuring the perception of light inconsistencies. Proceedings of the 7th Symposium on Applied Perception in Graphics and Visualization - APGV '10, 1(212), 25.

Marlow, P. J., Kim, J., & Anderson, B. L. (2012). The perception and misperception of specular surface reflectance. Current Biology, 22(20), 1909-1913.

Mury, A. a, Pont, S. C., & Koenderink, J. J. (2007). Light field constancy within natural scenes. Applied Optics, 46(29), 7308-7316.

Mury, A. a, Pont, S. C., & Koenderink, J. J. (2009). Representing the light field in finite three-dimensional spaces from sparse discrete samples. Applied Optics, 48(3), 450-457.

Nowrouzezahrai, D., Johnson, J., Selle, A., Lacewell, D., Kaschalk, M., & Jarosz, W. (2011). A programmable system for artistic volumetric lighting. ACM SIGGRAPH 2011 Papers on - SIGGRAPH '11, 1(212), 1.

O'Shea, J., Agrawala, M., & Banks, M. S. (2010). The influence of shape cues on the perception of lighting direction. Journal of Vision, 10(12), 21.

Ostrovsky, Y., Cavanagh, P., & Sinha, P. (2005). Perceiving illumination inconsistencies in scenes. Perception, 34, 1301-1314.

Pellacini, F., Battaglia, F., Morley, R. K., & Finkelstein, A. (2007). Lighting with paint. ACM Transactions on Graphics, 26(2).

Pont, S. C., & te Pas, S. F. (2006). Material - Illumination ambiguities and the perception of solid objects. Perception, 35(10), 1331-1350.

Pont, S. C., & Koenderink, J. J. (2007). Matching illumination of solid objects. Percep-

tion & Psychophysics, 69(3), 459-468.

Pont, S. C. (2013) Spatial and Form-Giving Qualities of Light. In Handbook of Experimental Phenomenology, Liliana Albertazzi (Ed.). John Wiley and Sons, Ltd.

Pont, S. C., van Doorn, A. J., Wijntjes, M. W. A., & Koenderink, J. J. (2015). Texture, illumination, and material perception. Proc. of SPIE, 9394, 93940E.

Pont, S.C. (2018) Optical and Perceptual Phenomena of Light - and the brilliance of fire flies. In: Ivana Franke: Retreat into Darkness. Towards a Phenomenology of the Unknown. (Editors: Ivana Franke, Heike Catherina Mertens, Katja Naie). Schering Stiftung, Berlin, Germany.

Ramamoorthi, R., & Hanrahan, P. (2001a). An efficient representation for irradiance environment maps. Proceedings of the 28th Annual Conference on Computer Graphics and Interactive Techniques SIGGRAPH 01, 64, 497-500.

Ramamoorthi, R., & Hanrahan, P. (2001b). On the relationship between radiance and irradiance: determining the illumination from images of a convex Lambertian object. Journal of the Optical Society of America. A, Optics, Image Science, and Vision, 18, 2448-2459.

Ramamoorthi, R., Mahajan, D., & Belhumeur, P. (2007). A First-Order Analysis of Lighting, Shading, and Shadows. ACMTransactions on Graphics, 26(1).

Reiner, T., Kaplanyan, A., Reinhard, M., & Dachsbacher, C. (2012). Selective inspection and interactive visualization of light transport in virtual scenes. Computer Graphics Forum, 31(2), 711-718.

Russell, S. (2008) The Architecture Of Light. Conceptnine.

Schirillo, J. a. (2013). We infer light in space. Psychonomic Bulletin & Review, 20(5), 905-15.

Schmidt, T., Nov, J., Meng, J., Kaplanyan, A. S., & Nowrouzezahrai, D. (2013). Path-Space Manipulation of Physically-Based Light Transport. ACM Trans. Graph., 32(4).

Schmidt, T., Pellacini, F., Nowrouzezahrai, D., Jarosz, W., & Dachsbacher, C. (2016). State of the art in artistic editing of appearance, lighting, and material. Computer Graphics Forum, 35(1), 216-233.

Schultz , T.& Kindlmann, G. L. (2010) Superquadric glyphs for symmetric second-order tensors. IEEE Transactions on Visualization and Computer Graphics, 16.6, 1595-

1604.

Simons, G., Ament, M., Herholz, S., Dachsbacher, C., Eisemann, M., & Eisemann, E. (n.d.). An Interactive Information Visualization Approach to Physically-Based Rendering, 1-9.

Sorger, J., Ortner, T., Luksch, C., Schwaerzler, M., Groeller, E., & Piringer, H. (2016). LiteVis: Integrated Visualization for Simulation-Based Decision Support in Lighting Design. IEEE Transactions on Visualization and Computer Graphics, 22(1), 290-299.

Toscani, M., Zdravkovic, S., & Gegenfurtner, K. R. (2017). Lightness perception for surfaces moving through different illumination levels. Journal of Vision, 16(2016), 1-18.

Velten, A., Wu, D., Jarabo, A., Masia, B., Barsi, C., Joshi, C., Lawson, E., Bawendi, M., Gutierrez, D., & Raskar, R. (2013). Femto-photography: Capturing and visualizing the propagation of light. ACM Transactions on Graphics (TOG) - SIGGRAPH 2013 Conference Proceedings, 32(4), 44.

Ward, J, G. (1989). The RADIANCE Lighting Simulation and Rendering System. 21st Annual Conference on Computer Graphics and Interactive Techniques, 459-472.

Westin, C., Maier, S., Khidhir, B., Everett, P., Jolesz, F. A., & Kikinis, R. (1999). Image processing for diffusion tensor magnetic resonance imaging. Int. Conf. on Medical Image Computing and Computer-Assited Interventions, 441-452.

van Doorn, A. J., Koenderink, J. J., Todd, J. T., & Wagemans, J. (2012). Awareness of the light field: the case of deformation. I-Perception, 3(7), 467-480.

Xia, L., Pont, S. C., & Heynderickx, I. (2014). The visual light field in real scenes. I-Perception, 5(7), 613-629.

Xia, L., Pont, S. C., & Heynderickx, I. (2016a). Light diffuseness metric Part 1 : Theory. Lighting Res. Technol., 49(4), 411-427.

Xia, L., Pont, S. C., & Heynderickx, I. (2016b). Light diffuseness metric , Part 2 : Describing , measuring and visualising the light flow and diffuseness in three-dimensional spaces. Lighting Res. Technol., 49(4), 428-445.

Xia, L., Pont, S. C., & Heynderickx, I. (2017). Separate and Simultaneous Adjustment of Light Qualities in a Real Scene. I-Perception.

Yot, R. (2011) Light for Visual Artists: Understanding and Using Light in Art and Design. London: Laurence King Publishing.

Zhang, F., de Ridder, H., & Pont, S. C. (2015). The influence of lighting on visual perception of material qualities, 9394(0), 93940Q.

Zirr, T., Ament, M., & Dachsbacher, C. (2015). Visualization of Coherent Structures of Light Transport. Eurographics Conference on Visualization, 34(3).

6

A TOOLBOX FOR VOLUMETRIC VISUALIZATION OF LIGHT PROPERTIES

Abstract

In this paper, we introduce to the light research and design audience a toolbox for perceptually-based visualization of light in a volume, focusing on visual effects of illumination. First, our visualizations extend the conventional methods from a 2D representation on surfaces to the whole volume of a scene. Second, we extend the conventional methods from showing only light intensity to visualizing three light properties (mean illuminance, primary direction and diffuseness). To make our methods generally available and easily accessible we provide a web-based tool, to which everybody can upload data, measured by a cubic or simple illuminance meter or even a smart-phone-app, and generate a variety of 3D visualizations of the light field. The importance to consider the light field in its full complexity (and thus the 3D vector field instead of its 2D sections) is widely acknowledged (Boyce, 2013; Cuttle, 2010; Lynes, 1966). Our toolbox allows easy access to sophisticated methods for analyzing the spatial distribution of light and its primary qualities as well as how they vary throughout space. We aspire that our results and tool could raise discussions in support of "3rd stage" (Cuttle, 2010) approaches to light(ing) research and design and implementation approaches to this complex problem in a practical manner.

In review as: Kartashova, T., de Ridder, H., Pas, S. F., & Pont, S. C. (2018) A toolbox for volumetric visualization of light properties, xx(x).

6.1. INTRODUCTION

Illumination visualization plays an important role in evaluating a lighting design of a space or a building. An image or a schematic representation of a scene provides designers with an instant grasp of the information, whereas descriptional texts or data tables are more likely to require effort for interpretation. As a Russian proverb says, "better to see <something> once than to hear <about it> a hundred times". One of the common methods of showing scene illumination is a straightforward rendering of light in a scene via sketching or a computer-generated image. Sketching lighting on paper or in software is a fast way for capturing and communicating lighting ideas (Innes, 2012). It can show shapes of light beams or identify objects and surfaces which require to be lit (Russel, 2008). However, this approach does not allow (and does not intend) to produce an accurate representation of light in a scene (Ganslandt & Hofmann, 1992), so it is mostly suitable for the early stages in the design process (Livingston, 2014). A photorealistic rendering, on the other hand, gives a glimpse of how a lighting design would look as a final result. However, such rendering has also disadvantages such as a narrow dynamic range of the resulting image and extensive time required to produce renderings (Innes, 2012). Murdoch et al. (2015) demonstrated how difficult it is to estimate the brightness of the illumination in a modelled scene, showing that an image of a dimly-lit room is often judged as an underexposed image of a normally-lit room. Additionally, such images show only how lighting affects scene walls, floors and ceilings plus the objects which are already placed in the scene. This might be not enough if, for example, a final arrangement of furniture is not known yet. Nor does it represent the visual experience of a user who moves through such a scene. For a more accurate examination of an illumination design, light professionals use visualizations based on light measurements. The most common of those is a false color image (see Figure 6.1) that encodes luminance/illuminance values on either all visible surfaces (Ochoa et al., 2012, Sorger at al., 2016) or planes of interest (Autodesk 3ds Max Lighting Analysis Assistant; Diva (Jakubiec & Reinhart, 2011)). False color visualizations allow a designer to assess the illumination levels in order to, for instance, check whether they satisfy lighting standards. These standards set illumination requirements including minimal illumination at horizontal and vertical planes.

There is a growing conviction that the focus of the lighting profession (and, therefore, light standards and light visualization methods) will be extended beyond illumination on planes, to light in 3D volumes (see Section 2.1). Additionally, the light level intensity is

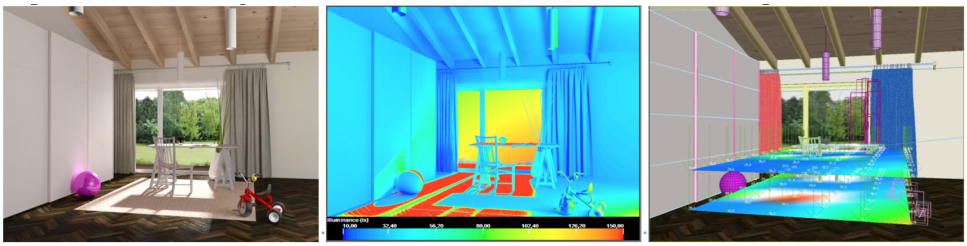

Figure 6.1: The leftmost image shows a scene, the middle image is a falsecolor representation of the illuminance over all surfaces of a scene, the right is a falsecolor representation of the illuminance over planar cross-sections in the space.

not the only light property influencing the appearance of objects and spaces. Thus, other light properties might be also worthy to visualize explicitly (see Section 2.2). Our interactive tool fills these gaps by providing a method for volumetric visualization of multiple light properties (mean illuminance, direction, and diffuseness) simultaneously.

In the next section, we further explain the motivation for creating our tool and list previous work. In Section 3 we describe the light visualization tool and provide examples of its application for light design. Section 4 contains insights on volumetric physical measurements, including a comparison of the visualizations obtained via three physical measuring tools that vary in precision — including a method that allows general use of our toolbox with smartphone measurements.

6.2. MOTIVATION AND PREVIOUS WORK

6.2.1. FROM SURFACES TO VOLUMES

There are many situations in which a researcher or designer might need information about light in (empty) space. For example, in studies on daylight and glare (e.g. Cantin & Dubois, 2011; Inanici & Navvab, 2006; Wienold, 2009), measurements were often made at a position where a person is expected to be seated. Indeed, in many cases an employee spends the majority of time in almost the same position. However, this approach does not suit open spaces where employees can change their positions around, or meeting rooms where seating positions are not strictly arranged or any space where humans move around (shops, museums, sport halls or even outside spaces). In those cases, there is a need for multiple measurements within the spaces. Lam (1992) criticized conventional lighting approaches for isolating the task of reading a carbon copy, which outdated

a long time ago, as the basis for lighting everywhere in an illuminated space. Obviously, human activities vary in tools, time and position over spaces. He also stated that criteria for a light design should not only be about eliminating negative elements, e.g. visual discomfort, but also about providing positive aspects of the luminous environment. The latter can be achieved by considering expected activities in a designed space and "biological information need", the need for information coming from the surrounding visual environment. Boyce (2003, 2013) agreed that following existing guidelines will usually ensure avoiding poor quality lighting, but will do little to ensure good quality lighting. Cuttle et al. (1967, 2003, 2010) suggested that the next development stage of the lighting profession requires that instead of accounting for the light on surfaces, designers should consider for light arriving at the observer's eye. In order to capture a full description of all light in a space that may potentially arrive at an observer's eye, we need a human-centered or perception-based description of the light field, that is the light as a function of position and direction (Gershun, 1939).

Another reason for visualization of light in a volume is that it might be difficult to see at a glance which component of a design produced a certain light effect while working with complex spatial geometries and multiple light sources. Psychophysical studies show that human observers are able to infer light fields, but their impression seems to be simplified with respect to the real physical distribution of light in a scene (Kartashova et al., 2016; Koenderink et al., 2007; van Doorn et al., 2012). Therefore, a simplified volumetric visualization could be helpful for a better understanding of light in space.

Light travels in every direction through every (transparent) point. This feature makes it difficult to visualize or even describe all information resulting from interaction of light with the geometry and material in a 3D space. A solution for this was first proposed by Gershun (1939) by introducing the concept of the light field, a 5-dimensional function determining the radiance arriving at a point x, y, z from directions θ, ϕ. In our implementations, we use luminance instead of radiance, because we are interested in the visual appearance of light. Additionally, he defined the light vector as the net transport of radiant power (in other words: the average luminance direction). Cuttle (2010) proposed panoramic ("field of view") imaging for capturing the light field in a point. Yet, in order to measure an entire light field one would have to make spherical photographs in every point of a measured volume. Doing so would require a lot of labor and storage place, also it is not clear how all this information could be used. Moreover, as mentioned before, humans seem to have a simplified impression of the light field, thus we do not

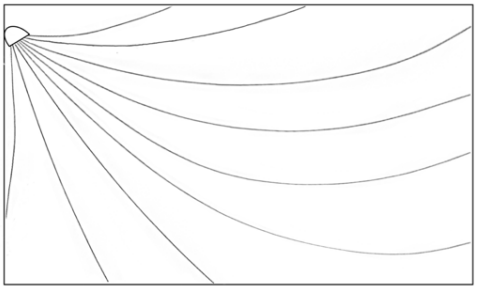

Figure 6.2: A drawing of lines of flow for a single light source in the top left corner of a room. The room is empty with walls and ceiling covered with a diffuse material that reflects some portion of light. The lines are slightly curved because of light reflection from the floor.

need the full approach. Later, Mury (2007) developed the concept further, finding that the lower order components of physical light fields (equivalent to ambient and directed light plus squash tensor) vary smoothly over spaces and therefore can be reconstructed using relatively few measurement points and interpolation to obtain values in-between measurements.

Light design researchers studied light in a 3D volume using the concept light flow. Lynes et al (1966) recommended the scalar and vector illumination for analyzing the structure of light. They visualized the flow of light via lines of flow that show (variations of) the light direction for a cross section in a space (see example in Figure 6.2). The authors emphasized that the flow lines are not rays of light, thus there is no contradiction between light traveling in straight lines, and a flow line being curvy. The reason is that flow lines in any point in space represent the average direction of all rays, similarly to the "lines of force" for magnetic fields. Cuttle (1971, 1973) explained the influence of the light flow and sharpness of light on object appearance, where the first concept describes the strength and direction of light and the second reflects shadows and highlights patterns. Dale et al. (1972) proposed an elegant method for determining the direction of a light vector using two pieces of paper, both marked with a wax creating a translucent spot. These pieces of paper were mounted on a stick perpendicularly to each other. For each paper holds that if the direction of the light vector was in the plane of the paper the grease spot looked equally bright as the surrounding paper, because the illuminance on both sides would then be equal. Thus, when both spots "disappeared", the stick was aligned with the light vector in that spot. Interestingly, without an evident relation to light design research, physicists came up with an idea very similar to light flow. Wun-

scher et al. (2001) called it the energy flow (of light), and visualized it as vectors or stream lines. They also related the concept to the structure of electric fields, thus applying similar rules to (light) energy flow lines: they never cross one another, they originate on light sources and end on absorbers, and they run parallel to a reflecting surface in their immediate vicinity.

In all studies mentioned above the visualizations were restricted to cross sections through spaces. Until recently it was not possible to produce 3D visualizations for the quite extensive data sets that a full light field usually encompasses, because the technical possibilities simply were not available. But with the development of computing, modelling and visualization technologies, it became possible to create complex 3D models leading to a new leap of development on light in volumes. In light field research, researchers measured the virtual light field (Ashdown, 1998), modelled and visualized the light field as density and vector field plots (Tregenza, 2000), presented light direction and mean illuminance as a grid of arrows of varying size (Jacobs, 2014), and visualized light flow as light tubes (Mury et al., 2009; Xia et al., 2016b). In computer graphics, striving for realism stimulated the development of illumination algorithms (Greger, 1998; Krivanek et al., 2010; Ritschel et al., 2012; Schmidt et al., 2016). Studies in this field visualized light rays (Nowrouzezahrai et al., 2011; Simons et al. 2016) avoiding clutter (Schmidt et al., 2013), and showed various light properties (Chajdas et al. 2011; Jacobs, 2014; Reiner et al., 2012). Although the listed studies demonstrate a variety of light visualizations methods, they are mostly targeted at the computer graphics audience and often take advantage of rendering methods. It makes them difficult or sometimes even impossible to apply for physical measurements.

In our toolbox, volumetric visualization of the light field is based on Mury et al.'s (2009) grid measurement approach, simplified by using Cuttle's (2003, 2013) formulas for cubic measurements. The resulting method is much simpler with regard to the measurements and calculations than most of the methods listed above, and allows efficient and robust reconstructions of the variations of light properties over either physical or virtual 3D space. The main difficulty of our method lies in the steps that need to be taken from raw data to the actual 3D visualizations, for which we provide our web-based publicly available tool.

6.2.2. MEASUREMENTS

It is impossible to have a meaningful visualization of light while preserving all the information of the light field, because there are infinitely many light rays passing through every point of (empty) space. However, it is possible to extract a few important features/properties and visualize their variation. The next question is, which light properties are important?

The mean illuminance, direction and diffuseness are the main properties that appear in the literature on lighting design (Cuttle 2003; Descottes and Ramos 2013; Innes 2012; Kelly, 1952; Livingston, 2014; Russell, 2008), computer graphics (Birn 2013; Brooker 2006), photography and drawing (Hunter et al. 2007; Yot, 2001). In visual perception studies, results showed that human observers are highly sensitive to the mean illuminance, diffuseness and average direction of light, not only on surfaces, but also in empty space (Gerhard & Maloney, 2010; Kartashova et al., 2016; Koenderink et al., 2007; Morgenstern, 2014; Xia et al., 2014; Xia et al., 2017). Often, authors use different terms to describe those light properties, but it is usually clear that the authors mean the same quality. For example, diffuseness (Koenderink et al., 2007), softness (Birn, 2013) and contrast (Hunter et al., 2007) all seem to describe the same basic property of light, namely the ratio between the directed and ambient light.

Based on the above-mentioned considerations, we chose to visualize the (variations of) values of mean illuminance, direction and diffuseness of the light, introduced in this combination by Xia et al. (2016ab). We did this via shapes and variation of their proportions. In order to obtain the values of the light properties we use Cuttle's (2003, 2013) approach of cubic illuminance adopted for multiple measurements, physical (Kartashova et al., 2016; Xia et all., 2016ab) as well as virtual (Kartashova et al., 2018).

6.3. VISUALIZATION TOOLBOX

6.3.1. OVERVIEW

The algorithms constituting the visualization toolbox are explained in detail by Kartashova et al. (2018), and here we will provide a general description of the key features of the toolbox. It contains two main components. The first component translates for each measurement position the input of six cubic light measurements into the following three light properties: mean or scalar illuminance, strength and direction (of the light vec-

tor), and diffuseness (ranging from 0, fully collimated light, to 1, fully diffuse light). The second component creates the resulting visualizations by expressing the values of these light properties through varying the proportions of various shapes (arrows, ellipses and tubes). The resulting visualizations were psychophysically and evaluated by Kartashova et al. (in review)

The arrows visualization adapts Jacobs' (2014) representation of light vectors pointing at the direction where the light comes from for every point of a vector grid. It is important to note that the chosen direction is that of the illumination, which is actually the physically important quantity – such that the component of the light vector in the direction of the surface normal of any given surface element represents the net flux density (Gershun, 1939; Moon & Spencer, 1981; Mury 2007). We visualize the mean illuminance via the arrow length, and the diffuseness via the width of the arrow shaft: the thicker the shaft, the more diffuse (less directed) the light is. The diffuseness judgments do not suffer from perspective distortion, since the arrowhead is always of the same size whereas the ratio of the arrowhead size and the shaft thickness varies.

The second type concerns visualization using ellipsoids (Westin et al., 1999). The long axis orientation of an ellipsoid is aligned with the light vector. The size of each ellipsoid corresponds to the mean illuminance. The proportion between the short and long axes corresponds to the diffuseness. The more elongated the ellipsoid is, the more directed (lower in diffuseness) light is. Fully diffuse light does not have a dominant direction, and is thus represented by a sphere.

The third type of visualization is done via light tubes (Mury et al., 2009). A tube is locally tangential to the light vector and in our visualizations its width is inversely proportional to the mean illuminance (in Gershun's (1936) and Mury et al.'s (2009) approach its width was inversely proportional to the strength of the light vector). The intuition behind this choice comes from fluid flow representations: the smaller the tube, the faster / stronger the flow. The set of tubes represents the "light flow" (Cuttle, 1973) and often shows a structure diverging out from the source to light absorbing surfaces (Kartashova et al., 2016, Mury, 2009). These "superpatterns" can also be seen in the vector and ellipsoid visualizations as a global structure formed by the ensembles of shapes.

Figure 6.3 demonstrates the shapes and their variations visualizing several light conditions, plus photographs of a white sphere in those conditions — to show the relation with how objects appear in those conditions — since this is usually what we see and how we judge the light in realistic contexts. For arrows and ellipsoids, the first and second

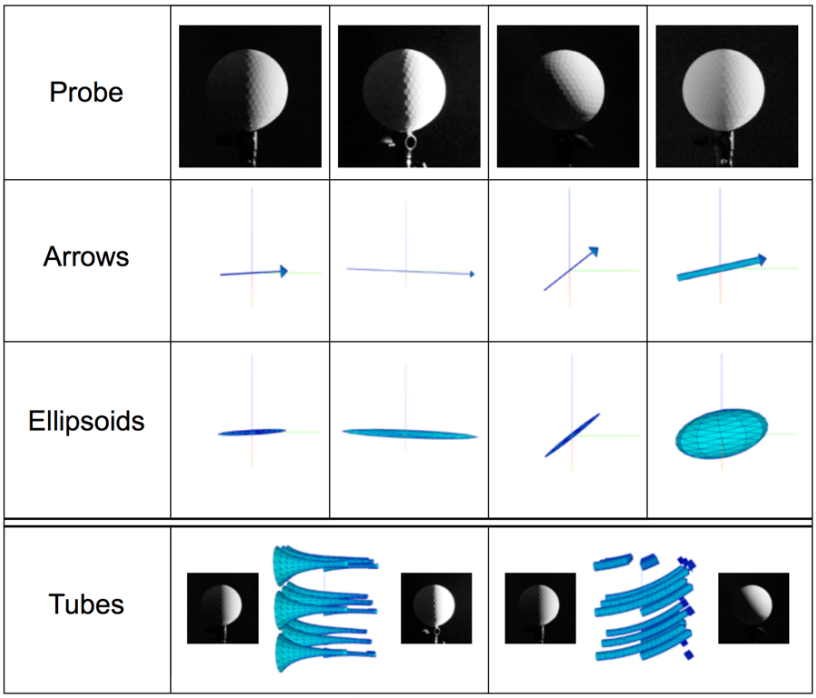

Figure 6.3: Examples of shapes visualizations and photographs of various light conditions. Note that the arrow and ellipsoid in the column with the strongly directly illuminated sphere are scaled twice smaller than the other shapes to show the whole visualization.

columns of images show differences in mean illuminance, the first and third columns show differences in direction, and the first and fourth show differences in diffuseness. The slight differences in direction between columns one, two and four are due to that a real scene was used for the measurements and photographs. The interreflections and slight variations between light source and the probe positions influence the resulting light direction. The tubes illustrate the variation of the parameters over the volume, with variation of the mean illuminance in the first column and variation of the direction in the second column.

We evaluated the visualizations via a user test (Kartashova et al., 2008). Participants were first asked to compare the light properties between three positions in scenes and secondly to match the appearance of illuminated objects to their positions in three scenes. Both tasks were performed using scene renderings and each of the visualizations. The main result was that all of the visualizations gave better or not significantly different performance compared to the renderings. We did not compare the visualizations between

each other, because the goal of the study was to test the performance of the introduced tool compared to renderings. Moreover, an informal survey with our participants confirmed that the choice of shape type was probably a matter of personal preference. In order to demonstrate the visualizations in action and make our tool available for everybody, we created a web-based visualization toolbox. It allows to load files with light measurements or to pick example data files, and transform the data into interactive 3D visualizations.

6.3.2. WORKFLOW

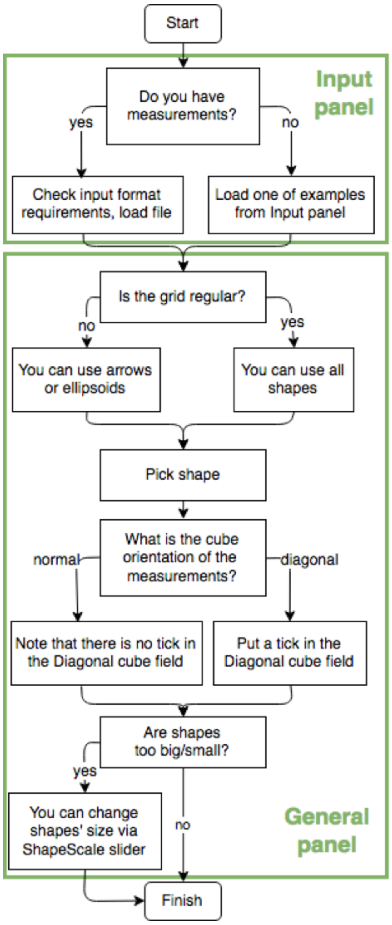

Figure 6.4: Workflow of interaction with the. First the user is supposed to upload his/her own measurements or one of the provided examples, then select and adjust adjust shapes in order to show the light properties variations in the best way.

The workflow of the tool is the following (see the scheme in Figure 6.4). After loading the webpage (see Figure 6.5), one should load a light measurements file or pick one of the example measurements files from the list. The light measurements file should be comma-separated and saved with the corresponding extension (*.csv). Every line represents a measurement point containing six measurements (one on every side of a cube) and the three coordinates of the measurement point in space. See details of the measurement procedure in section 3. If the file format is correct, the webpage will immediately show a visualization. The interface allows changing the viewing direction and zooming in/out using mouse click-and-drag and center wheel respectively.

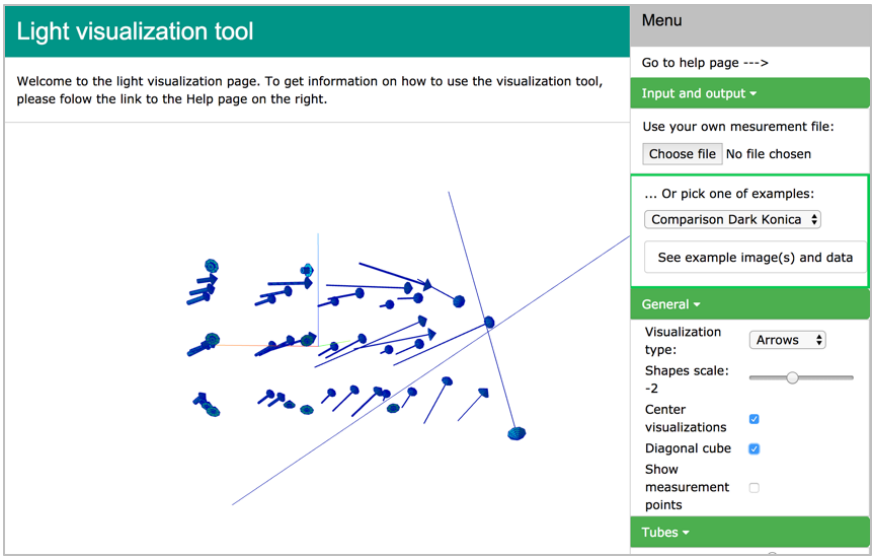

Figure 6.5: Light visualization interface. Most of the webpage is taken by an interactive view of the visualization. On the right is the menu for loading and controlling the visualization.

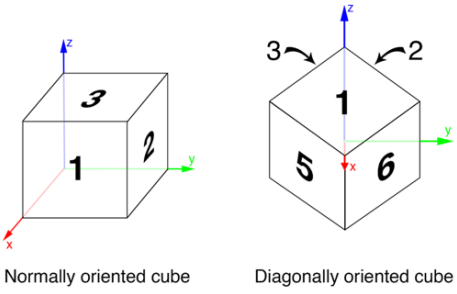

Figure 6.6: Two possible orientations of the cubic measurements.

Next, one should address if the measurements were done with a cube which was oriented normally (sides of the cube faced according to the XYZ axes) or diagonally (one of the main diagonals of the cube is oriented vertically), see Figure 6.6. If the measurements were made with a diagonally oriented cube, a tick should be placed in the "Diagonal cube" tick box. Then a shape type can be chosen (by default it is Arrows). Note that if the measurement grid is not regular, the demo cannot produce tubes, because of the interpolation difficulties of that particular case.

The resulting visualizations may be adjusted. They can be rotated by the mouse or touchpad using dragging and dropping, and they can be zoomed in or out using scrolling. All shapes may be scaled using the "Shapes scale" slider. This determines the size of the ellipsoids, the lengths of the arrows' shafts and widths of the tubes. By default, the coordinate origin (center of rotation) is placed in the center of the measured volume. It can be placed according to the measurements origin by removing a tick in the "Center visualizations" tick box. The tubes visualization has its own adjustment menu. There, one can choose step size, number of steps and number of tubes on each axis. Step size regulates the size of the steps between the points of the tubes at every interpolation point. It is important to note that the starting points of the tubes are placed such that the tubes originating on the edge of the volume can make at least one step within the measured volume. The number of steps regulates how many points will be calculated for each tube.

6.3.3. VISUALIZATION EXAMPLES

In this section, we present two examples of practical use of our visualizations toolbox. The first example demonstrates the influence of scene content on the resulting light field in the volume of the scene. The second example shows daylight measurements visualizations for two different sky conditions.

The scene for the first example was constructed in a lab with no windows and a single light source. One wall was always black, another was black for one set of measurements and white for another. The third side was covered with a black curtain, which also occluded the light source from a part of the measured volume. The fourth side was open to an unilluminated part of the room which was not included in the measurements. The ceiling was white and the floor was black. We measured a grid of four points in width and length and three points in height (see Figure 6.7). The grid was 2 meters in width and length. Measurements were taken at heights of 1, 1.5 and 2 meters from the floor.

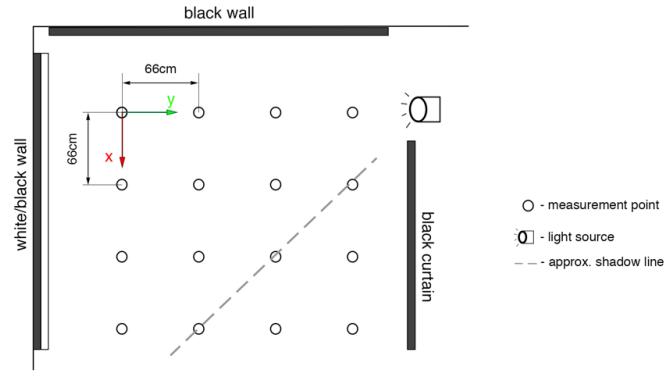

Figure 6.7: Example one. Room scheme, top view.

We used a Konica Minolta T-10MA illuminance meter with six mini sensor heads placed on a cube (see more in Section 4).

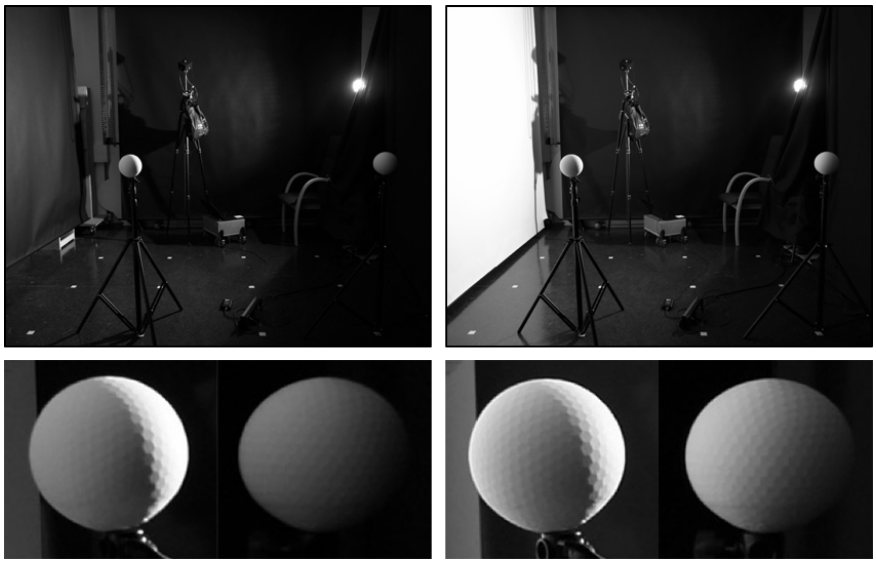

Figure 6.8: Example one. Room and light probe photographs.

Figure 6.8 shows photographs of the measured scene, left for the black and right for the white wall condition, produced with the same camera settings. It is clear from the enlarged white spherical probes below the scene images that the white wall dramatically changes the light conditions in the room (note that the light source and camera exposure were the same).

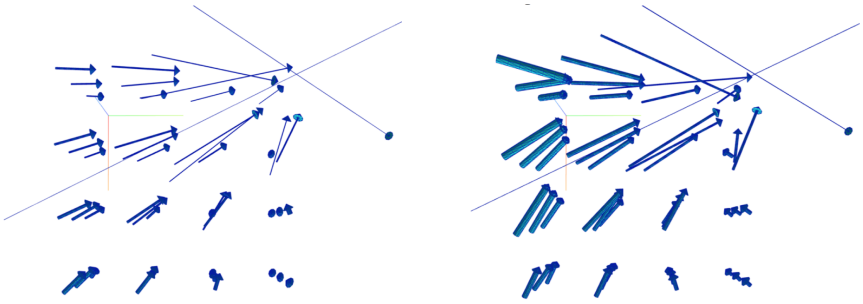

Figure 6.9: Example one. Arrows visualizations of the measurements, from a top view as in Figure 7. Note the difference in lengths, directions and thickness of the arrows.

Figure 9 demonstrates the visualizations of the measurements for both scenes. Close to the light source arrows do not seem to differ between the scenes whereas the remainder of the arrows in the light wall condition are longer and thicker than the ones in the dark wall condition. This is, because the white wall reflected more light than the dark wall and made the light in the scene denser and more diffuse. Additionally, the arrows in the left side of the grid, closest to the wall, show dissimilar directions in the scenes, because the reflected light influenced the average light direction in those points. Thus, the visualizations here give clear insights into the complex effects of material-light interactions and how these affect the structure of the light field.

For the second example, we measured an office room illuminated with daylight. We measured a grid of three points in the width, four points in the depth of the room with respect to the window and three points in height (see Figure 10). The grid was 1,2 meters in width, 2,4 meters in length. Measurements were taken at heights of 1, 1.5 and 2 meters from the floor. The measurements were made at roughly the same time of the day, on two days with different weather. One day it was sunny (see Figure 11, left), the other day it was rainy with the sky fully covered with clouds (see Figure 11, left). Measurements on the sunny day were made between 15:06 and 15:21, on the rainy day between 15:22 and 15:40. Note, that the photographs of the room were made with different camera settings, because the dramatically different lighting conditions made it impossible to capture photographs at the same exposure level. To evaluate the difference one can take into account that the brightness of the laptop screen was the same between conditions. Whereas the laptop screen on the left image of Figure 11 looks dim, it is completely overexposed on the right image.

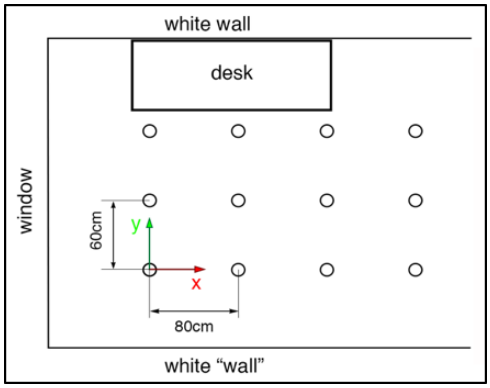

Figure 6.10: Example two. Room scheme.

Figure 6.11: Example two. Room scheme.

Similar to the photographs, the measurements are also presented with different scales, because for the sunny scene (see Figure 12, left column) the resulting mean illuminances ranged between 945 and 9338 lux, yet for the rainy one (see Figure 12, right column) the range was between 22 and 102 lux. The tube images show the light field from a top and side view, with the window at the left side. There are clear differences in the structures of

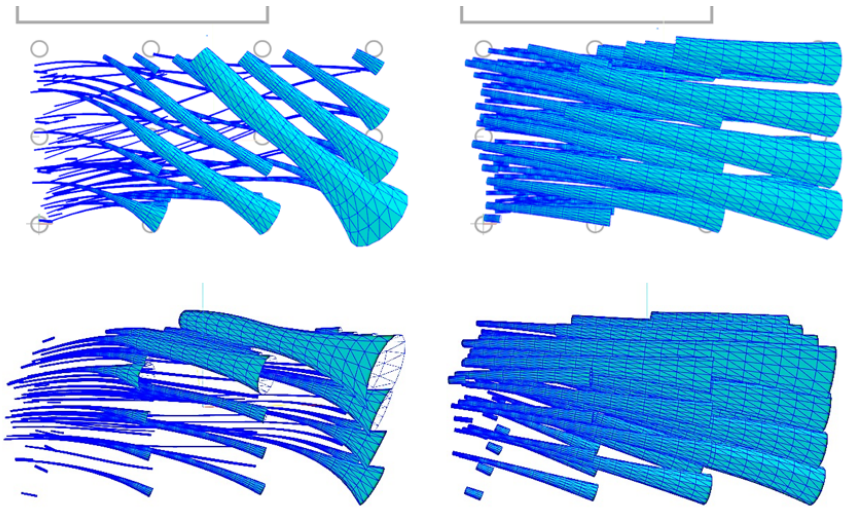

Figure 6.12: Example two. Tubes visualizations of the measurements. The first row shows top views as in Figure 10. The second row shows side views, with the window on the left. The left column shows the light flow for the sunny scene, the right for the rainy scene.

the light fields between the conditions. The measurements of the sunny scene have two distinct parts. Most of the scene was illuminated with strongly directed sunlight, except for the volume close to the ceiling and the volume far away from the window in depth of the room, which were occluded from the sun. The thin, uniformly directed tubes illustrate that the sunlit part has strongly directed light from the window at the left of the room (see Figure 12, left column). The sunlight-occluded part of the scene results in much thicker tubes — lower light densities — and light directions at large angles to the sunlit part due to light reflected from the wall on the left (see also the light gradient on the ceiling in Figure 11, left). In contrast, the rainy scene represents rather uniform illumination with a smooth gradient in the mean illuminance from the window to the back of the room. As a result, for example, the white relief with symbol in the back right of the room (enlarged in Figure 11, bottom row) is illuminated differently between conditions which results in dramatic differences in its appearance.

We demonstrated that our visualizations provide a strong support to understanding variations of light over spaces for several examples of illumination. Moreover, they allowed to see subtle light effects throughout the empty space in a glance, which cannot be fully captured from the photographs. We believe that these analyses might also help to understand interactions between lighting (artificial plus day lighting) and a scene ge-

Figure 6.13: Measurement devices. Left to right: cubic meter based on Konica Minolta system (Xia et al., 2016ab), luxmeter, smartphone with Luxi.

ometry as well as the dynamics resulting from combinations of artificial and (varying) day lighting.

6.4. VOLUMETRIC LIGHT MEASUREMENTS

6.4.1. COMPARISON OF VISUALIZATIONS FOR THREE MEASUREMENT DEVICES

Here we compare measurements visualizations for three tools with varying precision (see Figure 13) in order to see to what extent a tool precision influences the resulting visualization. The first device was a cubic meter (Xia et al., 2016b) based on a Konica Minolta T-10MA illuminance meter with six mini sensors heads connected together for cubic measurements. Thus, the device provided simultaneous measurements of all six sensors. The second device was rather cheap a common luxmeter (Voltcraft MS-1300) with a single sensor. We made cubic measurements with this device by placing it consecutively on the six faces of a cube and recording its output values. The third device was a smartphone with a white diffusion cap (Luxi) and the corresponding app (see measurements evaluation study by Gutierrez-Martinez et al., 2017). We used the Luxi for cubic measurements in the same manner as the luxmeter. Of these three devices the cubic meter has the highest accuracy and the Luxi the lowest. The same order applies to the price of the devices, ranging from a few thousands of Euro's for the Konica Minolta system to around 30 Euro for the Luxi.

The measurements were performed in the black wall scene described in Section 3.3 (see Figure 7 and Figure 8, left). We compared deviations of light properties between the

Table 6.1: Deviations of resulting properties measurements between the common luxmeter based device and baseline and between the Luxi based device and baseline. The baseline properties were obtained from measurements made with a Konica Minolta based cubic meter.

Property	Device	Median	Min	Max	Histogram
Direction (angular difference, degrees)	Common luxmeter	8,44	2,75	51,94	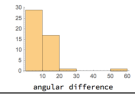
	Luxi	16,52	2,73	38,35	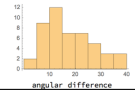
Mean illuminance (lux)	Common luxmeter	61,76	1,56	1666,8	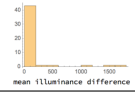
	Luxi	103,14	6,24	900,89	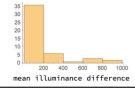
Diffuseness (diffuseness scale, ranges from 0 to 1)	Common luxmeter	0,013	0,001	0,122	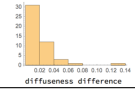
	Luxi	0,055	0,001	0,354	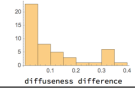

Konica Minolta system as baseline and the two other devices. The results are presented in Table 1. For direction we calculated the angular difference between the light vectors. For mean illuminance and diffuseness we calculated the absolute difference between the measurements. Maximum deviations for the mean illuminance occur close to the light source where large differences occur between the illumination in different directions. The range of mean illuminances in the room, according to the Konica Minolta device, was between 34.51 and 13500 lux. As one could expect, all median deviations for the common luxmeter are lower than for the Luxi, for all parameters.

Visualizations of the measurements are presented in Figure 14. The cubic meter and luxmeter produced visually similar results. The luxmeter visualizations have barely noticeable deviations in the pattern, which are almost entirely averaged out by the tubes visualization. The individual Luxi results are considerably noisier, as expected, but as a set they still produce a similar pattern, which allows to see the flow of light through the scene. In the tubes visualizations it can be seen that with noisier data the tubes become somewhat noisier, yet the main structure stays the same. Thus, the light field structure

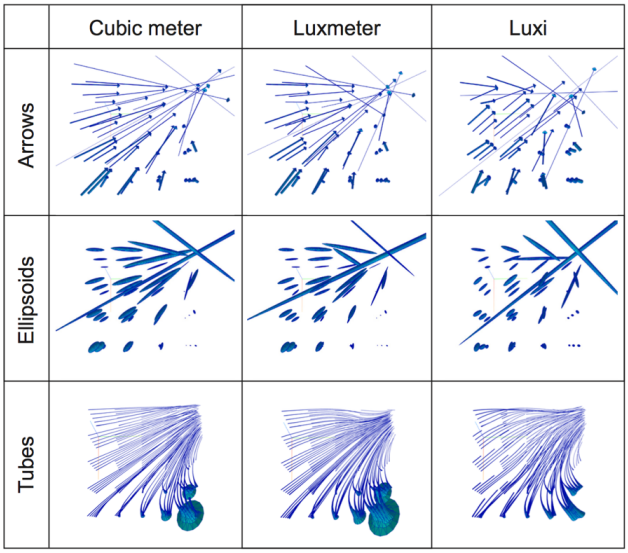

Figure 6.14: Measurement results, top view as in Figure 7.

can be measured robustly, even with extremely cheap devices. This result, plus our publicly available tool, now allow anybody to measure and visualize the structure of the light throughout any space. In this way we hope to support the lighting profession in its third stage (Cuttle, 2010) that is characterized by a focus on the light arriving at the eye, instead of the conventional approach focussing on light on planes.

6.4.2. RECOMMENDATIONS FOR MEASUREMENTS

In Section 3.1, we described the requirements for the input file content. This section contains practical recommendations for making measurements. Making a grid of physical cubic measurements might seem labor-intensive. However, after some practice, even measurements taken with a single lux meter (as in Section 4.1) might take less than half a minute per point. Moreover, even a single measurement can be visualized using the arrows or ellipsoids, whereas the tubes images may be created based on a minimum of a 2x2x2 measurements grid. If the light field is expected to be complex (for instance because there are many light sources and occlusions), more measurements are needed to reflect its light structure variations than in the case of a simple light field (for instance a single light source in relatively empty space). One approach to produce a grid of measurements consists of the following actions:

- Picking the size of the measurement volume and the number of measurements over each axis. It is worthy to mark the measurement positions on the floor.

- Setting up the measurement device and a table for keeping measurement records. Besides that, it is necessary to prepare the device, e.g. install the corresponding software and calibrate the device. The table serves for saving the illuminance measurements and position coordinates.

- Taking the measurements. In order to minimize the disturbance of measurements by being present in the scene, it is suggested to avoid occluding main and secondary light sources from the sensors. We achieved that by making remote measurements with the Konica Minolta device. With the hand-held luxmeter and Luxi devices the experimenter stayed in the darkest region possible and then reached out with the devices to do the measurements.

In addition to measurements in a real scene, our method can also be used in virtual scenes. Conducting cubic light measurements in virtual scenes requires a modelling environment that contains light measurement tools, e.g. Lighting Analysis Assistant (LAA) in the Autodesk 3ds Max system or calculation surfaces in DIALux. To make measurements in a modelled scene one should arrange the available light sensors in groups, such that in every group six sensors would face six directions, as if placed on a cube. The resulting measurements should be converted to the visualization tool input format by the user.

6.5. DISCUSSION AND CONCLUSIONS

The main goal of the current paper was to introduce our volumetric light visualization tool and demonstrate how such visualizations can be performed and applied for the analysis of the structure of light throughout a space. Our tool translates sets of cubic measurements into light properties values (that may be exported as a table) and visualizes them through variation of the shapes' proportions. Two main features of our tool are visualizing light volumetrically and visualizing essential light properties. The first one allows obtaining a comprehensive impression of the structure of the light field in a measured space. The second one translates the important information in easy to read visualizations. Together they provide a perception-based visualization of the 3D structure of the light flow. Visualization results were presented for two example scenes. Finally,

we showed that the necessary physical measurements might be performed with light measuring tools of varying precision, all producing acceptable results.

The current implementation of our toolbox limits the visualized information to only three light properties: mean illuminance, direction and diffuseness. We chose those lower order light properties because they majorly determine the appearance of matte objects (Ramamoorthi & Hanrahan, 2001). The appearance of objects made of glossy materials, such as glass and metals, is determined also by higher order light properties (Mury, 2009), e.g. Kelly's (1952) "play of brilliants" or the light texture (Pont, 2013). These properties cannot be extracted from our measurements, because of their low angular resolution. In order to take the light texture into account, one could take a spherical photograph and use different means of processing. This light texture can safely be assumed to be rather constant throughout a scene (in the statistical sense in which it is relevant to human perception). Such, a combination of our toolbox plus a statistical summary of the higher order properties of a spherical photograph would then complete such a perception-based light field analysis.

Further development of the tool implementation could include the following features. An output of the resulting geometry would allow inserting the visualization into a model of the geometry of a scene or into a rendering of the scene. The visualization shapes are currently scaled linearly, i.e. if the mean illuminance is a hundred times bigger in one position than another, the corresponding shapes will be a hundred times bigger in size/length. The possibility of logarithmic scaling might be a suitable addition for scenes with a very high dynamic range. Finally, the interpolation methods could be more advanced in order to support the usage of irregular grids of measurement points.

The lighting design profession is using more and more digital technologies. A survey of building design professionals (Reinhart & Fitz, 2006) revealed that already ten years ago 71% of the respondents used computer simulations for daylighting design. This is not surprising, these days a digital model is much cheaper and less labor-consuming to create and modify than a physical mockup. Moreover, digital simulation allows designers to perform more types of analysis and different visualizations of a design, as well as quick explorations and iterations of a design. We introduced a new tool for volumetric light measurements visualization via a web interface and demonstrated how this method can be used in several light analyses and design tasks, serving a large range of applications and research in the light(ing) realm.

The importance to consider the light field in its full complexity (and thus the 3D vec-

tor field instead of its 2D sections) is widely acknowledged1,15,22, but in practice incurs difficulties in 2D media presentations (where knowledge about mechanisms underlying visual perception in pictorial space will be helpful). We hope that lighting community will find interest in the ideas that we gathered in this paper and in the resulting implementation. We invite light researchers and designers for discussion, comments and suggestions about ?3rd stage? approaches to light(ing) research and design and how to implement approaches to this complex problem in a practical manner.

BIBLIOGRAPHY

Ashdown, I. (1998). The Virtual Photometer - Modeling the Flow of Light. 1998 IESNA Conference Proceedings, (October), 437—452.

Birn, J. 2013. Digital Lighting and Rendering (3rd Edition). New Riders.

Boyce, P. R. (2003). Human factors in lighting, 2nd ed. Boca Raton, FL: CRC Press.

Boyce, P. R. (2013). Lighting Quality for All. CISBE & SLL International Lighting Conference- Dublin 2013. Session 3, 1—5.

Brooker, D. 2006. Essential CG Lighting Techniques with 3ds Max. Waltham: Focal Press.

Cantin, F., & Dubois, M.-C. (2011). Daylighting metrics based on illuminance, distribution, glare and directivity. Lighting Research and Technology, 43(3), 291-307.

Chajdas, M. G., Weis, A., & Westermann, R. (2011). Assisted Environment Map Probe Placement. Proceedings of SIGRAD 2011.

Cuttle C, Valentine W, Lynes J, Burt W. (1967) Beyond the working plane. Proceedings of the CIE, Washington, DC, P-67- 12.

Cuttle, C. (1971). Lighting patterns and the flow of light. Lighting Research and Technology, 3(3), 171—189.

Cuttle, C. (1973). The sharpness and the flow of light. In R. Kuller (Ed.), Architectural psychology. Proceedings of the conference held at Lund University (pp. 12—22). Lund, Sweden: Lund University.

Cuttle, C. (2003). Lighting by Design. Oxford: Architectural Press.

Cuttle, C. (2010). Towards the third stage of the lighting profession. Lighting Research and Technology, 42(1), 73—93.

Cuttle, C. (2013). Research Note: A practical approach to cubic illuminance measurement. Lighting Research and Technology, 46(1), 31—34.

Dale, N., J, B., & P, C. (1972). Research note: Measuring the direction of the flow of light. Lighting Research and Technology, 4(1), 43—44.

Descottes H. and Ramos C. E. 2013. Architectural Lighting: Designing with Light and Space. Princeton Architectural Press.

Ganslandt, R., & Hofmann, H. (1992). Handbook of Lighting Design. (E. Edition, Ed.), Architecture. Vieweg publishing company.

Gerhard, H. E., & Maloney, L. T. (2010). Estimating changes in lighting direction in binocularly viewed three-dimensional scenes. Journal of Vision, 10, 14.

Gershun A. (1939) The light field. J. Math. Phys., 18, 51151 (translated by P. Moon and G. Timoshenko).

Greger, G., Shirley, P., Hubbard, P. M., & Greenberg, D. P. (1998). The Irradiance Volume. Distribution, 1—20.

Gutierrez-Martinez, J.-M., Castillo-Martinez, A., Medina-Merodio, J.-A., Aguado-Delgado, J., & Martinez-Herraiz, J.-J. (2017). Smartphones as a Light Measurement Tool: Case of Study. Applied Sciences, 7(6), 616.

Hunter, F., Biver, S., & Fuqua, P. 2007. Light Science and magic. Burlington, MA: Focal Press.

Inanici, M. N., & Navvab, M. (2006). The Virtual Lighting Laboratory: Per-pixel Luminance Data Analysis. Leukos, 3(February 2015), 89—104.

Innes, M. (2012) Lighting for interior design. Laurence King Publishing Ltd.

Jacobs, A., & Jacobs, A. (2014). Radiance Cookbook. http://www.jaloxa.eu/resources/radiance/documentation/docs/radiance_cookbook.pdf

Jakubiec, J. A., & Reinhart, C. F. (2011). DIVA 2.0: Integrating daylight and thermal simulations using rhinoceros 3D, DAYSIM and EnergyPlus. Proceedings of Building Simulation 2011: 12th Conference of International Building Performance Simulation Association, 2202—2209.

Kartashova, T., Sekulovksi, D., de Ridder, H., Pas, S. F., & Pont, S. C. (2016). The global structure of the visual light field and its relation to the physical light field. Journal of Vision, 16(9).

Kartashova, T., Pas, S. F., de Ridder, H., & Pont, S. C. (2018) Light Shapes: Perception-Based Visualizations of the Global Light Transport. Transactions on Applied Perception. In press.

Kelly, R. (1952). Lighting as an Integral Part of Architecture. College Art Journal, 12(1), 24—30.

Krivanek J., Fajardo M., Christensen P. H., Tabellion E., Bunnell M., Larsson D., Kaplanyan A.: Global illumination across industries. SIGGRAPH Course (2010).

Koenderink, Pont, S. C., van Doorn, A. J., Kappers, A. M. L., & Todd, J. T. (2007). The visual light field. Perception, 36(11), 1595—1610.

Lam, W. A. (1992). Perception and Lighting as formgivers for architecture. New York: Van Nostrand Reinhold.

Livingston, J. (2014) Designing with light: the art, science, and practice of architectural lighting design. Hoboken: John Wiley & Sons.

Lynes, J., Burt, W., JACKSON, G., & Cuttle, C. (1966). The Flow of Light into Buildings. Transactions of the Illuminating Engineering Society, 31(3), 65—83.

Morgenstern, Y., Geisler, W. S., & Murray, R. F. (2014). Human vision is attuned to the diffuseness of natural light. Journal of Vision, 14(2014), 1—18.

Murdoch, M. J., Stokkermans, M. G. M., & Lambooij, M. (2015). Towards perceptual accuracy in 3D visualizations of illuminated indoor environments. Journal of Solid State Lighting, 2(1), 12.

Mury, A. A, Pont, S. C., & Koenderink, J. J. (2007). Light field constancy within natural scenes. Applied Optics, 46(29), 7308—7316.

Mury, A. A. (2009). The light field in natural scenes. Thesis (PhD). Technical University of Delft, Delft, The Netherlands.

Mury, A. A, Pont, S. C., & Koenderink, J. J. (2009). Representing the light field in finite three-dimensional spaces from sparse discrete samples. Applied Optics, 48(3), 450—457.

Nowrouzezahrai, D., Johnson, J., Selle, A., Lacewell, D., Kaschalk, M., & Jarosz, W. (2011). A programmable system for artistic volumetric lighting. ACM SIGGRAPH 2011 Papers on - SIGGRAPH '11, 1(212), 1.

Ochoa, C., Aries, M., & Hensen, J. (2012). State of the art in lighting simulation for building science : a literature review. Journal of Building Performance Simulation, 5(Oc-

tober), 37—41.

Pont, S. C. (2013). Spatial and Form-Giving Qualities of Light. In L. Albertazzi (Ed.), Handbook of Experimental Phenomenology. John Wiley and Sons, Ltd.

Ramamoorthi, R., & Hanrahan, P. (2001). An efficient representation for irradiance environment maps. Proceedings of the 28th Annual Conference on Computer Graphics and Interactive Techniques SIGGRAPH 01, 64, 497—500.

Reiner, T., Kaplanyan, A., Reinhard, M., & Dachsbacher, C. (2012). Selective inspection and interactive visualization of light transport in virtual scenes. Computer Graphics Forum, 31(2), 711—718.

Reinhart, C., & Fitz, A. (2006). Findings from a survey on the current use of daylight simulations in building design. Energy and Buildings, 38(7), 824—835.

Ritschel, T., Dachsbacher, C., Grosch, T., & Kautz, J. (2012). The state of the art in interactive global illumination. Computer Graphics Forum, 31(1), 160—188.

Russell, S. (2008) The Architecture Of Light. La Jolla: Conceptnine.

Schmidt, T., Nov, J., Meng, J., Kaplanyan, A. S., & Nowrouzezahrai, D. (2013). Path-Space Manipulation of Physically-Based Light Transport.

Schmidt, T., Pellacini, F., Nowrouzezahrai, D., Jarosz, W., & Dachsbacher, C. (2016). State of the art in artistic editing of appearance, lighting, and material. Computer Graphics Forum, 35(1), 216—233.

Simons, G., Ament, M., Herholz, S., Dachsbacher, C., Eisemann, M., & Eisemann, E. (n.d.). An Interactive Information Visualization Approach to Physically-Based Rendering, 1—9.

Sorger, J., Ortner, T., Luksch, C., Schwarzler, M., Groller, E., & Piringer, H. (2016). LiteVis: Integrated Visualization for Simulation-Based Decision Support in Lighting Design. IEEE Transactions on Visualization and Computer Graphics, 22(1), 290—299.

Tregenza, P. (2000). Luminous energy field: a finite-element model. International Journal of Lighting Research and Technology, 32(3), 103—109.

Westin, C., Maier, S., Khidhir, B., Everett, P., Jolesz, F. A., & Kikinis, R. (1999). Image processing for diffusion tensor magnetic resonance imaging. Int. Conf. on Medical Image Computing and Computer-Assited Interventions, 441—452.

Wienold, J. (2009). Dynamic daylight glare evaluation. Eleventh International IBPSA

Conference: Building Simulation, 944—951.

Wunscher, T., Hauptmann, H., & Herrmann, F. (2002). Which way does the light go? American Journal of Physics, 70, 599.

van Doorn, A. J., Koenderink, J. J., Todd, J. T., & Wagemans, J. (2012). Awareness of the light field: the case of deformation. I-Perception, 3(7), 467—480.

Xia, L., Pont, S. C., & Heynderickx, I. (2014). The visual light field in real scenes. I-Perception, 5(7), 613—629. Retrieved from unknown

Xia, L., Pont, S. C., & Heynderickx, I. (2016a). Light diffuseness metric Part 1: Theory. Lighting Res. Technol.

Xia, L., Pont, S. C., & Heynderickx, I. (2016b). Light diffuseness metric Part 2: Describing , measuring and visualising the light flow and diffuseness in three-dimensional spaces. Lighting Res. Technol.

Xia, L., Pont, S. C., & Heynderickx, I. (2017). Separate and Simultaneous Adjustment of Light Qualities in a Real Scene. I-Perception.

Yot, R. 2001. Light for Visual Artists: Understanding and Using Light in Art and Design. London: Laurence King Publishing.

7

Conclusion

7.1. CONTRIBUTIONS

My thesis was funded by an EU grant and the faculty of Industrial Design Engineering. The EU project was called Perceptual Representation of Illumination, Shape and Material. Its goal was to "understand how the brain creates a richly detailed representation of the world by looking at how all three factors (3D shape, the material properties of objects, and the illumination within a scene) interact simultaneously". At my faculty, Industrial Design Engineering, research is conducted to develop and support human-centered design methods and applications. Together, these two factors, plus my personal preferences shaped my studies to be multidisciplinary and to be directed towards practical implementations and applications.

The main focus of the thesis was on light in spaces. From a perceptual point of view, we extended existing (local) visual light field studies to the exploration of global structures of the visual light field. From an application-oriented point of view, we created a tool for visualization of global variations of perceptually-relevant light properties and demonstrated its advantages for computer graphics and architectural light design. The research questions raised in the Introduction have been addressed in the Chapters 2-6. Below, these questions are completed with delivered scientific and practical contributions.

1. **Can we reconstruct the visual light field and compare it to the physical light field? (Chapter 2)**

   Contributions: We confirmed that it is indeed possible to reconstruct a global visual light field from local measurements. The obtained visual light fields were compared to physical light fields. Our results suggest that human observers have a robust impression of the light field, yet, this impression is simplified with respect to the physical truth. In particular, the observers neglected the curvature of the physical light field.

2. **Are inferences of light on objects (based on a single object appearance) and in empty space (based on appearance of surrounding objects) congruent with each other? (Chapter 3)**

   Contributions: We found that the congruency of inferences of light on objects and in empty space seems to depend on painting contents, in particular on illumination patterns pictured. The results showed that for four paintings with uniform

or diverging light, the settings were highly consistent both between conditions and within paintings. However, for two paintings containing zones of contrasting light, individual differences became prominent. We believe that the most plausible explanation of our results is that observers interpreted uniform and diverging patterns consistently. However, more complex patterns, such as resulting from multiple light zones, led to idiosyncratic behavior.

3. **How does the presence and mutual orientation of light zones (i.e. neighboring light fields with contrasting differences in one or more light properties) influence the perception of light properties in them? (Chapter 4)**

   Contributions: The results suggest that observers were able to distinguish the light conditions between the light zones and were quite sensitive to the difference in the light flow of the light zones. However, participants showed idiosyncratic behavior in cases of front-back oriented light zones. In particular, they often made settings on the probes in the back light zone as if they were illuminated in the same manner as the front light zone, ignoring the difference in illumination between the zones. This effect might be used in computer graphics, similarly to shadow cascades (reducing resolution of far away shadows in order to improve rendering).

4. **Do visualizations of light properties in a volume show light fields structures better than renderings? (Chapter 5)**

   Contributions: In this chapter we introduced and tested a novel approach to light visualization. The user study showed that our visualizations are at least as good as renderings for comparing light properties between the parts of the scenes and inferring the resulting appearance of objects. The developed visualizations show perceptually relevant properties of light as a 3D tensor field in a manner that can be easily understood by lighting artists.

5. **How can volumetric light visualizations be used in lighting design? (Chapter 6)**

   Contributions: We introduced a web-based tool and explained how it can be used for light design purposes. Moreover, we described the measurement method and compared three measurement tools demonstrating that visualizations can be obtained simply and cheaply. Our visualizations satisfy the needs of light designers for volumetric lighting visualizations that was expressed by established light design researchers and help to enhance understanding of the light field as a spatial structure.

7.2. RECOMMENDATIONS AND FUTURE WORK

As this thesis consists of published works, detailed recommendations for various aspects of light field research and design are presented in corresponding chapters. Here I list only the most essential of those and a few recommendations that were not included in the papers. First, understanding visual perception and light in particular is important for a range of professionals creating anything that is intended to be perceived visually. Thus, a painter or a product designer is supposed to know how a highlight on a glass vase is produced and how to reproduce the same effect in an image using drawing tools. An architect and computer graphics light designer should be able to use their theoretical knowledge on light effects in order manipulate lights and scene geometry to create an intended impression. Therefore, extending the body of knowledge of how the human visual system processes illumination information will help all these professionals.

Second, in our papers we described applications of existing tools and new tools for light fields measuring and visualization that we consider potentially useful for the light professionals community. The light probing tool, the white matte sphere first introduced by Koenderink et al (2007) and extended with defining a position via pole by Pont (2011), was used for systematic measurements of the structure of visual light fields (see Chapters 1, 2 and 3). Such a tool might be used for obtaining quick references of observers' perception of the light distribution in spaces. Moreover, we created a tool for volumetric visualization of light properties (see Chapters 1, 3, 4 and 5). This tool uses very simple translation from 6 cubic illuminance measurements to a graphical representation of light intensity, direction and diffuseness and then shows the variation of these properties over spaces via variation of the visualization shapes. Our visualization tool might be implemented on many platforms for real-time or close to real-time light visualizations.

Certainly, the performed studies did not just answer the raised research questions, but also raised many more questions for future studies. Again, here I list only some of the most notable and interesting, in my opinion, of potential follow-ups.

From the perceptual perspective, it would be interesting to investigate the perception of more light field structures and try other experimental approaches. In particular, in our studies we tested only a few scenes with only uniform, diverging structures and combinations of those (see Chapters 1 and 3). More research could be done into for example 3D versions of rotational and deformation structures(van Doorn et al., 2011, 2012). Then, all the light inferences described in this thesis were performed on the images shown on a

computer screen with a probe superimposed on an image of a scene. There might be other approaches to test the perceived illumination, including usage of different means of experimentation. For example, virtual reality seems to reach high enough fidelity for such experiments and also generates a much greater feeling of immersion than a computer screen. Another interesting topic is light in dynamic environments i.e. changing light or an object moving through a space over which light varies. There are already some studies on local light variations (Gilchrist et al., 1999; Toscani & Gegenfurtner, 2017) but it would be also interesting to study, for example, if human observers would notice that a change of illumination on a moving object does not match the variations of the light in a space through which it is moving.

For light visualization it is important to continue developing tools for volumetric light measurements and visualization. Our tool for light visualization could be improved by applying flow visualization techniques, for example streamline seeding techniques for placing the shapes, variations of grids' representation in terms of density, shapes' size, scale and transparency, using different shapes. Moreover, the measurement scenarios might be improved. For example, some image processing algorithms might allow replacing cubic measurements with spherical photographs making the measurement process less laborsome. Volumetric light visualization is a great support for making light designers think not on planes but in volumes. Therefore, advances in the visualization would move the lighting profession further towards its third stage (Cuttle, 2010).

BIBLIOGRAPHY

Cuttle, C. (2010). Towards the third stage of the lighting profession. Lighting Research and Technology, 42(1), 73—93.

Gilchrist, A. (1977). Perceived lightness depends on perceived spatial arrangement. Science (New York, N.Y.), 195(4274), 185—187.

Koenderink, Pont, S. C., van Doorn, A. J., Kappers, A. M. L., & Todd, J. T. (2007). The visual light field. Perception, 36(11), 1595—1610.

Pont, S. C. (2011). An ecologically valid description of the light field. In Proceedings VSS 2011 . Toscani, M., Zdravkovic, S., & Gegenfurtner, K. R. (2017). Lightness perception for surfaces moving through different illumination levels. Journal of Vision, 16(2016), 1—18.

van Doorn, A. J., Koenderink, J. J., & Wagemans, J. (2011). Light fields and shape from shading. Journal of Vision, 11, 1—21.

van Doorn, A. J., Koenderink, J. J., Todd, J. T., & Wagemans, J. (2012). Awareness of the light field: the case of deformation. I-Perception, 3(7), 467—480.

SUMMARY

It is impossible to see the light in an empty space, we can only observe light as emission from a light source or reflections from objects. Yet, human observers can estimate the illumination in empty parts of an observed scene, based on the appearance of surrounding objects. This dissertation presents studies on human sensitivity to the light field structure in empty spaces and description of the development of a light visualization tool that implements our knowledge of light fields, light design and perception.

In our perceptual studies, we reconstructed and compared physical and visual light fields. Physical measurements of the illuminance were made in real and modelled scenes with Cuttle's cubic measurement approach. The measurement device was a cube (a simulated one for modelled scenes) with small sensors on each side. The device was positioned over a grid of points in scenes creating regular measurements. For each position six measurements were translated to light properties (intensity, vector direction, diffuseness) with Cuttle's formulas. Then the resulting data was interpolated in order to obtain a full light field. In psychophysical experiments we used a probe proposed by Koenderink et al., a white matte sphere on which the illumination could be controlled by an observer. The task was to make the probe visually fit to a scene or an object. Placing the probe over grids of positions we obtained user data that was proven to be robust enough to reconstruct the global visual light field. We demonstrated that observers' data is robust enough to reconstruct the global structure of the visual light field. We also found that the visual light field is simplified with respect to the physical truth. In particular, it does not reflect subtle variations of the physical light field. In studies on scenes with complex light field structures (i.e. light zones, neighboring light fields with contrasting differences in one or more light properties), we found that observers are quite sensitive to the difference in light properties between the light zones. However, they showed idiosyncratic behavior especially for light zones with diferences in depth of a scene (front-back), rather than in the picture plane (left-right).

The second goal of this thesis was to develop a tool that incorporates our knowledge in measurement and perception of light in its visualization. Modern light visualizations

often focus on surfaces or show light in a sophisticated manner understandable only for experts. We augment existing approaches with our tool that visualizes light in 3D volumes and in a perceptually-relevant manner. The measurement approach was the same as the physical measurements used for the perceptual studies above. The measurement cubes could be implemented physically, for real, or virtually, for modelled scenes. Resulting measurements were translated into light properties — mean illuminance, vector direction and diffuseness of light — and represented via variation of shapes' proportions. We tested our visualizations performance compared to image renderings and found that the visualizations led to at least as good task performance as renderings. Moreover, we developed a web-based tool, which can be used for visualizing of cubic measurements by anyone and described applications of this tool for architectural lighting design.

Our findings expand knowledge on the structure of the visual light field and help to understand it better. This can contribute to applied areas, such as computer graphics and architectural lighting design. Moreover, our visualization tool can immediately be used by lighting artists or architectural light designers for increasing their work efficiency by providing quick and quantitative representation of the light conditions.

SAMENVATTING

Het is onmogelijk om het licht in een lege ruimte te zien, we kunnen alleen licht waarnemen als emissie van een lichtbron of reflectie van objecten. Toch kunnen menselijke waarnemers de verlichting schatten in lege delen van een waargenomen scene, gebaseerd op de uiterlijke verschijning van omringende objecten. Dit proefschrift presenteert onderzoek naar de menselijk sensitiviteit voor de structuur van het lichtveld in lege ruimtes en een omschrijving van de ontwikkeling van een licht-visualisatie tool. Deze tool implementeert onze kennis van lichtvelden, licht ontwerp en perceptie.

In onze perceptuele onderzoeken, hebben wij fysische en visuele lichtvelden gereconstrueerd en vergeleken. Met Cuttle?s kubieke meetmethode hebben we fysische metingen van de verlichtingssterkte gedaan in echte en gemodelleerde scenes. Het meetinstrument was een kubus (een gesimuleerde in gemodelleerde scenes), met kleine sensoren op elke zijde. Het instrument werd gepositioneerd op roosters van punten in de ruimtes, wat regelmatige metingen opleverde. Zes metingen per positie zijn vertaald naar lichteigenschappen (intensiteit, vector richting en diffusiteit) met de formules van Cuttle. De resulterende data is daarna geinterpoleerd om een volledig lichtveld te verkrijgen. In psychofysische experimenten hebben we gebruik gemaakt van een zogenaamde probe, ontwikkeld door Koenderink et al., een witte matte bol waarop de verlichting aangepast kan worden door de waarnemer. De taak was om de probe visueel te laten passen in een scene of bij een object. Door de probe op een grid van posities te plaatsen, verkregen we gebruikersdata waarvan we bewezen dat die robuust genoeg was om het globale lichtveld te reconstrueren. We hebben gedemonstreerd dat de data van de waarnemers robuust genoeg is om de globale structuur van het visuele lichtveld te reconstrueren. We ontdekten ook dat het visuele lichtveld versimpeld is ten opzichte van de fysische werkelijkheid. Met name de subtiele variaties van het fysische lichtveld ontbreken. In onderzoeken naar scenes met complexe lichtveldstructuren (d.w.z. lichtzones, naast elkaar gelegen lichtvelden met contrasterende verschillen in een of meer lichteigenschappen), vonden we dat waarnemers vrij gevoelig zijn voor verschillen in lichteigenschappen tussen de lichtzones. Echter, zij vertoonden idiosyncratisch gedrag, in het bijzonder voor

lichtzones met verschillen in de diepte van de scene (voor-achter), in plaats van in het beeldvlak (rechts-links).

Het tweede doel van deze thesis was om een visualisatie tool te ontwikkelen die onze kennis over het meten en de perceptie van licht belichaamt. Moderne lichtvisualisaties leggen vaak de nadruk om oppervlaktes of laten licht zien op een geavanceerde manier die alleen te begrijpen is voor experts. Wij breiden bestaande aanpakken uit met onze tool die licht visualiseert in 3D volumes en op een perceptueel relevante manier. De meetmethode was hetzelfde als in de fysische metingen die gebruikt werden in de hierboven genoemde onderzoeken. De meetkubussen kunnen fysiek, voor echte, en virtueel, voor gemodelleerde scenes, worden geimplementeerd. De resulterende metingen worden vertaald naar lichteigenschappen — gemiddelde verlichtingssterkte, vector richting en lichtdiffusiteit — en gerepresenteerd worden via variaties van de verhoudingen van vormen. We hebben de doelmatigheid van deze visualisaties getest in vergelijking met gerenderde beelden en vonden dat de visualisaties voor onze taken ten minste net zo doelmatig waren als de renderingen. Bovendien hebben we een web-gebaseerde tool ontwikkeld, welke voor de visualisatie van kubieke metingen gebruikt kan worden door iedereen, en we hebben toepassingen van deze tool voor architectonisch lichtontwerpen beschreven.

Onze bevindingen breiden de kennis uit over de structuur van het visuele lichtveld en helpen het beter te begrijpen. Dit kan bijdragen leveren in toepassingsgebieden, zoals computer graphics en architectonisch licht ontwerpen. Bovendien kan onze visualisatie tool direct gebruikt worden door lichtkunstenaars of architectonisch lichtontwerpers, om hun werk efficiënter te maker door hen een snelle en kwantitatieve representatie van de licht condities aan te reiken.

ACKNOWLEDGEMENTS

At the end of this thesis, I would like to express my deepest gratitude to many people who helped me during my PhD. Without them I would never make it this far.

The first thank goes of course to Sylvia, my promotor and main supervisor. Dear Sylvia, I will be forever grateful for picking me for this job. By making this decision, you changed my life and it went beyond my dreams. Delft was the best place for me to be. I am very lucky to have you as a supervisor for many reasons, including but not limited to your hospitality, patience and care. You will always be my role model.

Huib, thank you for joining my supervisory team and guiding me through most of my time in Delft, for adding a different perspective to many discussions, for the extremely valuable suggestions in studies and in writing and for your support. Susan, it was great to have you as my third promotor! I always appreciated your openness, confidence and serenity. Ingrid, thank you for helping in starting up my studies.

Thank you to all the lab members. Fan, at first it was not clear what is behind your poker face, but over years I found out how fun, smart and reliable you are. I'm happy we became friends. Ling, since the first day you were welcoming and warm to me. You are a wonderful person, incredibly strong and kind. I miss you a lot. Qian, not part of vision lab, but you feel inseparable from us, so close we were. You showed me how a person can be incredibly talented and modest at the same time. Also, it was amazing to see you becoming a beautiful strong woman and a loving mother to Oscar. Maarten, thank you for always creating the atmosphere of fun and joy around you. I will always remember your optimism, awesome sense of humor and your fascinating research. Willemijn, what a great development we had in our relationship over years! =D Now that I know you more, I deeply respect and awe your strength and bravery together with smartness and ability to deliver on your goals. Together these qualities will probably bring you to greatness. Jess, I'm very happy that I met you and learned from you so different approaches of interacting with people, much more tactful than mine =D. I hope we'll keep meeting (not in small part because of Sasha, very curious how your clever boy will develop). Mitchell,

I envy your communicative skills so much and already miss our lunch chats on techs and tv-shows. Francesca and Cristina, you make a new, cool facet of the lab, keep it up and good luck with your studies!

I thank all members of Pi-lab, especially Yi, Ernestasia, Reineer and Elif. We had great lunches together and I wish you all the best. Thank you also to the section people, I enjoyed our monthly meetings, at which I could hear about the faculty life and "kitchen" behind the scenes. Special note here to Jie. Oh my God, you are incredible! Balancing a scientific career, a child and a business — I did not think it is possible in real life. Now I know it is.

Thanks to to all people whom I met in the faculty, most of all to the secretary office. Amanda, Daphne, Denise, Charleyne and Joost, you helped me a lot during my appointment in the faculty and over all stages of my PhD. I am very grateful for that. Bertus, thank you for your support in technical issues and for always cheering everyone up.

I feel very lucky to belong to the PRISM network. It was a blast of experience. We had a great group of principal investigators and young researchers. Starting from the first meetings, we got spoiled by the talks from some of the best people in the field. We went to nice places for meetings and had awesome parties. I hope I will stay connected to the people that I met there. Roland, Sylvia and other PI-s, you did such a tremendous job! I think it was a success, and wish the DyVito to be as good.

Thank you to Alex Mury for putting his trust in me and good advices on science and communication ("be diplomatic, Tatiana"). =)

During these years, I was also supported by my friends. Some old-but-gold at the distance — Ira D., Max R., Tatiana A., Katja Ch., and some acquired already here — Olja and Dima, Elena and Fabiano, Encar, Camilla, Anna A., The Lunch Club, PDEngs. Thanks guys, I love you and you are great!

Thank you to my parents who were always there for me. And to my whole family, which got a few times bigger (and louder =D) when I got married. I feel warm among you.

Finally, Stefano, my beloved husband. You brighten my world. You make me a better person. I cannot express all the gratitude to the universe for having you in my life. And I'm looking forward of having many more adventures together =)

CURRICULUM VITÆ

Tatiana KARTASHOVA

08-06-1989	Born in Ermak, Kazakh Soviet Socialist Republic, USSR.
1996–2006	Gymnasium N85, Saint Petersburg, Russia
2006–2012	Engineer of Automated Systems of Information Processing and Control Saint Petersburg Electrotechnical University "LETI" (ETU), Russia
2010–2013	Technical writer General Satellite corp., Saint Petersburg, Russia
2013-2018	PhD. Delft University of Technology, Delft, The Netherlands *Thesis:* Structures of Physical and Visual Light Fields: Measurement, Comparison and Visualization *Promotors:* Prof. dr. S. C. Pont, Prof. dr. H. de Ridder, Prof. dr. S. F. te Pas